CONTENTS

LIST OF FIGURES

LIST OF ABBREVIATIONS

Abbreviation	Meaning
AE	Allee effect
BB	Backward bifurcation
BTB	Bovine tuberculosis
DFE	Disease-free equilibrium
EEP	Endemic equilibrium point
GAS	Globally-asymptotically stable
LAS	Locally-asymptotically stable
ODE	Ordinary differential equation

LIST OF TABLES

Title	Epidemiological models with density-dependent demographics
Name	Salisu Usaini
Supervisor	Prof. Ruomen Anguelov
Co-supervisor	Dr. Salisu Mohammed Garba
Department	Mathematics & Applied Mathematics
Degree	Philosophiae Doctor

Abstract

The Allee effect is characterized by a positive relationship between population density or size and the *per capita* population growth rate in small populations. There are several mechanisms responsible for the Allee effects. In light of these Allee mechanisms, we modeled both the birth and the death rates as density-dependent quadratic polynomials. This approach provides an ample opportunity for taking into account the major contributors to the Allee effects and effectively captures species' susceptibility variation due to the Allee effect. We design an SI model with these demographic functions and show that the host and/or disease persistence and extinction are characterized by threshold values of the disease related parameters (λ and μ). For special cases of the model, verifiable conditions for host population persistence (with or without infected individuals) and host extinction are derived. Numerical simulations indicate the effects of the parameter β on the host population persistence and extinction regions.

Furthermore, an SEI model with frequency-dependent incidence and the same quadratic demographics is presented. This is aimed at investigating the combined impact of infectious disease and the Allee effect at higher population levels. Indeed, the model suggests that the eventual outcome could be an inevitable population crash to extinction. The tipping point marking the unanticipated population collapse at high population level is mathematically associated with a saddle-node bifurcation. The essential mechanism of this scenario is the simultaneous population size depression and the increase of the extinction threshold owing to disease virulence and the Allee effect.

Finally, the role of repeated exposure to mycobacteria on the transmission dynamics of bovine tuberculosis is addressed. Such exposure is found to induce the phenomenon of backward bifurcation. Two scenarios when such phenomenon does not arise are highlighted and for each case the model is proved to have a globally asymptotically stable equilibrium. The impact of vaccine is assessed *via* a threshold analysis approach.

CHAPTER 1

Introduction

Population dynamics are regulated by numerous biological processes that affect fertility, mortality and migration. Cooperative phenomenon and parasitism are among those processes that can have complex and non-trivial outcomes on the dynamics of a population. The type of cooperative process that affects the vital dynamics of a population known as 'Allee effect' is of interest here. Another scenario that has complex and non-trivial consequences on the resulting population dynamics is some sort of group structure. Such structure arises when either disease driven changes in behavior is incorporated or disease numerous stages are taken into account.

The objective of this thesis is two-fold:

(1) to provide a more realistic modeling tool to study the interplay between the Allee effect and infectious disease on population dynamics from a theoretical point of view.

(2) to investigate the role of group structure on the dynamics of a population owing to some disease stages and susceptibility variation.

In the first part of this introduction, we explain the term Allee effect and give a brief review of some relevant works in the literature. The second part gives a

brief account on group structure with review of some previous studies.

The Allee effect is a phenomenon in biology characterized by a positive relationship between population density or size and the *per capita* population growth rate in small populations [1]. That is, it is manifested by an increase in *per capita* growth rate with an increase of either population density or size. It is sometimes referred to as "undercrowding" and in the field of fishery sciences is also considered analogous to "depensation" [1]. The history of the term Allee effect can be traced back to the pioneering work of W. C. Allee [2]. The Allee effect is found in numerous species such as bacteria, protozoans, plants and animals [1, 3, 4]. Some species that suffer from both an Allee effect and disease include the island fox *Urocyon littoralis* [5, 6] and the African wild dog *Lycoan pictus* [7, 8].

Various mechanisms account for an Allee effect which are naturally related to survival and/or reproduction. This means that there are mechanisms that affect reproduction and those that affect survival. Indeed, some mechanisms affect both simultaneously and as a consequence have greater impact on individual fitness [9, 10, 11, 12]. A few examples of these mechanisms reported in the literature are given in Table 1.1.

The Allee effects are phenomenologically classified into two main pairs namely: component-demographic and weak-strong Allee effects. Component Allee effect describes a positive relationship between any measurable component of individual fitness and either density or numbers of conspecifics. On the other hand, a demographic Allee effect is characterized by a positive density-dependence at the overall fitness level. This means that at population level, a component Allee effect or various combination of component Allee effects can affect the overall mean fitness and cause a demographic Allee effect [12]. It is classically measured by the *per capita* population growth rate [1]. The *per capita* growth rate is the number of individuals that are added to a population per unit time, per individual. That is the growth rate of a population (dN/dt) divided by the number of individuals in that population (N). A demographic Allee effect can either be 'weak' or 'strong' depending on the strengths of the positive density-dependence and negative density-dependence [12]. A population exhibits a strong Allee effect if the growth rate is negative at low population size or density. This population size or density is commonly known as the Allee effect threshold below which species

collapses to extinction. When the population growth rate is positive at low population size or density, the Allee effect is said to be weak. For the weak Allee effect no threshold of the population size or density exists.

The Allee effect has a long history as far back as 1931, but it receives considerable attention recently in mathematical models of ecology and epidemiology (for the recent works see [13, 14, 15, 16, 17, 18, 19, 20] and the references therein). As reported in [20], the most difficult problem in modeling with Allee effect is the splitting of the *per capita* growth rate into fertility and mortality rates to effectively capture some of the aforementioned Allee mechanisms. In this regard, we briefly review the works of some authors in the literature on the models that incorporate the joint impact of Allee effect and infectious disease. We denote by $S(t)$ the susceptible population size, $I(t)$ the infected population size, and $N(t) = S(t) + I(t)$ the total population size at time t.

Single species models (both discrete and continuous) with demographic Allee effect were widely studied in the literature (see the review in [21] and the references therein). An SI model is introduced by Deredec and Courchamp in [22] for a population whose dynamics already face a strong Allee effect in the absence of disease infection. They compare the impact of Allee effect on the disease dynamics with following assumptions: (i) the host population occupies a constant area; (ii) disease transmission is horizontal (newborns are susceptibles); (iii) infection does not affect reproductive capacity of infected individuals; and (iv) there is additional disease-induced mortality at the rate α. Their model equations are then given by

$$\begin{aligned} \dot{S} &= bf(N)N - mf(N)S - \beta\phi(N)SI/N, \\ \dot{I} &= \beta\phi(N)SI/N - mf(N)I - \alpha I, \end{aligned} \tag{1.1}$$

with $f(N) = (1-N/K)$ for the case with no Allee effect and $f(N) = (1-N/K)(1-L/N)$ in the presence of the Allee effect. In the case when the infected hosts were capable of infecting newborns, the disease would be transmitted horizontally and vertically. In this scenario, the splitting of the growth rate into birth and survival parts would be avoided. Thus, system (1.1) is given by

$$\begin{aligned} \dot{S} &= bf(N)S - \beta\phi(N)SI/N, \\ \dot{I} &= \beta\phi(N)SI/N + rf(N)I - \alpha I. \end{aligned} \tag{1.2}$$

In addition, Deredec and Courchamp [22] developed an alternative model in which the Allee effect only manifests itself on mortality. That is, a growth rate is decomposed into constant birth rate and density-dependent death rate. The alternative model is as follows.

$$\begin{aligned} \dot{S} &= B(N)N - M(N)S - \beta\phi(N)SI/N, \\ \dot{I} &= \beta\phi(N)SI/N - M(N)I - \alpha I, \end{aligned} \tag{1.3}$$

with $B(N) = b, \quad M(N) = b - rf(N)$.

Deredec and Courchamp [22] compared the dynamics of populations facing the possibility of microparasitic infections in the absence and presence of the Allee effect. They discovered that the impact of the Allee effect could be considered the tradeoff between disease and the Allee effect. Of course, an Allee effect could safeguard native individuals by diminishing the population sizes that accelerate parasitic spread. On the other hand, when the disease invades the population, the Allee effect reduces the population size and increases the range of parasitic species that could drive the population to extinction.

Hilker *et al.* [23] studied a particular case of model (1.3) with $\phi(N) = N$ and the following quadratic fertility and linear density-dependent death rates.

$$B(N) = a[-N^2 + (K + L + e)N + c], \quad M(N) = a(eN + LK + c). \tag{1.4}$$

This leads to the following couple of ordinary differential equations:

$$\begin{aligned} \dot{S} &= a[-N^2 + (K + L + e)N + c]N - a(eN + LK + c)S - \beta SI, \\ \dot{I} &= \beta SI - a(eN + LK + c)I - \alpha I, \end{aligned} \tag{1.5}$$

where $e, c \geq 0$ measure the effect of density-dependence and independence on the demographic functions, respectively. They show that in the presence of a strong Allee effect in host demographics, model (1.5) exhibits rich dynamical behaviors such as sub- and super-critical bifurcations, homoclinic bifurcations and multiple stable steady-states. Moreover, they noted that high transmissibility rates could lead to disease-induced extinction. Friedman and Yakubu [24] reconsidered the SI model (1.5) to identify parameter regime of the model that leads to host population persistence (with or without infected individuals) and host extinction. In

particular, they proved that an Allee effect matters even at large population densities, as a small perturbation from the disease-free equilibrium can drive host's population to extinction. They also showed that additional deaths due to the disease infections increase the Allee threshold of the host population. Cai *et al.* [25] also used the same SI model (1.5) to analytically study the bifurcations and dynamical behaviors of the model. These researchers found that their qualitative conclusions support the numerical bifurcation analysis and conjunctures in Hilker *et al.* [23]. In addition, they explored some new bifurcations phenomena such as pitchfork bifurcation, Bogdanov-Takens (BT) bifurcation of codimension two, degenerate Hopf bifurcation and degenerate BT bifurcation of codimension three in elliptic case [25]. These bifurcations exhibit more complicated dynamical behaviors of model (1.5), such as multiple attractors, homoclinic loop, and limit cycles.

In a similar note, Thieme *et al.* [20] developed an SI model with a strong Allee effect in the host demographics that incorporated distinct fertility and mortality functions compared with those used in model (1.5). Indeed, they considered a constant death rate d and a nonlinear birth function of the form:

$$B(S) = \frac{aS}{b + S^{\gamma}}, \quad \gamma > 1. \tag{1.6}$$

Another distinguishing feature of their model with those in (1.3) and (1.5) is the assumption that the infected individuals do not reproduce. The model of Thieme *et al.* [20], is given by the following system of ODE:

$$\begin{aligned} \dot{S} &= (B(S) - d)S - \beta SI, \\ \dot{I} &= \beta SI - (\alpha + d)I, \end{aligned} \tag{1.7}$$

The authors [20] proved that the transition from host's population decline to extinction is mediated by a Hopf bifurcation and is marked by the occurrence of a heteroclinic orbit.

It is clear from these previous studies that the presence of the Allee effect in host demographics affects qualitatively the dynamics of a population. Furthermore, all these models have strength on their own right and weakness in some sense. More precisely, these models account for the impact of the Allee effect on

either one of the host's demographics (birth or death), neglecting the other. In particular, the choice of the demographic functions $B(N)$ and $M(N)$ in (1.5) is based on mate limitation/crowding effect and intraspecific competition, respectively. The assumption that $M(N)$ is linear in the presence of a strong Allee effect is not very realistic, for the fact that the effect of intraspecific competition on social and cooperative species is very low when population is small [1, 26]. In order to circumvent this problem, we modeled both the birth and the death rate functions as quadratic polynomials. In this thesis, using quadratic demographics in the presence of a strong Allee effect provides a more realistic representation of the population dynamics particularly at low population density or size. This is because for our chosen death rate function there is a positive relationship between individual survival probability and population density, which indicates that social and cooperative species suffer more Allee effect than non cooperative species. Indeed, this approach provides ample opportunity for taking into account the major contributors (Allee mechanisms) to the Allee effect and presents more realistic modeling tool as well.

It is well known, right from Kermack and McKendrick model [27] that classical epidemiological models were developed based on simplifying assumptions taking into account some mathematical complexity while forgetting reality. More precisely, various classical mathematical models assume that all susceptible individuals have the same epidemiological status, all infected individuals transmit infection at the same rate, and the course of infection is the same for all individuals in a population. In addition, such type of models assume that either immunity does not exist (the SIS model) or recovery from infection confers permanent or temporary immunity (the SIR and $SIRS$ models). However, there is an evidence that some infections provide partial immunity and spread among seropositive individuals, albeit at a lower rate [28, 29]. This means that seropositive individuals can pass on the infection during the second and subsequent infectious periods even without any observable clinical symptoms of the disease. In this case, a population is structured in such a way that some disease stages and/or susceptibility variation are taken into account. That is, either differential susceptibility (S_1IS_2 model) or differential infectivity (SI_1I_2 model) or both the two scenarios ($S_1I_1S_2I_2S_2$ or $SIS_1I_1S_1$ model) are usually considered in such situations [28, 29, 30, 31, 32, 33].

Such type of models exhibit complex dynamical behaviors such as backward bifurcations and forward hysteresis which do not exist in their classical counterparts. Some examples of animal and human diseases which are appropriately modeled using this approach can be found in [28] and [33], respectively. Another strange assumption for classical models and most of those models that account for either differential susceptibility and/or differential infectivity is the restriction to the situation where the affected population is of constant size. As this thesis focuses on the animal population dynamics, we will briefly review some related works in the literature that incorporate differential susceptibility and/or infectivity.

Greenhalgh *et al.* [28] introduced a two-stage SIS ($S_1I_1S_2I_2$) model to study the transmission dynamics of bovine respiratory syncytial virus ($BRSV$) amongst cattle. This is for the fact that $BRSV$ infection offers partial immunity and spreads among seropositive cattle. The basic idea of their model is that for animal diseases which confer partial immunity from initial infection recovery, an animal may become lightly infected again without necessarily showing clinical symptoms of the disease. This appear for some diseases at which such seropositive animals may transmit the infection at a lower rate than animals experiencing the infection for the first time. Analysis of the two-stage model in [28] shows the possibility of backward bifurcation, and that the higher of the two subcritical equilibria (one with larger number of infective individuals) is stable whereas the lower one (one with smaller number of infective individuals) is unstable. It is argued in [34] that using two-stage model to incorporate the effect of successive exposure to infectious agents is an oversimplification. This is based on the suggestion in [35] that in some cases greater level of exposure to infectious organism may overcome the immune system and leads to a more subsequent transmission of disease than a lower exposure. However, a three-stage model for the spread of Bovine respiratory syncytial virus in cattle may be more realistic than the two-stage one. The three-stage extended model considered in [34] is shown to exhibit more complex dynamics such as two subcritical endemic equilibria in the presence of forward bifurcation and multiple supercritical equilibria.

The models developed by Castillo-Chavez *et al.* [36, 37] and Huang *et al.* [38] seem to be the first account for the presence of backward bifurcation in epidemiological models. In both papers, the phrase 'backward bifurcation' was not actually

used even though Figure 1, in the article by Huang *et al.* [38] is a bifurcation diagram that clearly demonstrates the phenomenon of backward bifurcation. With progress in research, numerous authors investigated this phenomenon in several disease transmission models [28, 29, 34, 39, 40, 41, 42, 43, 44], as it plays a relevant role for effective disease control and elimination. Indeed, it is well known that in a disease transmission modeling, a classical necessary requirement for effective disease elimination is that the basic reproduction number, usually denoted by $\mathcal{R}_0$, must be below one. However, in the presence of a backward bifurcation, endemic equilibria also exist when $\mathcal{R}_0 < 1$. This means that the occurrence of this phenomenon has important public health implications. In fact, it might not be sufficient although necessary to reduce $\mathcal{R}_0$ below unity to eradicate the disease. In this case, the basic reproduction number must be further reduced below a critical value at the turning point in order to avoid endemic states and guarantee the effective disease elimination.

It is to be noted that both the two-stage and its three-stage extension in the previous studies [28, 34] are restricted to the situations where the affected population is of constant size. This assumption is reasonable for diseases that either spread quickly (i.e. in less than one year) through the population or those that spread slowly (i.e. over many years) with births approximately balanced by the natural deaths [45, 46, 47]. However, for diseases with either high disease-related mortalities or in which the births are not balanced by the deaths, this assumption is not very realistic. Several examples of animal diseases in which disease-related deaths have drastically decreased the population sizes are given in [47]. In this thesis, we present a two-stage SIS model, which is an extension of the model presented in [28] by incorporating vital dynamics in a population with varying size which makes the model more realistic and practically relevant. We study this model with aim to identify causes of backward bifurcation and to assess vaccine impact in the transmission dynamics of an epidemiological model with partial immunity and variable population [48].

The main contributions to knowledge in the thesis include:

(1) We provide a more realistic representation of a population dynamics particularly at low population density or size. This is achieved by splitting a *per capita* growth rate in which an Allee effect is manifested into quadratic fer-

tility and mortality rates that effectively capture the major contributors to the Allee effects and species' susceptibility variation due to the Allee effect. In other words, the Allee effect acts on both birth and death rates instead on one of them. Therefore, it generalizes some of the existing works in the literature (see for example the demographic functions in (1.3) and (1.4)).

(2) The models in Chapter 3 and Chapter 4 are subjected to rigorous mathematical analysis as dynamical systems. We explore the range of values of the parameters α and β that measure the intensity of the Allee effect on both demographics and determine the extinction risk of endangered species as well.

(3) It is highlighted that the synergistic impact of an Allee effect and infectious disease at high population level could lead to an unanticipated population crash to extinction, even though the definition of the Allee effect refers only to low population levels.

(4) Global stability results are rigorously proved for the imperfect vaccine model in Chapter 5.

(5) Threshold conditions on the vaccine coverage and vaccine efficacy that determine the impact of an imperfect vaccine are also identified.

(6) Implication of this control measure is discussed, suggesting that eradication of BTB *via* vaccination alone may not be an effective control strategy in the wildlife.

The thesis is organized as follows. In Chapter 2, we recall some of the basic concepts and mathematical theory relevant to the formulation and proof of the results in the thesis. In Chapter 3, an extended version of model (1.5) is presented. The SI model in Chapter 2, is extended to an SEI model with standard incidence formulation in Chapter 4. In Chapter 5, we study structured acquired immunity due to repeated exposure to mycobacteria in animal population using a two-stage SIS model.

Table 1.1: Main Allee effect mechanisms

Mechanism	How it works	Examples
	Reproduction	
(1) Mate limitation	Difficulty in finding mate at low population size or density	queen conch (Strombus gigas); Glanville fritillary butterfly.
(2) Reproductive facilitation	Some species less likely to reproduce in isolation. The situation more probable in small populations	Whiptail lizards; snail (Biomphalaria glabrata); queen conch.
(3) Cooperative breeding	Cooperation in raising the young less successful in small population	African wild dog (Lycaon pictus).
	Survival	
(4) Anti-predator behavior	Cooperative defence against predators is less efficient when population is small	Meerkat (Suricata suricatta); desert bighorn sheep (Ovis canadensis).
(5) Predator dilution (predator satiation or swamping)	Individual prey vulnerability increases as prey groups get smaller or prey population sparser	Meerkat; cod; woodland caribou (Rangifer trandus caribou).
	Reproduction and/or survival	
(6) Foraging efficiency	Ability to locate food, kill prey or overrule kleptoparasites decline in small foraging groups. It can, in turn, reduce individual survival and/or fertility	African wild dog; black-browed albatross (Thalassarche melanophris).
(7) Environmental conditioning	A mechanism in which individuals work together in order to improve their environment for the benefit of the species	Bark beetles; fruit fly (Drosophila melanogaster); alphine marmot.

CHAPTER 2

Mathematical background

In this chapter, we recall some of the basic concepts and mathematical theory relevant to the formulation and proof of the results in the subsequent sections.

2.1 Autonomous Systems

Differential equations are relations between a function and its derivatives. When the function depends on a single variable, the resulting differential equation is said to be *ordinary* as opposed to *partial*. An ordinary differential equation whose vector field does not depend explicitly on time is called *autonomous*. Throughout this thesis autonomous systems of ordinary differential equations (ODEs) are considered.

Consider the following equation [49]

$$\dot{x} = f(x),\ x(t_0) = x_0 \in \mathbb{R}^n, \tag{2.1}$$

where $x = x(t) \in \mathbb{R}^n$ denotes a vector valued function of $t \in \mathbb{R}$. We assume that $f \in C(\mathbb{R}^n, \mathbb{R}^n)$ and the initial condition is given at $t = 0$.

The overdot in (2.1) denotes differentiation with respect to time t (i.e. d/dt). The equation (2.1) is an autonomous *ordinary differential equation* (ODE) and

the function $f(x)$, is called a *vector field*.

A solution of equation (2.1) is a continuously differentiable function $x : W \to \mathbb{R}^n$ satisfying (2.1), where W is the time interval of existence. Note that, we may also refer to $x(t, x_0)$ as the trajectory or phase curve through the point x_0 at $t = t_0$ and the space of the dependent variables of (2.1) is referred to as the phase space. Therefore, an equilibrium point of equation (2.1) is a point $x = \bar{x} \in \mathbb{R}^n$ such that $f(\bar{x}) = 0$.

Definition 2.1.1 *[50] An orbit through a point x_0 in the phase space $E \subset \mathbb{R}^n$ of (2.1), denoted by $O(x_0)$, is a set of points in E that lie on a trajectory passing through x_0. That is*

$$O(x_0) = \{x(t) \in \mathbb{R}^n : x(t_0) = x_0, t \in \mathbb{R}\}.$$

Definition 2.1.2 *[51] A flow $\phi(t, x)$ $(\phi_t(x))$ is a one parameter, differentiable mapping $\phi : \mathbb{R}^n \to \mathbb{R}^n$, such that*

(i) *$\phi_{t_0}(x) = x$, and*

(ii) *for all t and $s \in \mathbb{R}$, $\phi_t \circ \phi_s \equiv \phi_{t+s}$.*

Thus, the vector field $f(x)$ in (2.1) is said to generate a flow $\phi : \mathbb{R}^n \to \mathbb{R}^n$, which transforms an initial state x_0 into some state $x(t) \in \mathbb{R}^n$ at time $t \in \mathbb{R}$

$$\phi_t(x_0) := x(t).$$

The function $f(x)$ is said to be *locally Lipschitz* on an open set E if for every point $z \in E$, there is a neighborhood N such that f is Lipschitz on N. That is, there exists $K_N \in \mathbb{R}$ such that

$$|f(x) - f(y)| \leq K_N |x - y| \text{ for } x, y \in N. \tag{2.2}$$

The function $f(x)$ is said to be globally Lipschitz or simply Lipschitz on E if (2.2) holds with a constant K which is independent of z and N.

Theorem 2.1.1 *(Fundamental Existence-Uniqueness Theorem [52, 51]). Let $E \subset \mathbb{R}^n$ be an open subset of real Euclidean space, let $f : E \to \mathbb{R}^n$ be locally Lipschitz at a point $x \in E$. Then for any $x_0 \in E$, there exists a real interval W containing t_0 such that (2.1) has a* unique *solution $x = x(t)$ which is defined on W.*

The above Existence-Uniqueness Theorem implies that the solution of (2.1) can be found in an open interval W containing t_0 when $f(x)$ is locally Lipschitz at a point x_0. The solution typically exists over a larger interval since the estimated interval W is not optimal. The largest such interval is known as the *maximal interval of existence*. This maximal interval of existence is the largest interval of time containing t_0 for which the solution, $x(t)$, of (2.1) exists.

Theorem 2.1.2 *(Maximal Interval of Existence [51]). Let $E \subset \mathbb{R}^n$ be an open subset of real Euclidean space and $f : E \to \mathbb{R}^n$ be locally Lipschitz. Then there is a maximal, open interval $W = (a, b)$ containing t_0 such that (2.1), has a unique solution, $x = x(t)$.*

It should be noted that, the existence of solutions as provided by Theorem 2.1.1 and Theorem 2.1.2 does not imply existence for $t \in [0, \infty)$ or $t \in (-\infty, +\infty)$. Such existence of solutions of (2.1) is covered by the concept of *dynamical system*. Intuitively, dynamical system is an evolution rule that defines a trajectory as function of time on a set of states.

Definition 2.1.3 *[49]. Equation (2.1) is said to define a* dynamical system *on a subset $E \subset \mathbb{R}^n$ if, for every $x_0 \in E$, there exists a unique solution of (2.1) which is defined for all $t \in [0, \infty)$ and remains in E for all $t \in [0, \infty)$.*

Theorem 2.1.3 *[49]. Let $f : \mathbb{R}^n \to \mathbb{R}^n$ be globally Lipschitz on $\mathbb{R}^n$. Then there exists a unique solution $x = x(t)$ to (2.1) for all $t \in \mathbb{R}$. Hence (2.1) defines a dynamical system on $\mathbb{R}^n$.*

Theorem 2.1.4 *(Existence and Uniqueness for locally Lipschitz problems [49]). Let $\mathbb{R}^n \to \mathbb{R}^n$ be Lipschitz on a neighborhood N of E where $E \subset \mathbb{R}^n$ is bounded. If it may be shown that for any $z \in E$, the solution $x(t)$ of (2.1) satisfies $x(t) \in E$ for each $t \geq 0$ such that the solution exists, then (2.1) defines a dynamical system.*

2.2 Hartman -Grobman Theorem

Definition 2.2.1 *The Jacobian matrix of the function f at the equilibrium point $\bar{x}$, denoted by $Df(\bar{x})$, is the matrix*

$$\begin{pmatrix} \frac{\partial f_1}{\partial x_1}(\bar{x}) & \cdots & \frac{\partial f_1}{\partial x_n}(\bar{x}) \\ \vdots & \vdots & \vdots \\ \frac{\partial f_n}{\partial x_1}(\bar{x}) & \cdots & \frac{\partial f_n}{\partial x_n}(\bar{x}) \end{pmatrix},$$

of partial derivatives evaluated at $\bar{x}$.

Definition 2.2.2 *[50]. Let $x = \bar{x}$ be an equilibrium point of (2.1). Then $\bar{x}$ is called hyperbolic if $Df(\bar{x})$ has no eigenvalues with zero real part.*

Recall that a vector function f is said to be C^r if it is $r \geq 1$ times differentiable and each derivative is continuous. If $r = 0$ then the function is said to be continuous. Let the following vector fields f and g

$$\dot{x} = f(x),\ x \in \mathbb{R}^n,$$
$$\dot{y} = g(y),\ y \in \mathbb{R}^n,$$

be two C^r $(r \geq 1)$ on $\mathbb{R}^n$ or sufficiently large open subsets of $\mathbb{R}^n$.

Definition 2.2.3 *The dynamics generated by the vector fields f and g are said to be C^k conjugate $(k \leq r)$ if there exists a C^k diffeomorphism h which takes orbits of the flow generated by f, $\phi(t, x)$, to orbits of the flow generated by $g, \psi(t, y)$, preserving orientation and parameterization by time.*

Theorem 2.2.1 *(Hartman and Grobman [50]). Consider a C^r $(r \geq 1)$ vector field f and the system*

$$\dot{x} = f(x),\ x \in \mathbb{R}^n, \tag{2.3}$$

with f defined on an open subset of $\mathbb{R}^n$. Suppose that (2.3) has hyperbolic equilibrium point at $x = \bar{x}$ and $Df(\bar{x})$ has no eigenvalues on the imaginary axis. Consider the associated linear ODE system

$$\dot{\xi} = Df(\bar{x})\xi,\ \ \xi \in \mathbb{R}^n. \tag{2.4}$$

Then the flow generated by (2.3) is C^0 conjugate to the flow generated by the linearized system (2.4) in a neighborhood of the equilibrium point $\bar{x}$.

Hartman-Grobman Theorem simply asserts that an orbit structure near a hyperbolic equilibrium point is qualitatively the same as the orbit structure given by the associated linearized dynamical system around the equilibrium point.

2.2.1 Local Stability of Equilibria

Let $\bar{x}$ be an equilibrium point of (2.1). Then $\bar{x}$ is *stable* if solutions starting "close" to $\bar{x}$ at a given time stay close to it at all future times. It is asymptotically stable if nearby solutions converge to $\bar{x}$ as t approaches infinity. More formally

Definition 2.2.4 *[49, 53] An equilibrium point $\bar{x}$ of (2.1) is said to be*

- *stable (Lyapunov stable) if, for any $\epsilon > 0$, there exists $\delta = \delta(\epsilon) > 0$ such that*
$$|x_0 - \bar{x}| < \delta, \quad then \ |x(t) - \bar{x}| < \epsilon, \ \forall t \geq 0;$$
- *unstable if it is not stable;*
- *asymptotically stable if it is stable and there exists a constant $q > 0$ such that, if*
$$|x_0 - \bar{x}| < q, \quad then \ \lim_{t\to\infty} x(t) = \bar{x};$$
- *globally-asymptotically stable if it is stable and $\lim_{t\to\infty} x(t) = \bar{x}, \forall x$.*

2.2.1.1 Linearization Theory

In order to determine the stability of an equilibrium point $\bar{x}$, the nature of solutions near $\bar{x}$ need to be understood. Let

$$x = \bar{x}(t) + \xi, \ \xi \in \mathbb{R}^n \tag{2.5}$$

and suppose that the vector field f in (2.1) is at least twice differentiable. Substitute (2.5) into (2.1) so that its Taylor series expansion gives

$$\dot{x} = \dot{\bar{x}}(t) + \dot{\xi} = f(\bar{x}(t)) + Df(\bar{x}(t))\xi + \mathcal{O}(|\xi|^2), \tag{2.6}$$

where $|.|$ denotes a norm on $\mathbb{R}^n$. Hence, (2.6) reduces to (noting that $\dot{x(t)} = f(x(t))$)

$$\dot{\xi} = Df(\bar{x}(t))\xi + \mathcal{O}(|\xi|^2). \tag{2.7}$$

Equation (2.7) describes the evolution of orbits near $x(t)$. The behavior of solutions arbitrarily close to $\bar{x}$ is then obtained by studying the following associated linear system

$$\dot{\xi} = Df(\bar{x})\xi. \tag{2.8}$$

However, if $x(t)$ is an equilibrium point of (2.1), i.e., $x(t) = \bar{x}$, then $Df(x(t)) = Df(\bar{x})$ is a matrix with constant entries, and the solution of (2.8) through the point $\xi_0 \in \mathbb{R}^n$ at $t = t_0$ is as follows:

$$\dot{\xi}(t) = \exp(Df(\bar{x})t)\xi_0.$$

It follows that, $\xi(t)$ is asymptotically stable if all eigenvalues of $Df(\bar{x})$ have negative real parts. Then, the Hartman-Grobman theorem, Theorem 2.2.1, leads to the following simple characterization of the stability properties of $\bar{x}$.

Theorem 2.2.2 *[50] Suppose all of the eigenvalues of $Df(\bar{x})$ have negative real parts. Then the equilibrium $x = \bar{x}$ of the system* (2.1) *is asymptotically stable.*

Further, Routh-Hurwitz stability criterion provides necessary and sufficient conditions for establishing the local stability of a dynamical system. Let

$$det(\lambda I - Df(\bar{x})) = 0,$$

be the characteristic polynomial of $Df(\bar{x})$. Then we obtain the following polynomial for λ.

$$a_0\lambda^n + a_1\lambda^{n-1} + \cdots + a_{n-1} + a_n = 0,\ a_0 > 0. \tag{2.9}$$

Then, we define the Hurwitz matrix associated with equation (2.9) as follows

$$H_n := (d_{2j-i})_{1\le i,j\le n} = \begin{pmatrix} a_1 & a_3 & a_5 & a_7 & \cdots & 0 \\ a_0 & a_2 & a_4 & a_6 & \cdots & 0 \\ 0 & a_1 & a_3 & a_5 & \cdots & 0 \\ 0 & 0 & a_2 & a_4 & \cdots & 0 \\ \vdots & \vdots & \vdots & \vdots & & \vdots \\ 0 & 0 & 0 & 0 & \cdots & a_k \end{pmatrix},$$

where $a_k = 0$ for $k < 0$ or $k > 0$.

Theorem 2.2.3 *(Routh-Hurwitz criterion [54, 55]) The roots of equation* (2.9) *have negative real parts if and only if* $a_k > 0$ *for all* $k = 0, 1, \ldots, n$ *and* $\det Hn[1, \ldots, n] > 0$ *for all* $k = 1, 2, \ldots, n$.

For $n = 2, 3$, and 4, the roots of (2.9) have negative real parts if and only if

$n = 2:\ a_0 > 0,\ a_1 > 0,\ a_2 > 0.$

$n = 3:\ a_0 > 0,\ a_1 > 0,\ a_2 > 0,\ a_3 > 0$ and $a_1 a_2 - a_0 a_3 > 0.$

$n = 4:\ a_i > 0, \text{for } i = 0, 1, \ldots, 4,\ a_1 a_2 - a_0 a_3 > 0,$ and $a_1 a_2 a_3 - a_0 a_3^2 - a_4 a_1^2 > 0.$

Example 2.2.1 *[56] Consider the following model for a homogeneously mixing population that includes compartments for the susceptible* (x_1)*, exposed* (y_1)*, infected* (y_2) *and recovered* (x_2) *individuals.*

$$\begin{aligned}
\dot{x_1} &= \Lambda - \beta x_1 \frac{y_2}{p} - \mu x_1, \\
\dot{y_1} &= \beta x_1 \frac{y_2}{p} - (\alpha + \mu) y_1, \\
\dot{y_2} &= \alpha y_1 - (\gamma + \mu) y_2, \\
\dot{x_2} &= \gamma y_2 - \mu x_2,
\end{aligned}$$

where $p = x_1 + y_1 + y_2 + x_2$ *is the total population size.*

This system has a disease-free equilibrium point $\bar{x} = (\bar{x}_1, \bar{y}_1, \bar{y}_2, \bar{x}_2) = (\Lambda/\mu, 0, 0, 0)$. The Jacobian of the system is given by

$$J(x_1, y_1, y_2, x_2) = Df(x) = \begin{pmatrix}
\frac{\partial f_1}{\partial x_1} & \frac{\partial f_1}{\partial y_1} & \frac{\partial f_1}{\partial y_2} & \frac{\partial f_1}{\partial x_2} \\
\frac{\partial f_2}{\partial x} & \frac{\partial f_2}{\partial y_1} & \frac{\partial f_2}{\partial y_2} & \frac{\partial f_2}{\partial x_2} \\
\frac{\partial f_3}{\partial x} & \frac{\partial f_3}{\partial y_1} & \frac{\partial f_3}{\partial y_2} & \frac{\partial f_3}{\partial x_2} \\
\frac{\partial f_4}{\partial x} & \frac{\partial f_4}{\partial y_1} & \frac{\partial f_4}{\partial y_2} & \frac{\partial f_4}{\partial x_2}
\end{pmatrix}$$

$$= \begin{pmatrix}
-Q_1 - \mu & \frac{\beta x_1 y_2}{p^2} & -Q_2 & \frac{\beta x_1 y_2}{p^2} \\
Q_1 & -\frac{\beta x_1 y_2}{p^2} - (\alpha + \mu) & Q_2 & -\frac{\beta x_1 y_2}{p^2} \\
0 & \alpha & -(\gamma + \mu) & 0 \\
0 & 0 & \gamma & -\mu
\end{pmatrix},$$

where $Q_1 = \frac{\beta y_2}{p}(1 - x_1/p),\ Q_2 = \frac{\beta x_1}{p}(1 - y_2/p)$.
Evaluating J at $\bar{x}$ gives

$$J = \begin{pmatrix} -\mu & 0 & -\beta & 0 \\ 0 & -(\alpha+\mu) & \beta & 0 \\ 0 & \alpha & -(\gamma+\mu) & 0 \\ 0 & 0 & \gamma & -\mu \end{pmatrix}.$$

Then the characteristic equation of the Jacobian matrix J evaluated at $\bar{x}$ is given by

$$(\lambda+\mu)^2[\lambda^2 + (\alpha+\gamma+2\mu)\lambda + (\alpha+\mu)(\gamma+\mu) - \alpha\beta] = 0. \tag{2.10}$$

We have the eigenvalues $\lambda_1 = \lambda_2 = -\mu < 0$. Then, the equilibrium $\bar{x}$ is asymptotically stable if the roots of equation (2.10) have negative real parts. Applying Theorem 2.2.3 with $n = 2$ we obtain that the real roots of 2.2.3 are negative provided

$$(\alpha+\mu)(\gamma+\mu) - \alpha\beta > 0. \tag{2.11}$$

Therefore, if (2.11) holds then $\bar{x}$ is asymptotically stable equilibrium.

Note that the epidemiological meaning of inequality (2.11) will be shown in Section 2.6, where it is equivalently represented in terms of the basic reproduction number.

2.2.1.2 Next generation method

The next generation method is a linearization method specifically used to establish local asymptotic stability of either disease-free equilibrium or boundary equilibrium as well as computing the associated basic reproduction number. This method was first introduced by Diekmann, Hesterbeek and Metz [57] and improved by van den Driessche and Watmough [58] for epidemiological models. The description of this method as in [58] is the following.

Let $x = (x_1, \cdots, x_n)^T$, with $x_i \geq 0$, be the number of individuals in each compartment and the first m compartments corresponding to the infected individuals. Then define by X_s the set of all disease-free states. That is

$$X_s = \{x \geq 0 : x_i = 0, i = 1, \cdots, m\}.$$

Thus a disease transmission model with nonnegative initial conditions is given by the following systems of equations:

$$\dot{x_i} = f_i(x_i) = \mathcal{F}_i(x) - \mathcal{V}_i(x),\ i = 1, \cdots, n, \tag{2.12}$$

with $\mathcal{V}_i = \mathcal{V}_i^- - \mathcal{V}_i^+$ and $\mathcal{F}_i(x)$ being the rate of appearance of new infections in compartment i. The function $\mathcal{V}_i^+(x)$ is the rate of transfer of individuals into compartment i and $\mathcal{V}_i^-(x)$ represents the rate of transfer of individuals out of compartment i. All these functions are nonnegative since each of them represents a directed transfer of individuals. It is assumed that each of these functions are at least twice continuously differentiable in each state variable.

Definition 2.2.5 *(M-Matrix). An $n \times n$ matrix A is said to be an $M-Matrix$ if and only if all the diagonal entries are positive and every off-diagonal entry of A is non-positive.*

Lemma 2.2.1 *(van den Driessche and Watmough [58]). Let $\bar{x}$ be a disease-free equilibrium of (2.12) and let $f_i(x)$ satisfy the following conditions:*

(A1) if $x \geq 0$, then $\mathcal{F}_i, \mathcal{V}_i^+, \mathcal{V}_i^- \geq 0$ for $i = 1, \cdots, n$.

(A2) if $x = 0$, then $\mathcal{V}_i^- = 0$. In particular, if $x \in X_s$ then $\mathcal{V}_i^- = 0$ for $i = 1, \cdots, m$.

(A3) $\mathcal{F}_i = 0$ if $i > m$.

(A4) if $x \in X_s$ then $\mathcal{F}_i = 0$ and $\mathcal{V}_i^+ = 0$ for $i = 1, \cdots, m$.

(A5) if $\mathcal{F}(x)$ is set to zero, then all eigenvalues of $Df(\bar{x})$ have negative real parts.

Then the derivatives $D\mathcal{F}(\bar{x})$ and $D\mathcal{V}(\bar{x})$ are partitioned as

$$D\mathcal{F}(\bar{x}) = \begin{pmatrix} F & 0 \\ 0 & 0 \end{pmatrix},\ D\mathcal{V}(\bar{x}) = \begin{pmatrix} V & 0 \\ J_3 & J_4 \end{pmatrix},$$

where F and V are the $m \times m$ matrices defined by

$$F = \left[\frac{\partial \mathcal{F}_i}{\partial x_j}(\bar{x})\right] \quad and \quad V = \left[\frac{\partial \mathcal{V}_i}{\partial x_j}(\bar{x}) \ \ with\ \ 1 \leq i,\ j \leq m\right].$$

Further, F is nonnegative, V is nonsingular M-matrix and J_3, J_4 are matrices of the transition terms and all eigenvalues of J_4 have positive real parts.

Theorem 2.2.4 *(van den Driessche and Watmough [58]). Consider the disease transmission model given by* (2.1) *with* $f(x)$ *satisfying conditions* $A1 - A5$. *If* $\bar{x}$ *is a disease-free equilibrium of the model, then* $\bar{x}$ *is locally asymptoticallystable if* $\mathcal{R}_0 = \rho(FV^{-1}) < 1$ *(where* $\rho(A)$ *is the spectral radius of a matrix* A*), but unstable if* $\mathcal{R}_0 > 1$.

2.3 Global Stability of Equilibria

An equilibrium point $\bar{x}$ of (2.1) is said to be globally-asymptotically stable if all solutions converge to it. In epidemiology, it is important to know whether an infectious disease will persist and stay at a positive level over time, after epidemic outbreak and whether this behavior depends on the initial size of the infection or not. This is addressed mathematically by the global asymptotic stability of an endemic (non-trivial) equilibria. One well known technique of global stability analysis is based on Lyapunov functions [50, 59]. Lyapunov functions are energy-like functions that decrease along trajectories. Lyapunov functions and Lyapunov theorems are introduced below.

2.3.1 Lyapunov functions and LaSalle's Invariance Principle

2.3.1.1 Lyapunov Functions

Definition 2.3.1 *[49]. A function* $U \in C^1(\mathbb{R}^n, \mathbb{R})$ *is said to be a Lyapunov function at an equilibrium point* $\bar{x}$ *for* (2.1) *if*

$$\frac{d}{dt}U(x(t)) \leq 0$$

for all x *in a neighborhood* E *of* $\bar{x}$. *It is said to be a positive definite Lyapunov function at* $\bar{x}$ *if, in addition,*

- $U(x) = 0$ *if and only if* $x = \bar{x} = 0$,
- $U(x) > 0$ *for all* $x \in E \backslash \{\bar{x}\}$,

Theorem 2.3.1 *[49]. Let $f \in C^2(\mathbb{R}^n, \mathbb{R}^n)$. If there exists a positive definite Lyapunov function U on some neighborhood E of an equilibrium point $\bar{x}$ of (2.1) then*

(i) $\bar{x}$ is stable. If, in addition,

(ii) $\frac{d}{dt}U(x) < 0$ for all $x \in E\backslash\{\bar{x}\}$ then $\bar{x}$ is asymptotically stable.

Note that, if E can be chosen to be the whole $\mathbb{R}^n$ such that U is a Lyapunov function and $\frac{d}{dt}U(x) < 0$ in $\mathbb{R}^n \setminus \{\bar{x}\}$, then $\bar{x}$ is globally-asymptotically stable (GAS).

Example 2.3.1 *Consider the following system on $\mathbb{R}^2$*

$$\begin{aligned} \frac{dx}{dt} &= y(1-xy), \\ \frac{dy}{dt} &= -x. \end{aligned}$$

The system has a non-hyperbolic equilibrium solution at $(x, y) = (0, 0)$. Let $U(x, y) = (x^2 + y^2)/2$, then clearly $U(0, 0) = 0$ and $U(x, y) > 0$ in any deleted neighborhood of $(0, 0)$. Further,

$$\begin{aligned} \frac{d}{dt}U(x,y) &= x\frac{dx}{dt} + y\frac{dy}{dt} \\ &= xy(1-xy) - xy \\ &= -x^2y^2 < 0. \end{aligned}$$

Hence, $\frac{d}{dt}U < 0$ if $(x, y) \neq (0, 0)$. Thus, the equilibrium $(0, 0)$ is asymptotically-stable.

2.3.1.2 Limit Sets and Invariance Principle

Population dynamics models monitor human, animal, cell or vector populations among others whose population sizes are always nonnegative. However, such models should be considered in the regions where nonnegativity property is preserved.

Definition 2.3.2 *[50]. A point $x_0 \in \mathbb{R}^n$ is called*

(i) an $\omega-$limit point of $x \in \mathbb{R}^n$, denoted by $\omega(x)$, if there exists a sequence $\{t_i\}$ such that

$$\phi(t_i, x) \to x_0 \text{ as } t_i \to \infty.$$

(ii) an $\alpha-$limit point of $x \in \mathbb{R}^n$, denoted by $\alpha(x)$, if there exists a sequence $\{t_i\}$ such that

$$\phi(t_i, x) \to x_0 \text{ as } t_i \to -\infty.$$

Definition 2.3.3 *[50]. The set of all $\omega-$limit points of a flow is called $\omega-$limit set. The $\alpha-$limit set of a flow is defined in a similar manner.*

Definition 2.3.4 *[50]. Let $S \subset \mathbb{R}^n$ be a set. Then, S is said to be invariant under the vector field (2.1) if for any $x_0 \in S$ we have $\phi_t(x_0) \in S$ for all $t \in \mathbb{R}$. Moreover, S is referred to as positively invariant set for positive times (i.e., $t \geq 0$) and, for negative time, as negatively invariant set.*

Theorem 2.3.2 *(LaSalle's Invariance Principle [52]). Suppose U is a Lypunov function on an open set $E \subset \mathbb{R}^n$. Let*

$$S = \{x \in \bar{E} : \dot{U} = 0\},$$

where $\bar{E}$ is the closure of E and let M be the largest invariant set of (2.1) in S. If $\gamma^+(x_0)$ is a bounded orbit of (2.1) which lies in E, then the ω-limit set of γ^+ belongs to M; that is, $x(t, x_0) \to M$ as $t \to \infty$.

Corollary 2.3.1 *[52] If $U(x) \to \infty$ as $|x| \to \infty$ and $\dot{U} \leq 0$ on $\mathbb{R}^n$, then every solution $x(t)$ of (2.1) is bounded and approaches the largest invariant set M of (2.1) in the set S. In particular, if $M = \{\bar{x}\}$, then the equilibrium point $\bar{x}$ is globally-asymptotically stable.*

2.4 Qualitative Analysis

At times it is almost impossible to find explicitly or implicitly the solutions of a system of differential equations (particularly nonlinear ones). The qualitative

approach as well as numerical one are important since they allow us to make conclusions whether the solutions are known or not. One useful qualitative technique for analyzing nonlinear systems of differential equations is the method of *nullclines* (*isoclines*) [60, 61]. This technique is particularly useful when the dimension is low (especially planar systems). Consider system (2.1) written in the form

$$\begin{aligned} \dot{x}_1 &= f_1(x_1, \cdots, x_n), \\ &\vdots \\ \dot{x_n} &= f_n(x_1, \cdots, x_n). \end{aligned}$$

Then the x_i-nullcline is the set of point which satisfies $f_i(x_1, \cdots, x_n) = 0$. The intersection point of all the nullclines is called an *equilibrium point* or *fixed point* of the system.

The x_i-nullclines usually separate $\mathbb{R}^n$ into a collection of regions in which the x_i-components of the vector field point in either the positive or negative direction. This is easy to understand in the case of planer system as follows

$$\begin{aligned} \dot{x} &= f(x, y), \\ \dot{y} &= g(x, y). \end{aligned}$$

On the x-nullclines, $\dot{x} = 0$, so the vector field only points straight up or down. Hence, the x-nullclines divide $\mathbb{R}^2$ into regions where the vector field points either to the left or to the right. In contrast, on the y-nullclines, the vector field is horizontal, so the y-nullclines separate $\mathbb{R}^2$ into regions where the vector field points either upward or downward. The vector field in any of the regions between the nullclines, is neither vertical nor horizontal, so it must point in one of four directions: left-down, left-up, right-down, and right-up. These regions are called *basic regions*. A simple sketch of the basic regions (as in Fig. 2.1(A)) allows us to understand qualitatively the phase portrait of the system.

Example 2.4.1 *For the system*

$$\begin{aligned} \dot{x} &= y - 2x, \\ \dot{y} &= 1 - x^2 - y, \end{aligned}$$

the x-nullcline is the line $y = 2x$ and the y-nullcline is the parabola $y = 1 - x^2$. These nullclines meet at one point, so this is the only equilibrium point. The nullclines divide $\mathbb{R}^2$ into four basic regions labeled I through IV in Figure 2.1 (A). In order to find the direction of the velocity vectors in each of these regions, we pick a point in the region and find the direction of the velocity vector at that point. For example, the point (0, 1/2) lies in region I and the vector field is (1/2, 1/2) at this point, which points right-up (northeast). Hence the vector field points right-up at all points in this region. Continuing in this fashion we obtain the direction of the vector field in all four regions, as in Figure 2.1 (B). The horizontal and vertical directions of the vector field on the nullclines are determined in a similar manner. It seems that the equilibrium point is a spiral sink, just from the direction field alone.

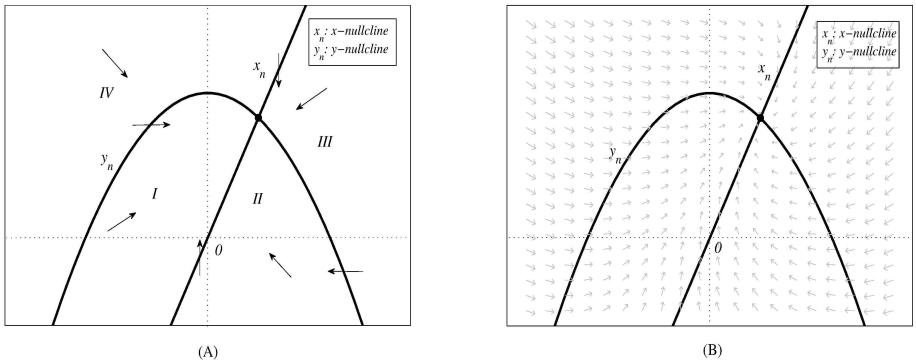

Figure 2.1: The (A) nullclines and (B) direction field.

In the case when the method of nullclines is not applicable or only the number of equilibrium solutions of the model is of interest, Descartes rule of signs would be useful. This is for the situation when the endemic equilibria correspond to the positive roots of a polynomial obtained at steady state. Such polynomial is usually obtained in terms of either one of the state variables or force of infection of the model. In order to state the Descartes theorem on the number of real roots

of polynomials, let

$$P_n(x) = a_n x^n + a_{n-1}x^{n-1} + \cdots, a_1 x + a_0,\ a_n \neq 0$$

be a polynomial of degree n with real coefficients.

Theorem 2.4.1 *(Descartes Theorem [62]). The number of positive (negative) roots (counted according to their multiplicity) of a polynomial $P_n(x)$ $(P_n(-x))$ is either equal to the number of sign alterations in the sequence of its coefficients or is by an even number less.*

Example 2.4.2 *Consider the following cubic polynomial*

$$P_3(x) = 3x^3 - 2x + 1.$$

Its coefficients have the signs $+ - +$, with two alterations of sign. Hence the number of positive roots of $P_3(x)$ is equal to either 2 or 0. On the other hand, $P_3(-x) = -3x^3 + 2x + 1$ whose sequence of coefficients changes sign only once. Therefore, $P_3(x)$ has one negative root.

2.5 Bifurcation Theory

Dynamics of differential equations system may change, if at least one parameter is allowed to vary. For example, an equilibrium can become unstable and either a periodic solution may appear or a new stable equilibrium may emerge. Such a qualitative change in behavior is called *bifurcation* and the value of the parameter at which these changes occur is known as a *bifurcation value*. Hence, the parameter that is varied is called a *bifurcation parameter*.

Definition 2.5.1 *[50]. Let*

$$\dot{x} = f(x, \mu) \equiv f_\mu(x), \quad x \in \mathbb{R}, \quad \mu \in \mathbb{R}, \tag{2.13}$$

where $x = x(t)$ denotes a vector valued function of $t \in \mathbb{R}$ be a general one-parameter family of one-dimensional ODE depending on the single parameter μ. Then an equilibrium point $\bar{x}$ of (2.13) is said to undergo bifurcation at μ_0 if the flow for $\mu < \mu_0$ near $\bar{x}$ and x near $\bar{x}$ is qualitatively different to the flow near $\bar{x}$ for $\mu > \mu_0$.

There are basically two types of bifurcations viz *local* and *global* bifurcations. A bifurcation that involves the degeneracy of some eigenvalue of the Jacobians associated with equilibria or cycles is called a *local bifurcation*. There are seven most important local bifurcations of continuous-time systems. These include transcritical, saddle-node, pitchfork, Hopf, the tangent of limit cycles, flip (or period-doubling) and Neimark-Sacker (or torus). The first three can be viewed as collisions of equilibria and the remaining four involve limit cycles. In contrast, global bifurcation involves the occurrence of homoclinic and heteroclinic orbits and cannot be revealed by eigenvalue degeneracies. That is, the dynamical properties cannot be deduced from local information. Homoclinic and heteroclinic bifurcations are some examples of global bifurcations [63].

2.5.1 Saddle-node bifurcation

This simply refers to collision of two equilibria at the bifurcation value $\mu = \mu_0$. Indeed, for $\mu < \mu_0$, the two equilibria are distinct and one is stable (the node) while the other is unstable (the saddle). As μ increases, the two equilibria approach each other and eventually collide when $\mu = \mu_0$ (and then disappear).

Theorem 2.5.1 *[50]. Suppose* (2.13) *has an equilibrium point at* $(x, \mu) = (\bar{x}, \mu_0)$. *Then* (2.13) *will undergo a saddle-node bifurcation if the following conditions hold:*

(i) $f(\bar{x}, \mu_0) = 0$,

(ii) $Df(\bar{x}, \mu_0) = 0$,

(iii) $\frac{d^2}{dx^2} f(\bar{x}, \mu_0) \neq 0$,

(iv) $\frac{d}{d\mu} f(\bar{x}, \mu_0) \neq 0$.

Conditions (i) and (ii) of Theorem 2.5.1 imply that $\bar{x}$ is a non-hyperbolic equilibrium point of (2.13) for $\mu = \mu_0$. Condition (iii) implies that a unique curve of equilibrium points passes through $(x, \mu) = (\bar{x}, \mu_0)$, whereas (iv) implies that the curve lies locally on one side of $\mu = \mu_0$.

Example 2.5.1 *Consider the following normal form of* (2.13).

$$\dot{x} = \mu + x^2, \tag{2.14}$$

Then, the set of equilibrium points of (2.14) is given by $\mu + x^2 = 0$. Thus, there is either one ($\mu = 0$) or two ($\mu < 0$) or none ($\mu > 0$) equilibrium points of (2.14).

- If $\mu > 0$, then there is no equilibrium point at all since there is no x-nullclines.
- If $\mu = 0$, then equation (2.14) has only one equilibrium point at the origin, which is a saddle-node,
- If $\mu < 0$, then equation (2.14) has two equilibrium points, which are a node $-\sqrt{-\mu}$ and a saddle $\sqrt{-\mu}$. Note that in the particular example shown in Figure 2.2 (A) the node is stable, the bifurcation can also be such that the node is unstable.

It follows that, equation (2.14) changes from having no equilibrium points to having two equilibrium points when the parameter μ is decreased through $\mu = 0$. The system is said to have a bifurcation when $\mu = 0$ and that $\mu = 0$ is a bifurcation point. At the bifurcation point itself, there is a special kind of equilibrium, a saddle-node. The qualitative bifurcation diagram for this case is depicted in Figure 2.2 (A).

2.5.2 Transcritical bifurcation

A transcritical bifurcation occurs when a stable equilibrium and an unstable equilibrium collide, cross through each other and exchange stability as μ varies. This bifurcation is also called *exchange of stability* for the fact that the two equilibria exchange their stability at the bifurcation value μ_0.

Theorem 2.5.2 *[50]. If* (2.13) *has an equilibrium point at* $(x, \mu) = (\bar{x}, \mu_0)$. *Then* (2.13) *will undergo a transcritical bifurcation if the following conditions hold:*

(i) $f(\bar{x}, \mu_0) = 0$, *for all* $\mu_0 \in \mathbb{R}$,

(ii) $Df(\bar{x}, \mu_0) = 0$,

(iii) $\frac{d}{d\mu} f(\bar{x}, \mu_0) = 0$,

(iv) $\frac{d^2}{dxd\mu}f(\bar{x},\mu_0) \neq 0$,

(v) $\frac{d^2}{dx^2}f(\bar{x},\mu_0) \neq 0$,

Conditions (i) and (ii) Theorem 2.5.2 imply that $\bar{x}$ is a non-hyperbolic equilibrium point of (2.13) for $\mu = \mu_0$. All the conditions show that orbit structure near $(\bar{x},\mu_0)$ of (2.13) is qualitatively the same as orbit structure near $(\bar{x},\mu_0)$ of

$$\dot{x} = x(\mu \pm x).$$

The transcritical bifurcation is typical for systems where an equilibrium is present regardless of the values of the parameter.

Example 2.5.2 *For the normal form*

$$\dot{x} = x(\mu + x), \tag{2.15}$$

there is a transcritical bifurcation at $\mu = 0$. In this case, there is either one ($\mu = 0$) or two ($\mu < 0$) equilibrium points. When $\mu = 0$ the only equilibrium point is the origin and for $\mu < 0$ there are two equilibrium points given by 0 and $-\mu$. So it is easy to see that the origin is an equilibrium point for all μ. For $\mu < 0$ the nonzero equilibrium point is stable, but for $\mu > 0$ the nonzero equilibrium point becomes unstable. Thus the stability of this equilibrium point has switched from stable to unstable. See Figure 2.2 (B) for the bifurcation diagram.

2.5.3 Backward bifurcation

Backward bifurcation involves the existence of transcritical bifurcation when the basic reproduction number is equal to one ($\mathcal{R}_0 = 1$), resulting in the emergence of two subcritical endemic equilibria and a saddle-node bifurcation at $\mathcal{R}_0 = \mathcal{R}_0^c < 1$. The qualitative description of this bifurcation scenario is the following. In the neighborhood of 1, a stable disease-free equilibrium (DFE) coexists with two endemic equilibrium points (EEPs): a smaller equilibrium (with a smaller number of infective individuals) which is unstable and a larger one (with a larger number of infective individuals) which is stable. These two endemic equilibria disappear

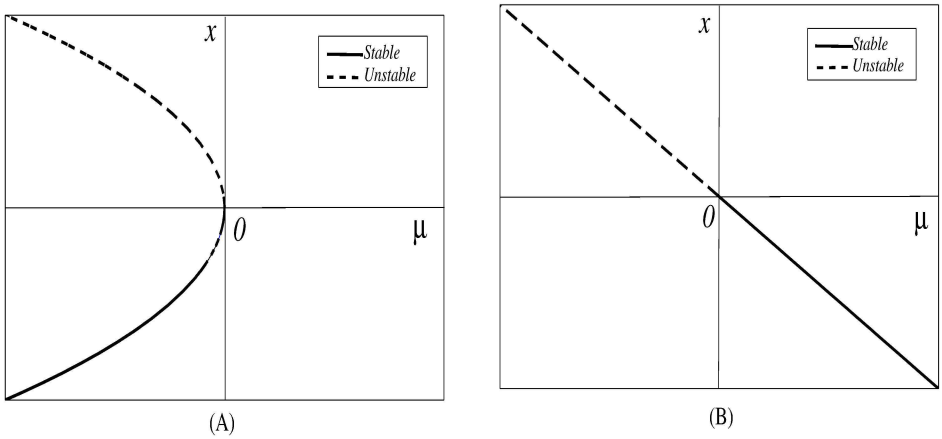

Figure 2.2: Bifurcation diagrams for (A) Saddle-Node and (B) Transcritical.

by a saddle-node bifurcation when $\mathcal{R}_0$ is reduced below the critical value $\mathcal{R}_0^c < 1$ [39].

For $\mathcal{R}_0 > 1$, however, there are only two equilibria: the unstable DFE and the stable EEP. In other words, the stable DFE and the unstable EEP exchange stability by transcritical (forward) bifurcation at $\mathcal{R}_0 = 1$. The bifurcation diagrams for these two types of bifurcation are depicted in Figure 2.3.

The existence of backward bifurcation in disease transmission models has an epidemiological implication for disease control. This is for the fact that if $\mathcal{R}_0$ is nearly below 1, then the disease control depends solely on the initial sizes of the infective sub-populations of the models. On the contrary, decreasing $\mathcal{R}_0$ below the critical value $\mathcal{R}_0^c$, results in effective disease eradication provided the disease-free equilibrium of the model is globally asymptotically stable. Hence, determining the sub-threshold $\mathcal{R}_0^c$ of the basic reproduction number results in effective disease control.

The phenomenon of backward bifurcation has been observed in various disease transmission models [28, 29, 34, 39, 40, 41, 42, 43, 44], such as those with sort of group structure, vaccination with an imperfect vaccine, and exogenous re-infection. Nonetheless, the mechanisms that cause backward bifurcation in disease transmission models are not fully identified (for detail explanation, see [41]).

However, the common causes of backward bifurcation in such models are the use of an imperfect vaccine and exogenous re-infection in the transmission dynamics of mycobacterium tuberculosis.

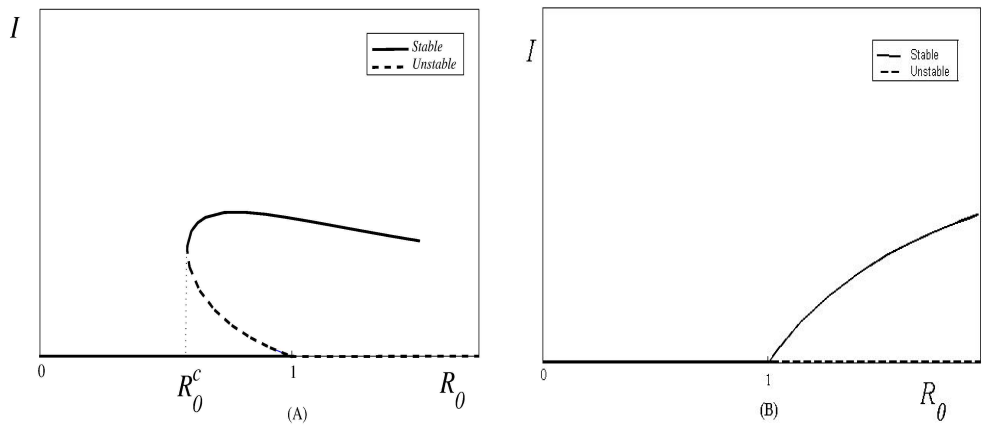

Figure 2.3: The (A) Backward bifurcation diagram and (B) Forward bifurcation diagram.

In the last decade, Hilker [16] identified a dynamic behavior similar to a backward bifurcation in an epidemiological model with Allee effect when the basic reproduction number is greater than unity. In the model with Allee effect, there is a transcritical bifurcation at $\mathcal{R}_0 = 1$, which can only be visualized by either plotting $\mathcal{R}_0$ against the total population or prevalence (not presented here for the basis of comparison). Moreover, a saddle-node bifurcation also occurs at $\mathcal{R}_0 = \mathcal{R}_0^c > 1$. In this case, the coexistence of a stable DFE with stable EEP arises when $\mathcal{R}_0 > 1$. The two equilibria coalesce and disappear by saddle-node bifurcation when $\mathcal{R}_0$ is increased above the critical value $\mathcal{R}_0^c > 1$. Similarly, for $\mathcal{R}_0 < 1$, a stable DFE coexists with unstable endemic equilibrium, which organizes the effective extinction threshold in the presence of the disease. Thus, the saddle-node bifurcation occurs beyond the disease invasion threshold $\mathcal{R}_0^u$ at $\mathcal{R}_0^c > 1$. The qualitative bifurcation diagram for the model with Allee effect is depicted in Figure 2.4 and the differences between models with backward bifurcation (BB) (epidemiological models without Allee effect) and models with Allee effect (AE) are given in Table

2.1.

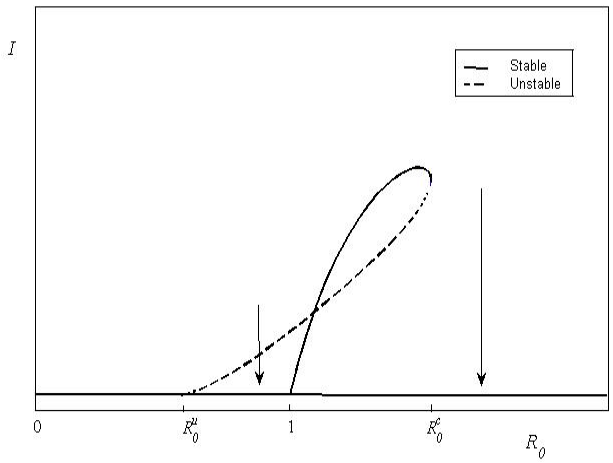

Figure 2.4: Backward bifurcation diagram for Allee effect model. The arrow indicates abrupt population collapse

2.6 Epidemiological Preliminaries

Generally speaking, disease control is related to some thresholds quantities, either in parameters or in population size. For instance, a disease may not be able to persist if the population is below some critical size or the fraction of immune individuals is above a certain level. Such thresholds can be characterized by the mean number of secondary infections a typical infective would produce in a susceptible host population, called the *basic reproduction number*, usually denoted by $\mathcal{R}_0$. Thus, $\mathcal{R}_0$ is a crucial quantity in epidemiological models, which is considered the determinant of disease persistence in a population. It is universally accepted that disease will spread if $\mathcal{R}_0 > 1$, and it will die out when $\mathcal{R}_0 < 1$. Moreover, population thresholds depend on transmission mechanisms of the disease. The most commonly assumed incidence (new infections per unit time) in disease modeling are: density-dependent (mass action) and frequency-dependent (also known

Table 2.1: Differences between models with BB and models with AE

Models with BB	**Models with AE**
(1) The disease can be endemic even if $\mathcal{R}_0 < 1$.	The disease can be endemic only for $\mathcal{R}_0 > 1$.
(2) The disease remains endemic in the host for all $\mathcal{R}_0 > 1$.	Both the disease and the host disappear when $\mathcal{R}_0 > \mathcal{R}_0^c$.
(3) The saddle-node bifurcation occurs before invasion threshold at $\mathcal{R}_0^c < 1$.	The saddle-node bifurcation takes place beyond the invasion threshold at $\mathcal{R}_0^c > 1$.
(4) Increasing $\mathcal{R}_0$ leads to emergence of the endemic equilibria. This is resulting in an abrupt explosion in infectives if $\mathcal{R}_0$ is increased above 1 and a sudden disease eradication if $\mathcal{R}_0$ is reduced below $\mathcal{R}_0^c$.	Increasing $\mathcal{R}_0$ leads to the disappearance of endemic equilibria, resulting for the abrupt population collapse.
(5) The bistability and endemic equilibria are induced by the characteristics of disease.	The bistability and endemic equilibria are due to the strong Allee effect.

as standard incidence or proportionate mixing). While the former assumes that the effective contact rate between susceptible and infected individuals increase linearly with population size, for the latter the number of contacts is independent of the population size. The choice of one of the two incidences over the other in a model for host-parasite dynamics depends on how the host population reacts to the disease impact [20]. The discussions on the appropriate form of incidence can be found in [22, 64, 65].

2.6.1 Incidence functions

Disease incidence is simply the number of new infections per unit time. Let $C(N)$ denote the number of effective contact rate (average number of contacts leading to

infection) per host per unit time in a host population of size or density N. Suppose p is the probability that the contact between susceptible host (S) and infected host (I) leads to infection. Then, $C(N)S$ is the rate of contacts made by all susceptible individuals and I/N is the probability that a susceptible individual actually makes a contact with infectious individual per unit time. Hence, the incidence is $pC(N)S(I/N)$, where $\lambda = pC(N)I/N$ is the force of infection. Thus, the number of new cases arising from all susceptible individuals is λS. If $C(N)$ is assumed to be proportional to N (i.e., $C(N) = CN$), then the resulting incidence λS is mass action. In contrast, assuming that $C(N)$ is a constant ($C(N) = C$) then λS is referred to as standard incidence [64, 66].

2.6.2 The basic reproduction number

The next generation method described earlier can be used to compute the basic reproduction number $\mathcal{R}_0$. This is achieved by finding the matrices F and V, for the infections and transition terms, respectively. Since F is nonnegative and V is a nonsingular M-matrix, V^{-1} is nonnegative [67], as is FV^{-1}. Following [57] and [58], the matrix FV^{-1} is defined as the next generation matrix for the model and set

$$\mathcal{R}_0 = \rho(FV^{-1}),$$

where $\rho(A)$ denotes the spectral radius of a matrix A. Then, by Theorem 2.2.4 the disease-free equilibrium of the model is locally asymptotically stable (LAS) if $\mathcal{R}_0 < 1$, and unstable when $\mathcal{R}_0 > 1$, but the positive endemic equilibrium exists and is LAS. In other words, the DFE and EEP exchange stability at $\mathcal{R}_0 = 1$, so that a transcritical bifurcation (forward bifurcation) occurs.

Example 2.6.1 *Consider the model for a homogeneously mixing population in Example 2.2.1.*

Then, the decomposition of $f(x)$ into the components $\mathcal{F}$ and $\mathcal{V}$ is as follows

$$\mathcal{F} = \begin{pmatrix} 0 \\ \beta x_1 \frac{y_2}{x} \\ 0 \\ 0 \end{pmatrix}, \quad \mathcal{V} = \begin{pmatrix} -\Lambda + \beta x_1 \frac{y_2}{x} + \mu x_1 \\ \beta x_1 \frac{y_2}{x} + (\alpha + \mu) y_1 \\ -\alpha y_1 + (\gamma + \mu) y_2 \\ -\gamma y_2 + \mu x_2 \end{pmatrix}.$$

The equilibrium solution when the infected compartments are empty ($y_1 = y_2 = 0$) is $x_0 = (\Lambda/\mu, 0, 0, 0)^T$. Then,

$$F = \begin{pmatrix} 0 & \beta \\ 0 & 0 \end{pmatrix}, \; V = \begin{pmatrix} \alpha + \mu & 0 \\ -\alpha & \gamma + \mu \end{pmatrix}$$

and

$$V^{-1} = \frac{1}{(\alpha + \mu)(\gamma + \mu)} \begin{pmatrix} \gamma + \mu & 0 \\ \alpha & \alpha + \mu \end{pmatrix},$$

Thus

$$\mathcal{R}_0 = \rho(FV^{-1}) = \frac{\alpha\beta}{(\alpha + \mu)(\gamma + \mu)}.$$

CHAPTER 3

Dynamics of SI epidemic with a demographic Allee effect

3.1 Introduction

In this chapter, the extended version of model (1.5) from Chapter 1 is presented. For the model (1.5) the birth rate and the death rate are assumed to be quadratic and linear functions (see Chapter 1, equation (1.4)) of the total population, respectively. More precisely, the fertility function is chosen based on mate limitation Allee mechanism and crowding effects with linearly decreasing offspring survival. The motivation behind the chosen mortality function is the density-dependent regulation induced by intraspecific competition. However, in the presented model, these demographic functions are both modeled as quadratic polynomials. This approach provides ample opportunity for taking into account the major contributors to the Allee effect given in Table 1.1.

In order to achieve this formulation, we chose as *per capita* growth rate function the one used in model (1.5). That is

$$G(N) = a(K_+ - N)(N - K_-),\ 0 < K_- \ll K_+, \tag{3.1}$$

where the strong Allee effect is manifested through the minimum viable density K_-. As usual, the parameter K_+ is referred as a carrying capacity and the coefficient $a > 0$ adjusts the maximum *per capita* growth rate. The decomposition of the growth rate into birth rate and death rate, $G(N) = B(N) - D(N)$, potentially can have a significant impact on epidemiological dynamics. The model presented in this chapter can be considered an extension of model (1.5) where the death rate is assumed linear. Using quadratic death rate and one additional parameter provides a more realistic representation of the population dynamics particularly at low population density or size. As this is a mortality rate in populations where there is a positive relationship between individual survival probability and population density due to factors like joint defence, cooperative feeding and/or breeding and lower exposure to predators. That is, the quadratic death rate effectively captures species' susceptibility variation due to the Allee effects. This follows from the fact that an Allee effect is more intense on some species than others [26, 68]. More precisely, species whose individuals benefit from the presence of conspecifics suffer heavy mortality when small because they rely on mass number and a strategy of predator dilution for survival.

The demographic functions $B(N)$ and $D(N)$ are represented in the following form

$$\begin{aligned} B(N) &= a\{-(1-\alpha)N^2 + [K_+ + (1-\beta)K_-]N + K_+\Gamma\}, \\ D(N) &= a(\alpha N^2 - \beta K_- N + K_+ K_- + K_+\Gamma), \end{aligned} \tag{3.2}$$

where α, β and Γ are real parameters. The parameter $\alpha \in [0, 1)$ determines the splitting of the quadratic term in (3.1) between the functions $B(N)$ and $D(N)$. Moreover, α and β determine the intensity of the Allee effects on both the demographic rate functions $B(P)$ and $D(P)$. As in [23], the parameter Γ determines the effect of density-independence of the demographic rate functions. The basic requirement that both demographic functions need to be nonnegative places some constraints on the values of β and Γ as follows:

The inequality $B(N) \geq 0$ holds provided

$$(1-\alpha)N - (K_+ + (1-\beta)K_-) \leq 0,$$

or equivalently

$$N \leq \frac{(1-\beta)K_- + K_+}{(1-\alpha)}.$$

Hence the model is applicable for population density $N \in [0, M)$, where

$$M = \frac{(1-\beta)K_- + K_+}{1-\alpha}. \tag{3.3}$$

We assume that $\beta < 1$ in order to ensure that $K_+ \in [0, M)$ for all $\alpha \in [0, 1)$. Indeed, if

$$\beta < 1 \tag{3.4}$$

we have

$$M = \frac{(1-\beta)K_- + K_+}{1-\alpha} > \frac{K_+}{1-\alpha} > K_+.$$

Further, the parameters of the model should be such that $D(N) \geq 0$. To prove this inequality, it suffices to show that the discriminant Δ of $D(N)$ is nonpositive. This follows from the following assumptions.

(A1) $K_- \leq \frac{1}{2}K_+$ (i.e. the minimum viable density is far from the carrying capacity),

(A2) $\beta \leq 2\sqrt{2\alpha}$ and $\Gamma \geq 0$.

Indeed, if (A1) and (A2) hold, we have

$$\begin{aligned} \Delta &= \beta^2 K_-^2 - 4\alpha K_+(K_- + \Gamma), \\ &\leq \beta^2 K_-^2 - 8\alpha K_-(K_- + \Gamma) \text{ by } (A1), \\ &= K_-^2(\beta^2 - 8\alpha) - 8\alpha K_-\Gamma \leq 0 \text{ by } (A2). \end{aligned} \tag{3.5}$$

Combining (3.4) and $(A2)$ leads us to the inequality

$$\beta \leq \min\{1, 2\sqrt{2\alpha}\}, \tag{3.6}$$

which we assume hereafter. To summarize under restriction (3.6) and $\Gamma \geq 0$ both demographic functions are nonnegative on the interval $[0, M]$. It should be noted that since $B(N)$ is a quadratic function with negative leading coefficient it cannot

be positive on an infinite interval. Therefore our aim is only to have it positive on a practically relevant interval. In this regard, let us remark that the interval $[0, M]$ contains all disease-free equilibrium states of the population. The decomposition of $G(N)$ in (3.1) into $B(N)$ and $D(N)$ given in (3.2) is intended to model the factors causing the Allee effect given in Table 1.1. More precisely, the steep gradient of $B(N)$ is when N is small. This reflects factors like improved access (e.g. *via* cooperative strategies) to abundant resources. For small populations $D(N)$ is either increasing at a slower rate ($\beta \leq 0$) or is decreasing ($\beta > 0$) representing what is referred to as safety in numbers (joint defence, lower individual exposure to predators, cooperation in raising the young). This allow us to basically divide all endangered species into two groups namely cooperative and non-cooperative. The mortality rate of cooperative species decreases ($\beta > 0$) when small because they need helpers for reproduction and/or survival. While the death rate of non-cooperative species increases when small because they do not need helpers for reproduction and/or survival. The graphs of the demographic functions given in (3.2) are depicted in Figure 3.1.

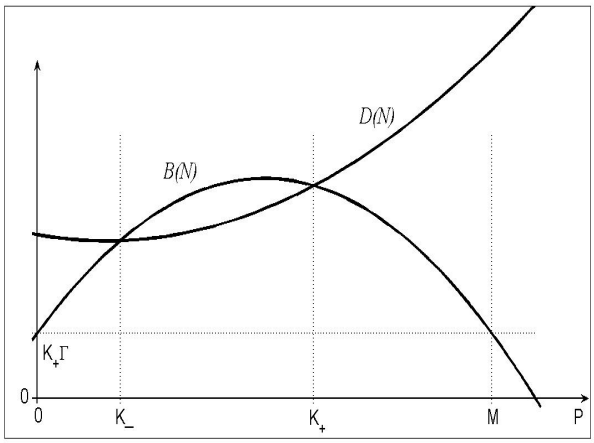

Figure 3.1: The demographic functions $B(N)$ and $D(N)$ for $\beta > 0$

The two graphs intersect at the unstable equilibrium K_{-}. This critical value

of N, a minimum survival level, is precisely the manifestation of the strong Allee effect. The graphs also intersect at the stable equilibrium K_+. When N is large, for example with values around K_+, the functions $B(N)$ and $D(N)$ exhibit the usual behavior of decreasing and increasing, respectively, due to adverse conditions caused by the larger population (food scarcity, stressful condition owing to a strong competition, rise in predator numbers).

As mentioned earlier, the demographic model presented in this chapter which is described in terms of the functions $B(N)$ and $D(N)$ in (3.2) extends model (1.5) (Chapter 1) by using quadratic functions for modeling both the birth and the death rates with the aim of providing more realistic modeling tool as explained above. Note that the demographic functions in Chapter 1, equation (1.4) are particular cases of those in (3.2) for $\alpha = 0$ and $\beta = -1/K_-$.

3.2 Model formulation

Let the host population density at time t be denoted by $N(t)$. The densities of susceptible and infected individuals when a disease divides the population into two parts are denoted by $S(t)$ and $I(t)$, respectively. The respective transfer rates are given on the flowchart depicted in Figure 3.2.

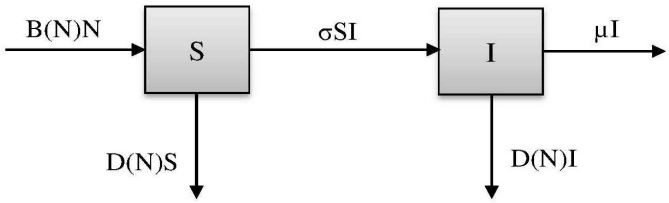

Figure 3.2: Schematic diagram of model (3.7)

We assume a density-dependent transmission, which is described by mass action rate σSI. There is no recovery from the disease and there is no vertical transmission (newborns of infected individuals move to the susceptible class). Thus,

the model equations are then described by the following system of differential equations:

$$\begin{aligned} \frac{dS}{dt} &= B(N)N - \sigma SI - D(N)S, \\ \frac{dI}{dt} &= \sigma SI - D(N)I - \mu I, \end{aligned} \tag{3.7}$$

where μ is an additional constant disease-related death rate assumed for infectious individuals. The birth rate $B(N)$ and the death rate $D(N)$ are given in (3.2).

To make the system (3.7) with (3.2) non-dimensional, we introduce the following dimensionless quantities as in [23]:

$$p = \frac{N}{K_+}, \quad i = \frac{I}{K_+}, \quad s = \frac{S}{K_+}, \quad u = \frac{K_-}{K_+} \in (0,1). \tag{3.8}$$

Using the first and the last relations in (3.8), we obtain the dimensionless forms of the *per capita* growth rate and the demographic functions presented in (3.1) and (3.2), respectively, as follows:

$$\begin{aligned} g(p) &= k(1-p)(p-u), \\ b(p) &= k\{-(1-\alpha)p^2 + [1+(1-\beta)u]p + \gamma\}, \\ d(p) &= k(\alpha p^2 - \beta up + u + \gamma), \end{aligned} \tag{3.9}$$

with $k = aK_+^2$, $\gamma = \Gamma/K_+$. It follows from (3.8) and (3.9) that, the equations of model (3.7) in the (p,i) phase plane become

$$\begin{aligned} \frac{dp}{dt} &= k(1-p)(p-u)p - \mu i, \\ \frac{di}{dt} &= [-\tau - kp(\alpha p - \beta u) + \lambda(p-i)]i, \end{aligned} \tag{3.10}$$

where $\lambda = K_+\sigma$, $\tau = \mu + k(u+\gamma)$. Furthermore, since N is considered in the practically relevant interval $[0, M]$, we have $p \in [0, m]$ where

$$m = \frac{M}{K_+} = \frac{1+(1-\beta)u}{1-\alpha}.$$

In the rest of this chapter, we will focus on the ecologically interesting case where the Allee threshold is far from the carrying capacity, i.e. $0 < u < \frac{1}{2}$.

3.3 Basic properties

3.3.1 Model (3.10) as a dynamical system.

Theorem 3.3.1 *The system of ordinary differential equations* (3.10) *defines a dynamical system in the domain*

$$\Omega = \{(p, i) : 0 \leq i \leq p \leq m\}.$$

Proof. We show first that all solutions of (3.10) initiated in Ω remain in Ω on the increasing interval of their existence. We consider the three line segments which make the boundary of Ω, see Figure 3.3.

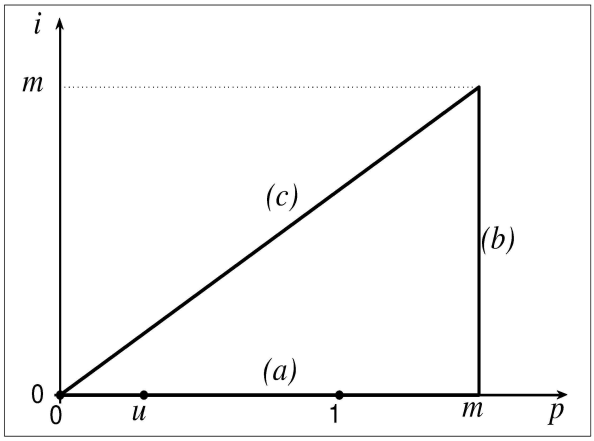

Figure 3.3: Domain Ω

(a) This line segment represents the disease-free state of the population. It is positively invariant and contains the three disease-free equilibria of the model.

(b) If $p = m$ one can see from the first equation of (3.10) that $dp/dt < 0$. Therefore the vector field defined by the system (3.10) is directed inwards at this segment.

(c) In order to prove that the vector field is directed inwards on this line segment we need to show that $dp/dt - di/dt > 0$. Let $i = p \in [0, m]$. Then

$$\begin{aligned}\frac{dp}{dt} - \frac{di}{dt} &= [k(1-p)(p-u)p - \mu p] - [-\tau - k(\alpha p^2 - \beta up)]p, \\ &= p(-kp^2 + kup + kp - ku - \mu + \tau + k\alpha p^2 - k\beta up), \\ &= kp\{-(1-\alpha)p^2 + [1 + (1-\beta)u]p + \gamma\}, \\ &= pb(p) > 0,\end{aligned}$$

which proves the required inequality.

Combining the results for the boundary segments (a), (b) and (c) we obtained that the solutions of (3.10) initiated in Ω do not leave this domain. Then using the fact that Ω is bounded, it follows from Theorem 2.1.4 that these solutions exist for $t \in [0, \infty)$. Hence (3.10) defines a dynamical system on Ω. ■

3.3.2 Threshold quantities

We introduce the critical host population density for disease establishment (the disease threshold) and the basic reproduction number, as in [23]. From the second equation of system (3.10) the replacement number of the disease is given by

$$\mathcal{R} = \mathcal{R}(p) = \frac{\lambda p}{\tau + k(\alpha p^2 - \beta up)}. \tag{3.11}$$

Notably, the replacement number is expressed as a function of p because the population size is variable. This threshold quantity $\mathcal{R}(p)$ is defined to be the average number of secondary infections produced by an infective individual during the entire infectious period [64]. It should be noted that some authors use the term reproduction number or ratio instead of replacement number as in [16, 23]. Since in the absence of the disease the population being above the Allee threshold will settle to its carrying capacity then setting $p = 1$ in equation (3.11) gives the basic reproduction number

$$\mathcal{R}_0 = \mathcal{R}(1) = \frac{\lambda}{\tau + k(\alpha - \beta u)}. \tag{3.12}$$

Note that $\tau + k(\alpha - \beta u) = \mu + ku(1-\beta) + k(\alpha+\gamma) > 0$ since $\beta \leq \min\{1, 2\sqrt{2\alpha}\}$.

For the disease threshold (also known as a critical community density or a critical host density), set $\mathcal{R} = 1$ in (3.11) and solve for p in the equation

$$k\alpha p^2 - (k\beta u + \lambda)p + \tau = \quad 0. \tag{3.13}$$

In the following analysis, we assume that $\alpha \neq 0$ so that equation (3.13) is a quadratic equation. We will see later that the results for model (1.5) can be obtained when $\alpha \to 0$. Note from equation (3.13) that

(i) there are two distinct real roots if $(k\beta u + \lambda)^2 > 4k\alpha\tau$,

(ii) there is one real root with multiplicity 2 if $(k\beta u + \lambda)^2 = 4k\alpha\tau$,

(iii) there is no real root if $(k\beta u + \lambda)^2 < 4k\alpha\tau$.

Denote by λ^* the threshold value of λ which discriminates between the three cases. Namely, $\lambda^* = 2\sqrt{k\alpha\tau} - k\beta u$ is such that (3.13) has two, one or zero real roots according as $\lambda > \lambda^*, \lambda = \lambda^*$ and $\lambda < \lambda^*$, respectively.

Note that $\lambda^* > 0$. Using the relation $\tau = \mu + k(u+\gamma) > ku$ and $\beta < 2\sqrt{2\alpha}$ we obtain

$$\begin{aligned}
\lambda^* =& 2\sqrt{k\alpha\tau} - k\beta u = 2\sqrt{k\alpha\tau} - \beta[\tau - (\mu + k\gamma)], \\
>& 2\sqrt{k^2\alpha u} - 2ku\sqrt{2\alpha}, \\
=& 2k\sqrt{2\alpha u}\left(\sqrt{\frac{1}{2}} - \sqrt{u}\right) > 0 \text{ since } u < 1/2.
\end{aligned}$$

It follows that, for $\lambda > \lambda^*$, equation (3.13) has the following two real roots.

$$(p_t)_{1,2} = \frac{(k\beta u + \lambda) \pm \sqrt{(k\beta u + \lambda)^2 - 4k\alpha\tau}}{2k\alpha\tau}. \tag{3.14}$$

Remark 3.3.1

(1) Note that, if $(\lambda + k\beta u) \leq 0$, then by the second equation of (3.10)

$$i(t) \to 0 \ \ as \ \ t \to \infty,$$

so that the infected population goes extinct. Hereafter, we assume that $(\lambda + k\beta u) > 0$.

(2) $\lambda > \lambda^*$ implies that $(\lambda + k\beta u) > 0$. Therefore, the roots $(p_t)_{1,2}$ are positive whenever they exists.

3.3.3 Existence and stability of equilibria

3.3.3.1 Disease-free equilibria

In the absence of the disease the steady states of system (3.10) are given by

(i) $\mathcal{E}_0 = (0, 0)$: the trivial extinction state,

(ii) $\mathcal{E}_1 = (u, 0)$: the Allee threshold state,

(iii) $\mathcal{E}_2 = (1, 0)$: the carrying capacity state.

It is obvious that $\mathcal{R}_0 \leq 1$ if and only if $\lambda + k\beta u - (\tau + k\alpha) \leq 0 \Rightarrow \lambda + k\beta u \leq 0$. The condition $\lambda + k\beta u \leq 0$ leads to the extinction of disease $i(t)$ of system (3.10) (see, Remark 3.3.1). Hence, the disease cannot establish itself from arbitrarily introductions into the host population at the carrying capacity whenever $\mathcal{R}_0 \leq 1$.

Theorem 3.3.2 *Model* (3.10) *has three disease-free equilibria* $\mathcal{E}_0, \mathcal{E}_1$ *and* $\mathcal{E}_2$. *Furthermore, each of the two equilibria* $\mathcal{E}_0$ *and* $\mathcal{E}_2$ *is a stable node, whereas* $\mathcal{E}_1$ *is a saddle point if* $\mathcal{R}_0 < 1$.

Proof. The Jacobian matrix of system (3.10) evaluated at a disease-free equilibrium $(p, 0)$, denoted by $J^\star(p, 0)$ is as follows:

$$J^\star(p,0) = \begin{pmatrix} -k[3p^2 - 2(1+u)p + u] & -\mu \\ 0 & A \end{pmatrix},$$

where $A = \lambda p - \tau - kp(\alpha p - \beta u)$. It follows that the trace and determinant of $J^\star(0, 0)$ are $tr(\mathcal{E}_0) = -(ku + \tau) < 0$ and $det(\mathcal{E}_0) = ku\tau > 0$, respectively. The eigenvalues of $J^\star(0, 0)$ have negative real parts and hence $\mathcal{E}_0$ is stable by Theorem 2.2.2. Moreover, $\mathcal{E}_0$ is a stable node since the eigenvalues $-\tau$ and $-ku$ are real and of negative sign. Similarly, the trace and determinant of the Jacobian matrix

$J^{\star}(1,0)$ evaluated at the disease-free equilibrium state $\mathcal{E}_2$ are, respectively, given by

$$\begin{aligned} tr[J(\mathcal{E}_2)] &= -\{k(1-u)+[\tau+k(\alpha-\beta u)](1-\mathcal{R}_0)\}, \\ &= -\{k(1-u)+\frac{\lambda}{\mathcal{R}_0}(1-\mathcal{R}_0)\} < 0 \text{ if } \mathcal{R}_0 < 1 \end{aligned}$$

and

$$\begin{aligned} det[J(\mathcal{E}_2)] &= k(1-u)[\tau+k(\alpha-\beta u)](1-\mathcal{R}_0), \\ &= \frac{k\lambda}{\mathcal{R}_0}(1-u)(1-\mathcal{R}_0) > 0 \text{ if } \mathcal{R}_0 < 1. \end{aligned}$$

Hence, $\mathcal{E}_2$ is a stable node since the eigenvalues of the Jacobian matrix $J(\mathcal{E}_2)$ are $-k(1-u)$ and $-\frac{\lambda}{\mathcal{R}_0}(1-\mathcal{R}_0)$, which are real and of negative sign whenever $\mathcal{R}_0 < 1$. Finally, the first eigenvalue of $J^{\star}(u,0)$ is $ku(1-u)$, which is positive since $0 < u < 1$ and the second eigenvalue is

$$-[\tau+ku^2(\alpha-\beta)]+\lambda u = -(\tau+ku^2\alpha)+u(\lambda+k\beta u),$$

which is negative if $\mathcal{R}_0 < 1$ since $(\lambda+k\beta u) \leq 0$. Therefore, $\mathcal{E}_1$ is a saddle point. ■

It can be deduced from Theorem 3.3.2 that if the host population is below the Allee threshold u, then the population goes extinct and it will survive otherwise. Thus, the dynamics of the system (3.10) is only determined by the Allee effect when $\mathcal{R}_0 < 1$ since the infectious agent could not establish itself from arbitrarily small introductions into the host population at carrying capacity. This leads to a bistable scenario in system (3.10).

3.3.3.2 Endemic equilibria

Endemic equilibrium of model (3.10) is the equilibrium point where the disease may persist in the population, that is when the infected compartment i is non empty. Hence, setting the right-hand side of (3.10) to zero, gives

$$\begin{aligned} i &= \frac{k}{\mu}(1-p)(p-u)p, \\ i &= \frac{1}{\lambda}[-\tau-k(\alpha p^2-\beta up)+\lambda p]. \end{aligned}$$

Then, we obtain the following cubic polynomial after equating and rearranging these equations.

$$Ap^3 + Bp^2 + Cp + D = 0, \tag{3.15}$$

where

$$A = -k, B = k\left[1 + u + \frac{\alpha\mu}{\lambda}\right], C = -\left[ku + \mu\left(\frac{k\beta u}{\lambda} - 1\right)\right], D = \tau.$$

Notice that A is negative, B and D are positive while C is negative or positive or zero. Therefore, there is at least one sign change in the sequence of coefficients $\{A, ..., D\}$. Hence, by Theorem 2.4.1, there is at least one positive real root of (3.15). Consequently, we obtain the following result.

Theorem 3.3.3 *If* $(p_t)_1 < 1$ *and* $(p_t)_2 > 1$ *then model* (3.10) *has:*

(i) a unique endemic equilibrium if $C \geq 0$;

(ii) a unique endemic equilibrium or three endemic equilibria if $C < 0$.

It should be noted that the results of Theorem 3.3.3 does not exclude the existence of two endemic states depending on the parameter values as in Figure 3.4. According to the first case of Theorem 3.3.3, it is possible for the model (3.10) to have a unique endemic equilibrium. Thus, we obtain the following results.

Theorem 3.3.4 *Let* $Q(p) = \frac{d}{dp}[k(1-p)(p-u)p]$. *If* $0 < u < (p_t)_1 < 1 < (p_t)_2$, *then model* (3.10) *has a unique endemic equilibrium point* $\mathcal{E}^* = (p^*, i^*)$ *with*

$$(p_t)_1 < p^* < 1, i^* > 0,$$

and $\mathcal{E}^*$ *is locally asymptotically stable if*

$$Q(p^*) < \frac{\lambda p^*}{\mathcal{R}(p^*)}[\mathcal{R}(p^*) - 1]. \tag{3.16}$$

Proof. It should be noted that $\mathcal{E}^*$ is an endemic equilibrium point with $i^* > 0$ if and only if $x = p^*$ is a zero of the function

$$\begin{aligned} q(x) &= kx(1-x)(x-u) - \frac{\mu}{\lambda}[\tau + k(\alpha x^2 - \beta u x)][\mathcal{R}(x) - 1] \\ &= kx(1-x)(x-u) - \mu x \frac{[\mathcal{R}(x) - 1]}{\mathcal{R}(x)}. \end{aligned}$$

This may occur only in the interval $(p_t)_1 < x < 1$. It can be verified that $q(1) < 0, q[(p_t)_1] > 0$ and $q''(x) < 0$ if $u < x < 1$. Thus, by Intermediate Value Theorem, $q(x)$ has precisely one zero $x = p^*$ in the interval $(p_t)_1 < x < 1$. But the slope of the i-nullcline is greater than that of the p-nullcline at $\mathcal{E}^*$, that is,

$$Q(p^*) < \frac{\mu}{\mathcal{R}(p^*)} \left\{ [\mathcal{R}(p^*) - 1] + \frac{p}{\mathcal{R}(p^*)} \frac{d}{dp}[\mathcal{R}(p^*)] \right\}. \tag{3.17}$$

The Jacobian matrix of system (3.10) at $\mathcal{E}^*$ is

$$J(\mathcal{E}^*) = \begin{pmatrix} Q(p^*) & -\mu \\ (\lambda - k(2\alpha p^* - \beta u))i^* & H_{i^*} \end{pmatrix},$$

where

$$\begin{aligned} H_{i^*} &= \frac{\lambda p^*}{\mathcal{R}(p^*)}[\mathcal{R}(p^*) - 1] - 2\lambda i^*, \\ i^* &= \frac{p^*}{\mathcal{R}(p^*)}[\mathcal{R}(p^*) - 1]. \end{aligned}$$

The trace and determinant of $J(\mathcal{E}^*)$ are respectively, given by

$$\begin{aligned} tr(\mathcal{E}^*) &= Q(p^*) + H_{i^*}, \\ &= Q(p^*) - \frac{\lambda p^*}{\mathcal{R}(p^*)}[\mathcal{R}(p^*) - 1] < 0, \end{aligned}$$

which is the inequality (3.16) and

$$\begin{aligned} det[J(\mathcal{E}^*)] =& Q(p^*)\{\frac{\lambda p^*}{\mathcal{R}(p^*)}[\mathcal{R}(p^*)-1]-2\lambda i\} \\ &+\frac{\mu}{\mathcal{R}(p^*)}\left\{[\mathcal{R}(p^*)-1]+\frac{p^*}{\mathcal{R}(p^*)}\frac{d}{dp}[\mathcal{R}(p^*)]\right\}i^*, \\ =&\frac{\lambda p^*}{\mathcal{R}(p^*)}[\mathcal{R}(p^*)-1] \\ &\times\left\{\frac{\mu}{\mathcal{R}(p^*)}\left([\mathcal{R}(p^*)-1]+\frac{p^*}{\mathcal{R}(p^*)}\frac{d}{dp}[\mathcal{R}(p^*)]\right)-Q(p^*)\right\}>0 \end{aligned}$$

only with inequality (3.17). Hence, the eigenvalues of $J(\mathcal{E}^*)$ have negative real parts. Thus, $\mathcal{E}^*$ is locally asymptotically stable by Theorem 2.2.2. ■

3.3.4 The effect of disease-induced mortality on the model

In order to explore the effect of disease related death on the stability results of model (3.10), we denote by λ_0, the denominator of the basic reproduction number $\mathcal{R}_0$. That is

$$\lambda_0 = \tau + k(\alpha - \beta u)$$

so that $\mathcal{R}_0 \leq 1$, if and only if $\lambda \leq \lambda_0$. Furthermore, the respective nontrivial nullclines of model (3.10) are represented as follows:

$$\begin{aligned} \Lambda_p : i = \phi_1(p) &:= \frac{k}{\mu}p(p-u)(1-p), \\ \Lambda_i : i = \phi_2(\lambda, p) &:= p - \frac{kp(\alpha p - \beta u)+\tau}{\lambda}. \end{aligned}$$

It is to be noted that $dp/dt = 0$ and $di/dt = 0$ on the curves Λ_p and Λ_i, respectively, and only Λ_i depends on the coefficient of the force of infection λ. Also, one can easily see that

$$\phi_2(\lambda, p) < p$$

and

$$\lim_{\lambda\to\infty}\phi_2(\lambda, p) = p.$$

The dynamical system (3.10) behaves in two essentially different ways depending on wether or not Λ_p intersects the line $i = p$. These two cases are distinguished below *via* the threshold value

$$\mu^* = \frac{k(1-u)^2}{4}$$

of the disease-induced mortality μ. This threshold value is obtained by using $i = p$ in the host nullcline Λ_p.

3.3.4.1 The model with low disease-induced mortality: $\mu < \mu^*$

For the case when $\lambda > \lambda_0$ the system (3.10) always has an equilibrium $\hat{\mathcal{E}}_2$ on the decreasing portion of Λ_p. Moreover, there may be a second equilibrium point $\hat{\mathcal{E}}_1$ on the increasing side of Λ_p.

Proposition 3.3.1 *Let $\lambda > \lambda_0$,*

(i) *then the endemic equilibrium $\hat{\mathcal{E}}_2$ is stable and attractive,*

(ii) *if the two endemic equilibria $\hat{\mathcal{E}}_1$ and $\hat{\mathcal{E}}_2$ exist, then $\hat{\mathcal{E}}_1$ is unstable (saddle point) and $\hat{\mathcal{E}}_2$ is stable and attractive. Therefore, for every $p \in (u, m]$ there exists $\delta > 0$ such that any solution of system (3.10) initiated at a point (p, i) with $i < \delta$ converges to $\hat{\mathcal{E}}_2$.*

This proposition simply asserts that if the population is above the minimum viable population, the disease will establish itself in the population. This is illustrated on Figure 3.4 (A) (one endemic equilibrium) and Figure 3.4 (B) (two endemic equilibria).

3.3.4.2 The model with high disease-induced mortality: $\mu > \mu^*$

In this case, for sufficiently large λ the graph of Λ_i is very close to the line $i = p$ so that Λ_i and Λ_p do not intersect. Denoting

$$\lambda_1 = \min\{\lambda : \phi_1(p) \leq \phi_2(\lambda, p)\}$$

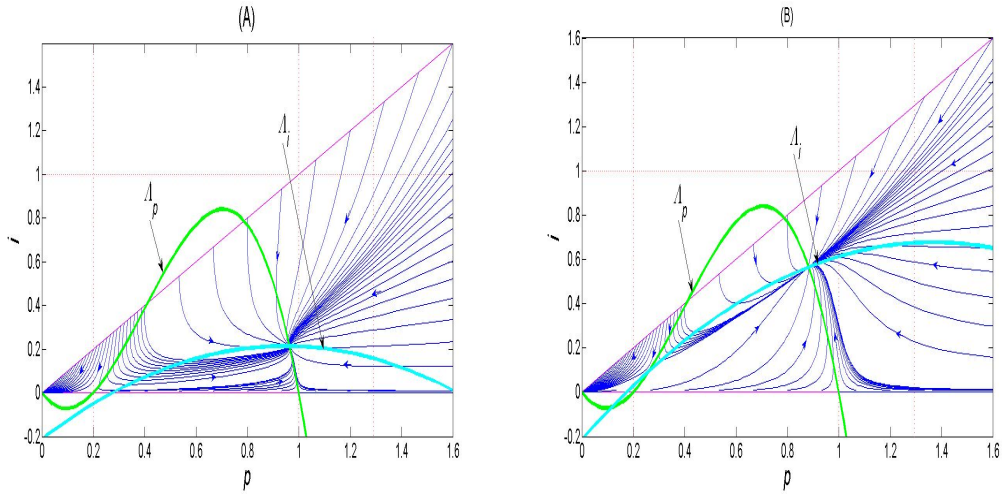

Figure 3.4: (A) Low disease induced mortality and unique endemic equilibrium; (B) Low disease induced mortality and two endemic equilibria. The green curve Λ_p is the p-nullcline and the cyan curve Λ_i is the i-nullcline. The diagonal magenta line is the line $p = i$. Parameter values used are: $\mu = 0.25, \gamma = 0.1, k = 2, u = 0.2, \alpha = 0.95, \lambda = 4$, and $\beta = -1, 3$, respectively.

and

$$\Omega_0 = \{(p, i) : i = 0\},$$

we obtain the following result.

Proposition 3.3.2 *If $\lambda > \lambda_1$ the only stable equilibrium of the dynamical system is the origin and its basin of attraction is $\Omega \setminus \Omega_0$.*

In simple terms, for $\lambda > \lambda_1$ the disease drive the host population to extinction (see Figure 3.5 (A)). On the other hand, when $\lambda \in (\lambda_0, \lambda_1)$ the disease can either persist endemically or drive the host population to extinction. That is, the eventual outcome (endemic state or extinction) depends on the host population size and the size of the initial number of infections. As λ decreases from λ_1 to λ_0 the dynamics presented in Figure 3.5 (B-D) can be observed.

Biologically, the results of propositions 1 and 2 follow from the fact that the maximum degree of depression of the host population equilibrium, here leading

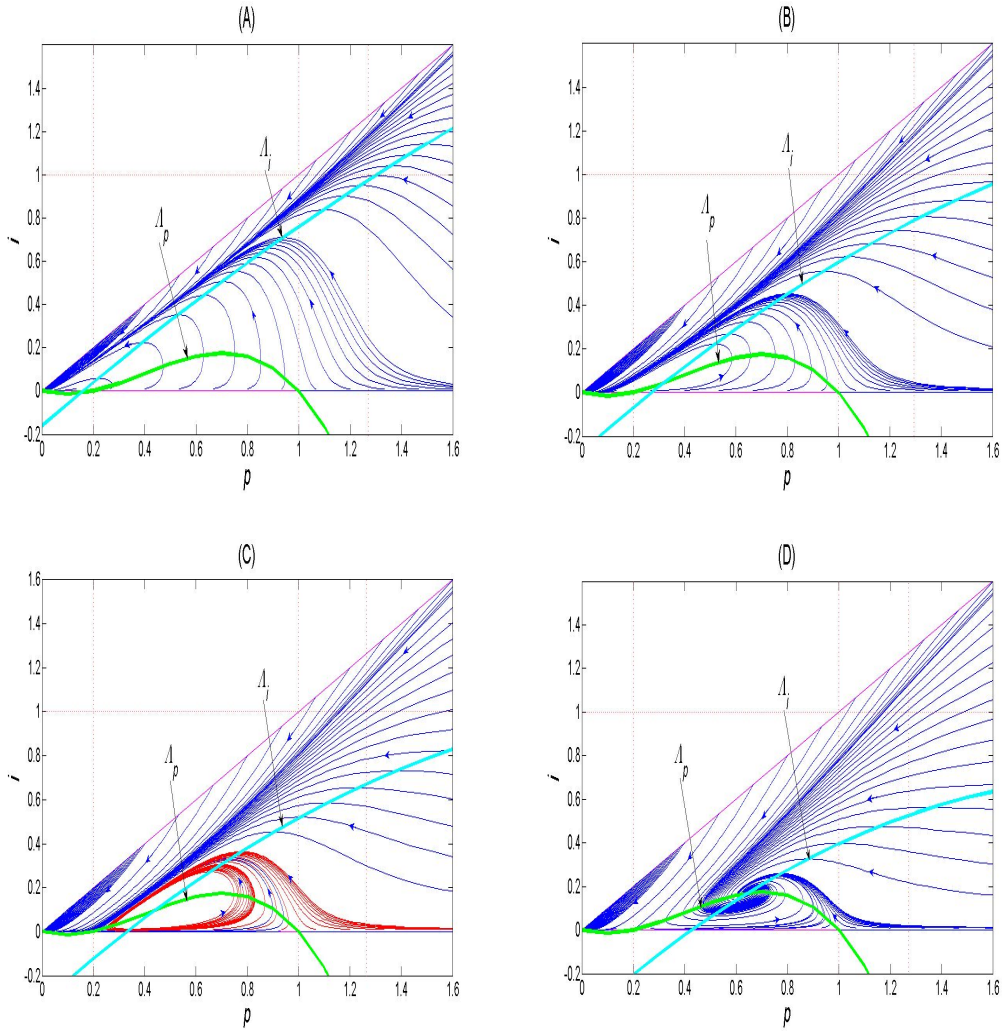

Figure 3.5: (A) Extinction: $\lambda > \lambda_1$; (B) Unique unstable endemic equilibrium; (C) Stable endemic limit cycles and (D) Stable Spiral point. The green curve Λ_p is the p-nullcline and the cyan curve Λ_i is the i-nullcline. The diagonal magenta line is the line $p = i$. Parameter values used are: $\mu = 0.6, \gamma = 0.01, k = 1, u = 0.2, \alpha = 0.5, \beta = 0.5$, and $\lambda = 2, 5, 3, 2.5$, respectively.

to extinction, is achieved by a disease with intermediate pathogenicity [69, 70]. If a disease pathogenicity is low ($\mu < \mu^*$), the disease has a little detrimental

effect on the host and so, the host persists at endemic state with large population density. On the other hand, if the disease pathogenicity is high, i.e. $\mu > \mu^*$ such that $\lambda \in (\lambda_0, \lambda_1)$, the infection can either be stably maintained in the population or drive the host to extinction depending on the initial sizes of the host and infected sub-populations owing to the strong Allee effect. Furthermore, if the disease pathogenicity is high ($\mu > \mu^*$) and $\lambda > \lambda_1$ then the disease drive the host population to extinction.

3.4 Special cases

In this section, we consider the dynamics of system (3.10) for the case when $\alpha = 0$ and $\beta \neq -\frac{1}{ku}$, which implies that the mortality function of system (3.10) becomes linear (i.e. different from the one in equation (1.4) of Chapter 1).

Case I: $\alpha = 0$ **and** $\beta \neq 0$

When $\alpha = 0$ and $\beta \neq -\frac{1}{ku}$, system (3.10) reduces to

$$\begin{aligned} \frac{dp}{dt} &= k(1-p)(p-u)p - \mu i, \\ \frac{di}{dt} &= [-\tau + (\lambda + k\beta u)p - \lambda i]i. \end{aligned} \tag{3.18}$$

The threshold quantities are obtained from (3.11), (3.12) and (3.13) by setting α to zero as follows: The replacement number reduces to

$$\mathcal{R} = \frac{\lambda p}{\tau - k\beta u p} \tag{3.19}$$

and the basic reproduction number becomes

$$\mathcal{R}_0 = \frac{\lambda}{\tau - k\beta u}. \tag{3.20}$$

For the disease threshold equation (3.13) reduces to a linear form so that

$$p_t = \frac{\tau}{\lambda + k\beta u}. \tag{3.21}$$

The threshold p_t is the point at which the linear infected nullcline crosses the horizontal axis (p-axis). Moreover, $0 < p_t < 1$ is equivalent to $\mathcal{R}_0 > 1$, and $p_t > 1$ is equivalent to $\mathcal{R}_0 < 1$.

Using a similar argument as for the threshold quantities, the results of Theorem 3.3.1, Theorem 3.3.2 and Theorem 3.3.3 follows. Furthermore, for $\alpha = 0$ and p_t as defined in (3.21), we obtain the following corollary.

Corollary 3.4.1 *Let* $Q(p) = \dfrac{d}{dp}[k(1-p)(p-u)p]$. *If* $0 < u < p_t < 1$, *then model* (3.18) *has a unique endemic equilibrium point* $\mathcal{E}^* = (p^*, i^*)$ *with*

$$p_t < p^* < 1, i^* > 0,$$

and $\mathcal{E}^*$ *is locally asymptotically stable if*

$$Q(p^*) < (\lambda + k\beta u)(p^* - p_t). \tag{3.22}$$

The proof follows easily from the proof of Theorem 3.3.4 for $\alpha = 0$.

It is worth mentioning here that, if $\alpha = 0$ and $\beta = -\frac{1}{ku}$, then model (3.10) reduces to model (1.5) in Chapter 1. Detailed analysis of model (1.5) can be found in [23, 24, 25].

Case II: $\alpha = \beta = 0$

For the case when $\alpha = \beta = 0$, model (3.10) reduces to

$$\begin{aligned} \frac{dp}{dt} &= k(1-p)(p-u)p - \mu i, \\ \frac{di}{dt} &= [-\tau + \lambda(p-i)]i. \end{aligned} \tag{3.23}$$

Using $\beta = 0$ in (3.19), (3.20) and (3.1) gives the following associated threshold quantities of model (3.23).

$$\mathcal{R}(p) = \frac{\lambda p}{\tau}, \tag{3.24}$$

$$\mathcal{R}_0 = \frac{\lambda}{\tau}, \tag{3.25}$$

and

$$p_t = \frac{\tau}{\lambda}. \tag{3.26}$$

In this case, Theorem 3.3.1 and Theorem 3.3.2 hold. For the endemic equilibria equation (3.15) becomes

$$Ap^3 + Bp^2 + Cp + D = 0, \tag{3.27}$$

where

$$A = -k, B = k(1+u), C = -(ku+\mu), D = \mu p_t,$$

so that A, C are negatives and B, D are positives. Then there are three sign changes in the sequence of coefficients of equation (3.27).

Corollary 3.4.2 *The model* (3.23) *has a unique endemic equilibrium or three endemic equilibria.*

If a unique endemic equilibrium exists, we have

Corollary 3.4.3 *Let* $Q(p) = \dfrac{d}{dp}[k(1-p)(p-u)p]$. *If* $0 < u < p_t < 1$, *then model* (3.18) *has a unique endemic equilibrium point* $\mathcal{E}^* = (p^*, i^*)$ *with*

$$p_t < p^* < 1, i^* > 0,$$

and $\mathcal{E}^*$ *is locally asymptotically stable if*

$$Q(p^*) < \lambda(p^* - p_t). \tag{3.28}$$

Setting $\alpha = \beta = 0$ in the proof of Theorem 3.3.4, gives the proof of corollary 3.4.3.

3.5 Persistence and Extinction

In this section, we state the conditions for persistence and extinction of the infected and host population of model (3.18) and model (3.23) using a similar approach in [24].

Before we state the conditions for persistence and extinction, we claim the following auxiliary results.

Lemma 3.5.1 *Let $0 < p_t < 1$. Then for any $0 < \rho_0 < 1 - u$, there exists a sufficiently small $\eta > 0$ and a function $t^0 = t^0[\rho, \rho_0, i(0)]$ such that if*

$$0 < i(0) < \rho \text{ and } u + \rho_0 < p(0) \leq 1,$$

then

$$i(t_1) = \rho \text{ for some } t_1 < t^0[\rho, \rho_0, i(0)].$$

Proof. Suppose

$$i(t) < \rho \quad for \quad all \quad t < t^{0*}. \tag{3.29}$$

Then we need to show that t^{0*} has a bound in terms of ρ, ρ_0, and $i(0)$. We claim that

$$p(t) > u + \rho_0 \quad for \quad all \quad t < t^{0*}. \tag{3.30}$$

Proof of the claim: If the assertion in (3.30) is not true, then there is a smallest $t = t_1$ such that $p(t_1) = u + \rho_0$, so that $\frac{dp(t_1)}{dt} \leq 0$. But by the first equation of (3.18) and inequalities (3.29) and (3.30)

$$\frac{dp}{dt} > k(1-p)(p-u)p - \mu\rho = k[1-(u+\rho_0)]\rho_0(u+\rho_0) > 0$$

at $t = t_1$ for

$$\rho < \frac{k[1-(u+\rho_0)]\rho_0(u+\rho_0)}{\mu},$$

which is a contradiction. Thus, inequality (3.30) holds.
We further claim that

$$\frac{dp}{dt} > 0 \text{ whenever } p(t) < 1 - \rho_1,$$

where $\rho_1 = v\rho$ and v is a positive constant such that $u + \rho_0 \leq 1 - \rho_1 \leq 1$. In fact, by the first equation of (3.18) and inequalities (3.29) and (3.30), at any time t_2 where $p(t_2) < 1 - \rho_1$, we have

$$\frac{dp}{dt} > k\rho_1\rho_0(u + \rho_0) - \mu\rho = \mu\rho$$

for

$$\rho_1 = \frac{2\mu\rho}{k\rho_0(u + \rho_0)} = v\rho.$$

It follows that,

$$p(t) > 1 - v\rho \;\; if \;\; t > t_1^0(\rho, \rho_0) \;\; for \;\; some \;\; t_1^0 = t_1^0(\rho, \rho_0). \tag{3.31}$$

Also, from the second equation of (3.18) and inequalities (3.29) and (3.31), we have

$$\begin{aligned}\frac{di(t)}{idt} &= -\tau + (\lambda + k\beta u)p - \lambda i, \\ &> -\tau + (\lambda + k\beta u)(1 - v\rho) - \lambda\rho, \\ &= \frac{1}{p_t}(1 - p_t)\tau - v_1\rho = \xi\tau - v_1\rho,\end{aligned}$$

where $t > t_1^0(\rho, \rho_0), \xi = \frac{1-p_t}{p_t} > 0$ and $v_1 > 0$ is a constant. Therefore,

$$i(t) > i[t_1^0(\rho, \rho_0)]e^{(1/2)\xi\tau[t - t_1^0(\rho,\rho_0)]} \;\; for \;\; \rho \leq \frac{1}{2v_1}\xi\tau.$$

Hence, $i(t_1) > \rho$ for some t_1, where

$$t_1 \leq t^{0*} \equiv t_1^0(\rho, \rho_0) + t_2^0(\rho, \rho_0, i[t_1^0(\rho, \rho_0)]). \tag{3.32}$$

It is to be noted that, $i[t_1^0(\rho, \rho_0)]$ depends on the initial condition $i(0)$, as such if $i(0) \to 0$, then $i[t_1^0(\rho, \rho_0)] \to 0$. Hence, the right-hand side of equation (3.32) is indeed a function t^0 of $\rho, \rho_0 \;\; and \;\; i(0)$ which approaches infinity as $i(0)$ approaches 0. ■

Lemma 3.5.2 *Let* $0 < p_t < 1$ *and*

$$i(t_a) = \rho, p(t_a) > u + \rho_0 \ \ for \ \ some \ \ \rho_0 \in (0, 1-u),$$

where, ρ *is a sufficiently small positive number depending on* ρ_0*. If* $i(t) \leq \rho$ *for* $t_a < t < t_b$*, then*

$$t_b - t_a < t^0(\rho, \rho_0).$$

Theorem 3.5.1 *If*

$$0 < u < p_t < 1 \tag{3.33}$$

and

$$\max_{u \leq x \leq p_t} \{k(1-x)(x-u)x\} > \frac{\mu(\lambda + k\beta u)}{\lambda}(1-p_t) \tag{3.34}$$

then for any solution $(p(t), i(t))$ *of* (3.18) *with* $p(0) > u + \rho_0$ *for some positive number* ρ_0*, there exists an* $\eta > 0$ *depending on* ρ_0 *and a time* $t^0 = t^0[\rho_0, i(0)]$ *such that*

$$i(t) \geq \eta \ \ for \ \ all \ \ t \geq t^0[\rho_0, i(0)]. \tag{3.35}$$

Proof. Considering Lemma 3.5.1, it suffices to show that $i(t)$ is bounded from below in the interval $t_a < t < t_b$, where $i(t) \leq \rho \ \ and \ \ t_a > 0$. Let (t_a, t_b) be a maximal interval for which $i(t) \leq \rho \ \ so \ \ that \ \ i(t_a) = \rho$ and then, $i(t) > \rho$ for some $t < t_a$. Suppose t_1 is the largest value of $t, t < t_1$ such that $i(t)$ is monotonically decreasing from $t_1 \ \ to \ \ t_a$. Then,

$$i(t) < i(t_1) \ \ for \ \ t_1 < t < t_a \tag{3.36}$$

and

$$\frac{di(t_1)}{dt} = 0,$$

or by the second equation of (3.18),

$$-\tau + (\lambda + k\beta u)p(t_1) - \lambda i(t_1) = 0. \tag{3.37}$$

Hence,

$$\lambda p(t_1) = p_t + \frac{\lambda}{\lambda + k\beta u} i(t_1) > p_t = u + \rho_1, \tag{3.38}$$

where $\rho_1 \equiv p_t - u > 0$.

Now, we claim that there exists $\rho_0^* \in (0, \rho_1)$ such that

$$p(t) > u + \rho_0^* \ \ for \ \ all \ \ t_1 < t \leq t_a. \tag{3.39}$$

In fact, since $p(t_1) > u + \rho_1 > u + \rho_0^*$, if the assertion (3.39) is not true, then there exists $t_1^* \in (t_1, t_a)$ such that

$$p(t) > u + \rho_0^* \ \ if \ \ t_1 < t < t_1^*, p(t_1^*) = u + \rho_0^*.$$

Thus,

$$\frac{dp(t_1^*)}{dt} \leq 0,$$

or by the first equation of (3.18), we have

$$k[1 - (u + \rho_0^*)]\rho_0^*(u + \rho_0^*) - \mu i(t_1^*) \leq 0$$

so that

$$i(t_1^*) \geq \frac{k}{\mu}[1 - (u + \rho_0^*)]\rho_0^*(u + \rho_0^*).$$

But, by inequality (3.36) and equation (3.37),

$$i(t_1^*) \leq i(t_1) = \frac{1}{\lambda}[(\lambda + k\beta u)p(t_1^*) - \tau] < \frac{1}{\lambda}[(\lambda + k\beta u) - \tau],$$

so that,

$$k[1 - (u + \rho_0^*)]\rho_0^*(u + \rho_0^*) < \frac{\mu}{\lambda}(\lambda + k\beta u)(1 - p_t).$$

Indeed, this is a contradiction to inequality (3.34) when ρ_0^* is chosen for $x = u + \rho_0^*$ to be the value at which the left-hand side of (3.34) attains the maximum. We infer that with this chosen value of ρ_0^*, (3.39) holds and specifically,

$$p(t_a) > u + \rho_0^*.$$

Therefore, by applying Lemma 3.5.2, we can now deduce that

$$t_b - t_a < t^0(\rho, \rho_0^*).$$

Considering the way ρ_0^* is determined, $t^0(\rho, \rho_0^*)$ may be taken as a function depending on ρ only (*i.e.* $t^0 = t^0(\rho)$). We also observe from the second equation of (3.18) that

$$\frac{di}{dt} \geq -ci \quad for \quad all \quad t > 0,$$

where $c > 0$ is a constant. Therefore,

$$i(t) \geq \rho e^{-c(t_b - t_a)} \geq \rho e^{-ct^0(\rho)} \equiv \eta \quad if \quad t_a < t < t_b.$$

Indeed, this estimate is true for any such interval $t_a < t < t_b$, where $i(t) \leq \rho \quad and \quad i(t_a) = \rho$. It follows that, $i(t) > \eta \quad if \quad t > t^0[\rho, \rho_0, i(0)]$ by combining this estimate and Lemma 3.5.1. ■

As mentioned earlier, in model (3.18), all the trajectories $(p(t), i(t))$ with $p(0) < u$ lead to the extinction of host population. But for $0 < p_t < 1$, Theorem 3.5.1 asserts that in the presence of disease infection, the host population size need to be larger than the Allee threshold, u in order to guarantee persistence of the infected population. That is, the Allee threshold is increased to $u + \rho_0$.

Remark 3.5.1

(i) If $g(x) = \frac{k}{\mu}(1-x)(x-u)x \quad and \quad x_c = \frac{1+u+\sqrt{(1+u)^2-3u}}{3}$, then (3.34) becomes

$$\begin{aligned} \frac{(\lambda + k\beta u)}{\lambda}(1 - p_t) &< \max_{u \leq x \leq p_t} g(x) \\ &= \begin{cases} g(p_t) & \text{if } u \leq p_t \leq x_c, \\ g(x_c) & \text{if } u < x_c < p_t. \end{cases} \end{aligned} \tag{3.40}$$

(ii) If $p_t \leq x_c$ as in the first case of (i), the inequality (3.34) becomes

$$k(p_t - u)p_t > \frac{\mu(\lambda + k\beta u)}{\lambda}. \tag{3.41}$$

We illustrate in Figure 3.6 that inequality (3.34) is satisfied whenever the maximum value of g, in the second case of (3.40), $g(x_c)$ is greater than $\frac{(\lambda+k\beta u)}{\lambda}(1-p_t)$, where $u < x_c < p_t$.

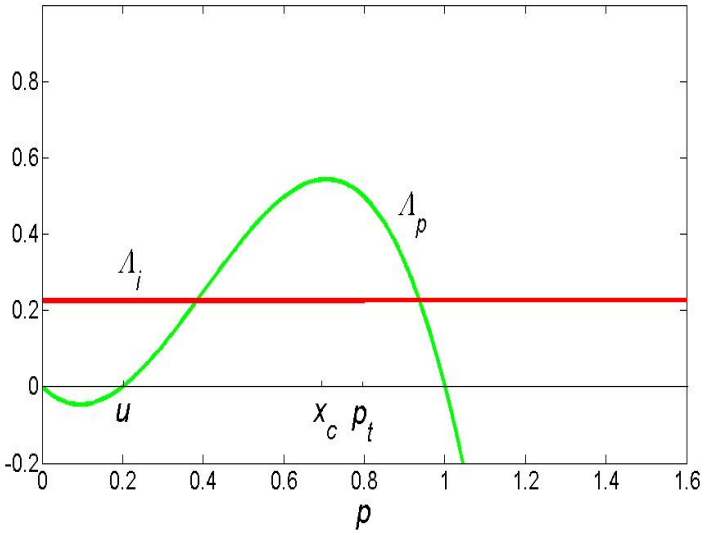

Figure 3.6: Inequality (3.34) holds where $u < x_c < p_t$ and the i-nullcline, $\Lambda_i = \frac{(\lambda+k\beta u)}{\lambda}(1-p_t)$, is below the maximum value of the p-nullcline, $\Lambda_p = \frac{k}{\mu}(1-p)(p-u)p$.

We observe that in model (3.18), it is possible for host population to go extinct with $0 < p_t < 1$ and $p(0) \geq u + \rho_0$. This can be seen when we consider $p_t < u$ instead of $p_t > u$ in (3.34). Hence, we obtain the following result.

Theorem 3.5.2 *If* $0 < p_t < u$ *and*

$$\max_{u \leq x \leq 1} \left\{ k(1-x)(x-u)x - \frac{\mu(\lambda + k\beta u)}{\lambda}(x - p_t) \right\} \leq \rho \tag{3.42}$$

for some small enough $\rho > 0$, then any solution of model (3.18) with $1 - \eta < p(0) \leq 1$ for any sufficiently small $\eta > 0$ and $i(0) > 0$ satisfies

$$p(t) \to 0 \text{ and } i(t) \to 0 \text{ as } t \to \infty.$$

Proof. Let Λ_i and Λ_p be the i- and p-nullclines of model (3.18) respectively. Define

$$\begin{aligned}
\Pi_1 =&\{(p,i) \in [0,\infty) \times [0,\infty) : i > 0, p_t < p < 1\},\\
\Pi_2 =&\{(p,i) \in [0,\infty) \times [0,\infty) : i = 0, 0 < p \leq p_t\},\\
\Pi_3 =&\{(p,i) \in [0,\infty) \times [0,\infty) : i > 0, u < p < 1\},\\
\Pi_4 =&\{(p,i) \in [0,\infty) \times [0,\infty) : i = 0, 0 < p \leq u\}.
\end{aligned}$$

We denote by Λ_i^+ the union of $\Lambda_i \cap \Pi_1$ and the interval, Π_2, that is

$$\Lambda_i^+ = (\Lambda_i \cap \Pi_1) \cup \Pi_2$$

and Λ_p^+ the union of $\Lambda_p \cap \Pi_3$ and the interval, Π_4, so that

$$\Lambda_p^+ = (\Lambda_p \cap \Pi_3) \cup \Pi_4.$$

Therefore,

$$\begin{aligned}
\frac{dp}{dt} > 0 \text{ below } \Lambda_p^+ \text{ and } \frac{dp}{dt} < 0 \text{ above } \Lambda_p^+,\\
\frac{di}{dt} > 0 \text{ below } \Lambda_i^+ \text{ and } \frac{di}{dt} < 0 \text{ above } \Lambda_i^+.
\end{aligned}$$

Considering condition (3.42), where

$$\max_{u \leq x \leq 1} \left\{ k(1-x)(x-u)x - \frac{\mu(\lambda + k\beta u)}{\lambda}(x - p_t) \right\} < 0$$

we have

$$\Lambda_i \cap \{(p,i) \in [0,\infty) \times [0,\infty) : i > 0\}$$

to be strictly above

$$\Lambda_p \cap \{(p,i) \in [0,\infty) \times [0,\infty) : i > 0\}.$$

Thus,

$$\frac{di}{dt} \geq \rho_1 \text{ below } \Lambda_p^+ \text{ and } \frac{dp}{dt} \leq -\rho_1 \text{ above } \Lambda_i^+, \text{ for some } \rho_1 > 0.$$

Hence, every trajectory of model (3.18) must cross Λ_i^+ at some time to enter the region above Λ_i^+ unless if it is initially above it. Then it remains there so that $p(t) \to 0$ and $i(t) \to 0$ as $t \to \infty$.

Consider now the case when equality holds in inequality (3.42) with $\rho = 0$. Then, Λ_p^+ and Λ_i^+ are tangent to each other with point of intersection $\omega = (p^*, i^*)$. The Jacobian matrix of (3.18) evaluated at ω

$$J(\omega) = \begin{pmatrix} Q(p) & -\mu \\ (\lambda + k\beta u)i^* & -\lambda i^* \end{pmatrix}$$

has eigenvalues 0 and $\frac{\mu(\lambda+k\beta u)}{\lambda} - \lambda i^*$. Therefore, ω is a single degenerate point (saddle), so that no trajectory $(p(t), i(t))$ which is above Λ_i^+ can converge to ω for some time $t = t_1$ as t approaches infinity.

It follows, as illustrated in Figure 3.7 that any trajectory $(p(t), i(t))$ with $(p(0), i(0)) = (1 - \eta_1, \eta_2)$ must cross Λ_p^+ and Λ_i^+, where $\eta_1 \geq 0$ is sufficiently small and $\eta_2 > 0$. Hence, $(p(t), i(t)) \to (0, 0)$ as $t \to \infty$ as in the first case considered above. Precisely, $p(t_\eta) < \frac{1}{2}u$ for some finite time t_η.

Furthermore, when ρ in condition (3.42) is small enough, the i-nullcline Λ_i intersects the p-nullcline Λ_p at two points ω_1 and ω_2 such that $|\omega_1 - \omega|$ and $|\omega_2 - \omega|$ are sufficiently small. Then, by continuity, the corresponding trajectory $(p^*(t), i^*(t))$ with $(p^*(0), i^*(0)) = (1 - \eta_1, \eta_2)$ satisfies $p^*(t_\eta) < u$, where $\eta_1 \geq 0$ is small enough and $\eta_2 > 0$. Hence, $p^*(t) \to 0$ as $t \to \infty$. ■

Inequality (3.42) holds whenever the p-nullcline, Λ_p, is below the i-nullcline, Λ_i, of system (3.18) (see Figure 3.8(A)). It is to be noted that, the assumption that ρ in condition (3.42) is small is necessary. As shown in Figure 3.8(B), for

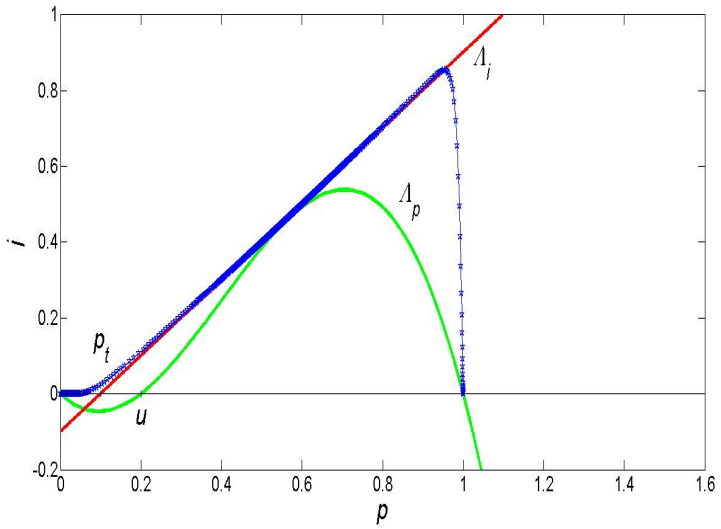

Figure 3.7: Phase plane of model (3.35) with Λ_i tangent to Λ_p and a solution (pentagrams) with initial condition (1, 0.0001) converges to (0, 0) as $t \to \infty$. Here, $k = 1.2, \mu = 0.232, \gamma = 1.27, u = 0.2, \beta = 0.07$ and $\lambda = 19.997$.

example, if the two nullclines intersect at two points ω_1 and ω_2 which are not sufficiently close, then the solution $(p(t), i(t))$ of model (3.18) converges to ω_2 as $t \to \infty$.

On the issue of persistence and extinction for model (3.23), Lemma 3.5.1 and Lemma 3.5.2 hold. But, Theorem 3.5.1 and Theorem 3.5.2, respectively become

Theorem 3.5.3 *If*

$$0 < u < p_t < 1 \tag{3.43}$$

and

$$\max_{u \le x \le p_t} \{k(1-x)(x-u)x\} > \mu(1-p_t) \tag{3.44}$$

then for any solution $(p(t), i(t))$ *of* (3.23) *with* $p(0) > u + \rho_0$ *for some positive number* ρ_0*, there exists an* $\eta > 0$ *depending on* ρ_0 *and a time* $t^0 = t^0[\rho_0, i(0)]$ *such*

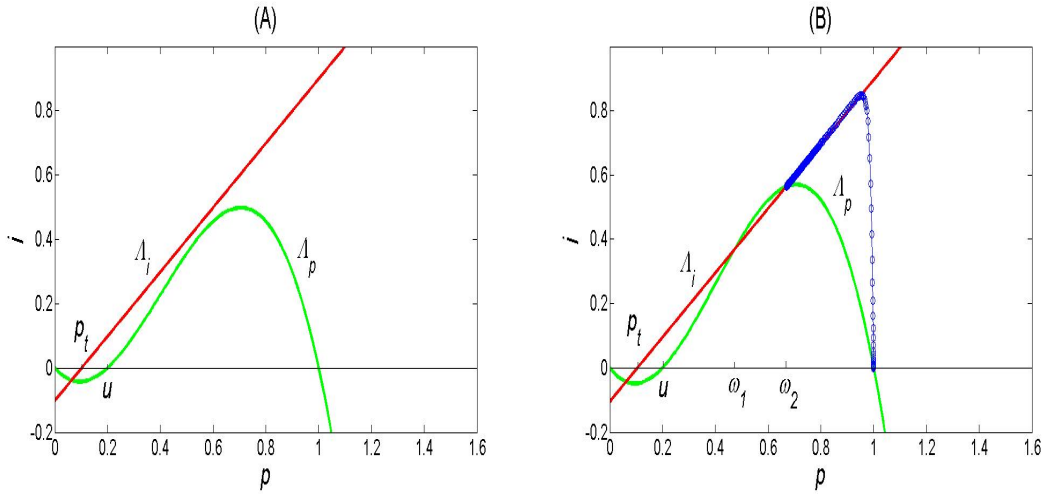

Figure 3.8: (A) Inequality (3.42) holds where $p_t < u < 1$ and the p-nullcline is below the i-nullcline; (B) Two interior positive equilibrium points of model (3.18) and a solution (pentagrams) with initial condition $(p, i) = (1, 0.0001)$ converges to an equilibrium point ω_2 as $t \to \infty$. Parameter values used $\gamma = 1.27, u = 0.2, \beta = 0.07$ and; (A) $k = 1.1, \mu = 0.232, \lambda = 17.997$; (B) $k = 1.2, \mu = 0.221$, and $\lambda = 18.797$.

that

$$i(t) \geq \eta \quad for \quad all \quad t \geq t^0[\rho_0, i(0)]. \tag{3.45}$$

Remark 3.5.2

(i) If $g(x) = \frac{k}{\mu}(1-x)(x-u)x$ *and* $x_c = \frac{1+u+\sqrt{(1+u)^2-3u}}{3}$, then (3.44) becomes

$$\begin{aligned}(1-p_t) &< \max_{u \leq x \leq p_t} g(x) \\ &= \begin{cases} g(p_t) & \text{if } u \leq p_t \leq x_c, \\ g(x_c) & \text{if } u < x_c < p_t. \end{cases}\end{aligned} \tag{3.46}$$

(ii) If $p_t \leq x_c$ as in the first case of (i), the inequality (3.44) becomes

$$k(p_t - u)p_t > \mu. \tag{3.47}$$

Theorem 3.5.4 *If* $0 < p_t < u$ *and*

$$\max_{u \le x \le 1} \{k(1-x)(x-u)x - \mu(1-p_t)\} \le \rho \tag{3.48}$$

for some small enough $\rho > 0$*, then any solution of model* (3.23) *with* $1-\eta < p(0) \le 1$ *for any sufficiently small* $\eta > 0$ *and* $i(0) > 0$ *satisfies*

$$p(t) \to 0 \text{ and } i(t) \to 0 \text{ as } t \to \infty.$$

The biological conclusion of the results of Theorems 3.5.2 and 3.5.4 is that the synergistic interplay between the Allee effect and infectious disease is death blow for the host population if the disease threshold p_t is low and the transmissibility λ is large. That is, the eventual outcome in such a situation is the extinction of the whole population.

3.5.1 Numerical simulations

Here, we will focus on the model parameters where a small number of individuals infected with a fatal disease cause the host population subject to the strong Allee effect in the vital dynamics with $p(0) = 1$, to persist or to go extinct. If extinction occurs for no matter how small the initial number of the infected individuals, $i(0)$ is, then the model parameters are in the *host extinction phase*; otherwise they are said to be in the *host persistence phase* [24].

According to Theorem 3.5.1, when $0 < p_t < 1$, under conditions (3.33) and (3.34), if $p(0) > u + \rho_0$ for some $\rho_0 > 0$ ($p(0) = 1$, in particular), the inequality (3.35) holds for any small number of infected individuals $i(0)$. Hence, (u, λ) is a point of persistence of the infected population and also of the host population by Theorem 3.3.1. If $0 < p_t < \min\{u, 1\}$ and inequality (3.42) holds, then by Theorem 3.5.2, (u, λ) is a point of host extinction.

For illustration, in Figure 3.9, we vary the Allee threshold, u and the transmissibility, λ, keeping all other parameters fixed, see Table 3.1 for the parameter values.

Define

(1) The curve $\Lambda_1 : \lambda = \lambda_1(u)$ by setting p_t to 1 in (3.21).

Table 3.1: Parameter values

Parameter	Nominal value	Reference
k	0.2	[23, 24]
γ	1.25 (scaled by k to 0.25)	[23, 24]
μ	0.1	[23, 24]
u	(0, 0.5)	[23, 24]
β	-0.6	Assumed

(2) The curve $\Lambda_2 : \lambda = \lambda_2(u)$ by setting p_t to u in (3.21).

(3) The curve $\Lambda_3 : \lambda = \lambda_3(u)$ such that with $\lambda = \lambda_3(u)$, equality holds in inequality (3.34). Then inequality (3.34) holds if $\lambda > \lambda_3(u)$.

(4) The curve $\Lambda_4 : \lambda = \lambda_4(u)$, such that with $\lambda = \lambda_4(u)$, equality holds in inequality (3.42). Then inequality (3.42) holds if $\lambda > \lambda_4(u)$.

By the assertion of Theorem 3.5.1, the region between Λ_3 and Λ_2 is a region of persistence of the infected population. The region $\lambda > \lambda_4(u) + \epsilon$ for some $\epsilon > 0$ is a region of host population extinction as asserted by Theorem 3.5.2. Points of disease population persistence or extinction may either be points in the regions between Λ_1 and Λ_3 and between Λ_2 and Λ_4. In Figure 3.9 (A), simulations depict points of host population persistence with no infected individuals (tildes), points of disease persistence (stars), and points of host population extinction (open circles).

For system (3.23), we define the curves Λ_1 and Λ_2 by replacing equation (3.21) with equation (3.26). The curves Λ_3 and Λ_4 are defined respectively, by replacing inequalities (3.34) and (3.42) with inequalities (3.44) and (3.48). Then, we have in Figure 3.9 (B), numerical simulations similar to that of system (3.18).

It should be noted that, if $\alpha = 0$ and $\beta = -\frac{1}{ku}$, then model (3.10) reduces to model (1.5) with $\lambda > 1$, see simulations in Figure 3.9 (C) and compare with Figure 5 in [24].

One can observe from Figure 3.9 that it is possible for the model parameters to shift from host population persistence phase to host population extinction phase

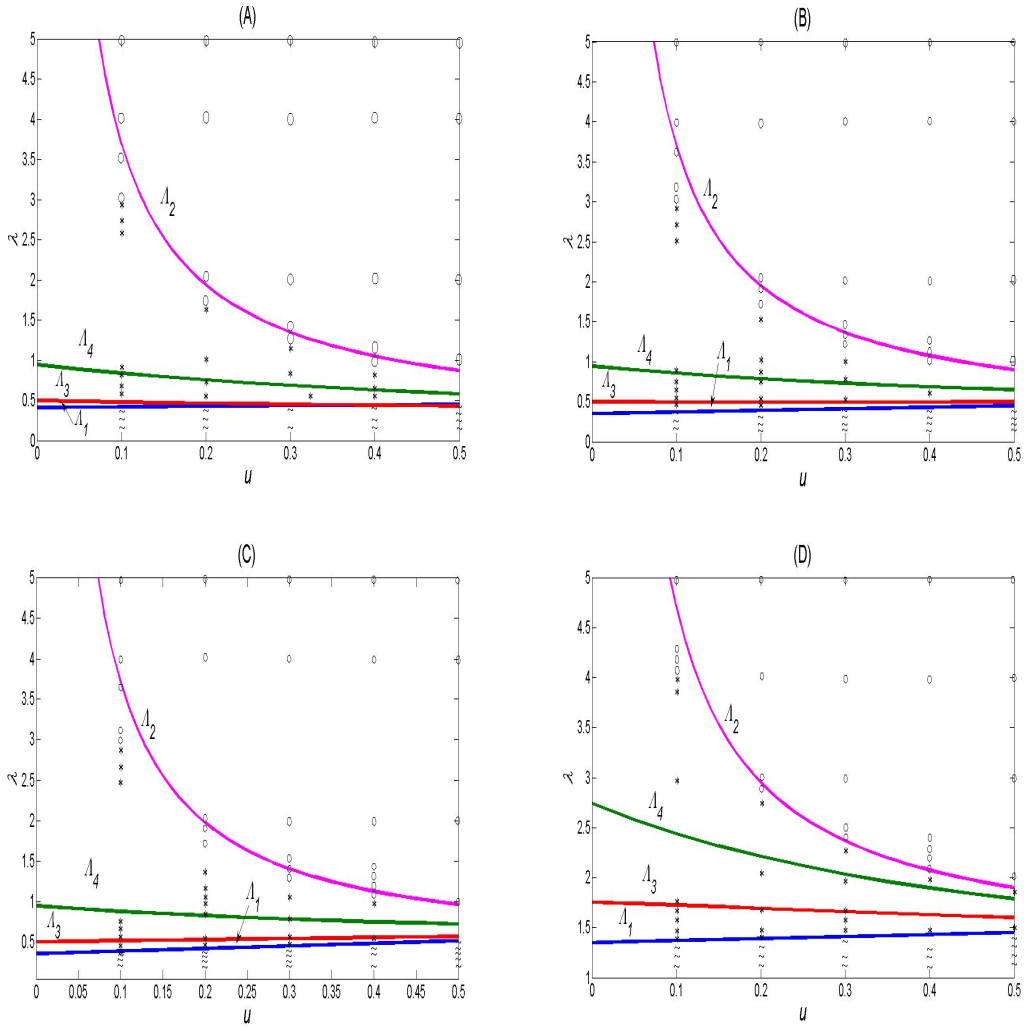

Figure 3.9: Region of disease extinction (host persistence) is denoted by 'tildes', region of disease persistence is denoted by 'stars', and region of host extinction is denoted by 'open circles' in (u, λ)-plane with initial condition $(p, i) = (1, 0.0001)$. (A) $\alpha = 0, \beta = 0.6, \lambda > 0$; (B) $\alpha = \beta = 0, \lambda > 0$; (C) $\alpha = 0, \beta = -0.6, \lambda > 0$; (D) $\alpha = 0, \beta = -\frac{1}{ku}$ and the values of other parameters are as stated in Table 1.

if we increase the transmissibility λ and the Allee threshold u, respectively, while

the values of all the other parameters are fixed. Moreover, it can also be seen that the regions for persistence and extinction vary in size with altering value of β, noting that Figure 3.9 (A-D) are drawn with $\beta = 0.6, 0, -0.6$, and $-\frac{1}{ku}$, respectively, and the same set of values of all the other parameters.

3.6 Summary

The Allee effect and infectious disease are some of the extinction drivers that recently received considerable attention in the extinction research. Their joint interplay have long been recognized to drive host population to extinction. An SI model with a strong Allee effect in which the vital dynamics (birth and death) are both modeled as quadratic polynomials is designed and analyzed in this chapter. This approach provides ample opportunity for taking into account the major contributors to the Allee effect. The main results of this chapter include the following:

(1) The model has bistable disease-free equilibria namely: the trivial extinction state $\mathcal{E}_0$ and the carrying capacity state $\mathcal{E}_2$, which are both stable nodes whenever the basic reproduction number $\mathcal{R}_0$ is below one. The biological interpretation of this result is that the presence of a strong Allee effect in host demographics plays a preventive and stabilizing role in relations to the invasion of disease;

(2) For $\mathcal{R}_0 > 1$, the model can have a locally asymptotically stable endemic equilibrium $\mathcal{E}^*$.

(3) The model suggests that additional disease related mortality increases the likelihood of population extinction. In fact, the host and/or disease persistence and extinction are characterized by a threshold value μ^* of the disease-induced death rate μ and two threshold values (λ_0, λ_1) of the transmissibility λ:

   (i) for $\mu < \mu^*$ and $\lambda > \lambda_0$ the disease will invade the population provided the host population is above the Allee threshold u (Proposition 3.3.1, Figure 3.4);

(ii) if $\mu > \mu^*$ and $\lambda > \lambda_1$ the disease drive host population to extinction and when $\lambda \in (\lambda_0, \lambda_1)$ the disease can either persist endemically or drive the host population to extinction (Proposition 3.3.1, Figure 3.5).

(4) For the special cases of the model, verifiable conditions that guarantee host persistence (with or without infected individuals) and extinction are derived. The extinction scenario shows that a small perturbation to the disease-free equilibrium can lead to the catastrophic extinction of the host population in the presence of a strong Allee effect.

(5) Numerical simulations show how the parameter β affects the dynamics of the model as the sizes of the persistence and extinction regions of the host population vary with altering value of β. This testify that the Allee effect is more intense on some species than others.

(6) It is proved that there is an effective increase in the Allee threshold u when a fatal disease invades the host population whose demographics are manifested with a strong Allee effect.

CHAPTER 4

Dynamical behavior of an epidemiological model with a demographic Allee effect

4.1 Introduction

While Chapter 3 is primarily concerned with providing ample opportunity for taking into account major contributors to Allee effect by modeling both demographic functions as quadratic polynomials, this Chapter focuses on bifurcation behavior of an extended version of model (3.7). We extend the SI model analyzed in Chapter 3 by adding a compartment of exposed individuals and considering frequency-dependent incidence instead of density-dependent transmission.

In recent years, a number of authors reported that models with Allee effect in the host demographics exhibit complex dynamics such as periodic oscillation, multiple stable steady states, and a series of bifurcations. Such bifurcations include sub- and super-critical bifurcations, Bogdanov-Takens bifurcation etc. (see for instance, [20, 23, 25]). In a similar note, the model developed by Hilker [16] seems to be the first account of the presence of another type of bifurcation behavior in an epidemiological model with a demographic Allee effect similar to the backward bifurcation discussed in Section 2.5.3 of Chapter 2. The author

explored the differences between bifurcation behaviors in epidemiological models without Allee effect that exhibit backward bifurcations and the epidemiological model with the Allee effect as given in Table 2.1 of Chapter 2. It is highlighted in [16] that another saddle-node bifurcation is possible in the Allee effect model, resulting in the re-emergence of two endemic equilibria since highly pathogenic parasites cause their own extinction but not that of their host. In addition, the author noted that the second saddle-node bifurcation might not be detected by any computer software such as MatCont [71], AUTO [72] or XPPAUT [73].

In conservation biology, one of the primary goals is to understand the ecological mechanisms that make some species more prone than others to population decline and extinction [74, 75]. Such information play relevant role for guiding management actions as it would allow biologists to predict the vulnerability of species to extinction even before they decline, thereby improving the species' chances of survival [74]. There is an evidence that some species are more vulnerable to extinction than others [76]. More precisely, the Allee effect is to be more likely to occur when individuals benefit from the presence of conspecifics [1, 26]. Some species, however, suffer heavy mortality at low population because they rely on mass numbers and a strategy of predator dilution for survival [77]. In light of this, we deduce that the mortality rate of species whose individuals benefit from the presence of conspecifics decreases when small, whereas the mortality rate of those whose individuals do not benefit from the presence of conspecifics increases in such a situation. As discussed in Chapter 3, when $\beta > 0$ the mortality rate decreases, while it increases if $\beta \leq 0$ for small population.

It can be observed that the definition of the Allee effect as given in the introductory part of Chapter 1, refers to low population levels. However, whether or not the mechanisms responsible for the Allee effect at low density or small population size affect the dynamics of a population at high density or large population size need to be investigated. The main purpose of this chapter is to investigate the combined impact of the Allee effect and infectious disease at high population level and to determine which species are more vulnerable to extinction than others under such a situation.

4.2 Model formulation

Let $N(t)$ be the host total population size at time t. This population is subdivided into three disjoint compartments of individuals that are susceptible ($S(t)$), exposed (have been infected but are not yet infectious) ($E(t)$) and infectious ($I(t)$), so that $N(t) = S(t) + E(t) + I(t)$. The respective transfer rates are given on the flow diagram depicted in Figure 4.1.

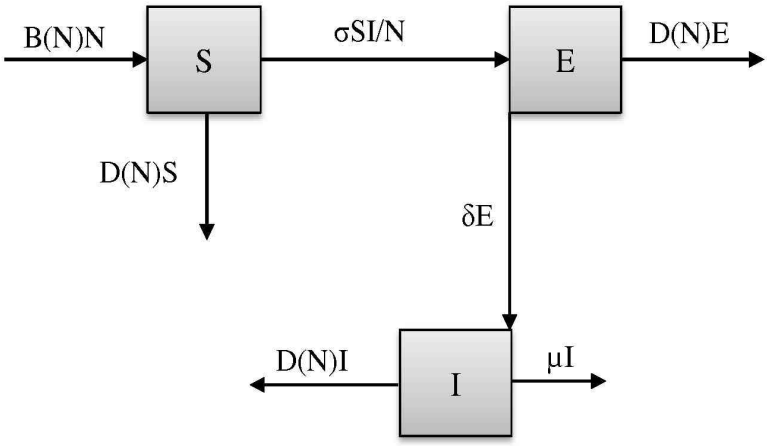

Figure 4.1: Schematic diagram of model (4.1)

We assume that the force of infection is given by standard incidence (frequency-dependent transmission) and there is no vertical transmission. The dynamics obey the following system of ordinary differential equations:

$$\begin{aligned}
\frac{dS}{dt} &= B(N)N - \sigma\frac{SI}{N} - D(N)S,\\
\frac{dE}{dt} &= \sigma\frac{SI}{N} - [\delta + D(N)]E,\\
\frac{dI}{dt} &= \delta E - [\mu + D(N)]I,\\
\frac{dN}{dt} &= G(N)N - \mu I,
\end{aligned} \tag{4.1}$$

where the parameter σ is the effective contact rate, δ is the rate at which exposed individuals become infected. It is assumed that infected individuals suffer additional disease induced mortality at a rate μ. The density-dependent demographic functions $B(N)$ and $D(N)$ are obtained by splitting a *per capita* growth rate, $G(N)$ in which a strong Allee effect is manifested. More precisely, we assume that $G(N) = B(N) - D(N)$ satisfies the following assumptions.

(A1) $G(N)$ is increasing on the interval $[0, N_{max}]$ and decreasing for $N > N_{max}$ so that G has a unique maximum at N_{max},

(A2) The equation $G(N) = 0$ has two positive roots K_- and K_+, such that $0 < K_- < N_{max} < K_+ < M$, where M is as defined in (3.3) of Chapter 3.

From (A1) and (A2) we obtain that $G(N) > 0$ for $N \in (K_-, K_+)$. Therefore (denoting $' = \frac{d}{dN}$)

(B1) $B(N) > D(N)$ for $N \in (K_-, K_+)$ with $B(K_+) = D(K_+)$ and $B'(K_+) < D'(K_+)$,

(B2) $B(N) < D(N)$ for $N \in [0, K_-) \cup (K_+, M)$ with $B(K_-) = D(K_-)$ and $B'(K_-) > D'(K_-)$.

In order to make system (4.1) non-dimensional, we re-scale the variables of the model (4.1) by

$$s = \frac{S}{N}, e = \frac{E}{N}, i = \frac{I}{N} \text{ and } p = \frac{N}{K_+}$$

so that $s + e + i = 1$ and system (4.1) becomes

$$\begin{aligned} \frac{dp}{dt} &= [g(p) - \mu i]p, \\ \frac{de}{dt} &= \sigma(1-i)i - [\delta + b(p) + (\sigma - \mu)i]e, \\ \frac{di}{dt} &= \delta e - [b(p) + \mu(1-i)]i, \end{aligned} \tag{4.2}$$

where $g(p)$ and $b(p)$ are the dimensionless forms of $G(N)$ and $B(N)$ respectively. More precisely, we have $g(p) = G(pK_+)$ and $b(p) = B(pK_+)$. Then the assumptions (A1) and (A2) imply that on $[0, m], m = \frac{M}{K_+}$, $g(p)$ has two positive roots $u = \frac{K_-}{K_+} \in (0, 1)$ and 1 with a unique maximum between the roots.

4.3 Basic properties

4.3.1 Model (4.2) as a dynamical system

Theorem 4.3.1 *The system of differential equations* (4.2) *defines a dynamical system in the domain*

$$\Omega = \{(p, e, i) \in \mathbb{R}^3_+ : 0 \leq p \leq m, 0 \leq e, i, e + i \leq 1\}.$$

Proof. We need to show that all solutions of (4.2) initiated in Ω do not leave Ω. Then the statement of the theorem follows from the boundedness of Ω, see Theorem 2.1.4. The region Ω is a triangular prism in the (p, e, i)-space. It is easy to see that the line $e = i = 0$ and the plane $p = 0$ are invariant sets of system (4.2). Then it remains to show that the vector field defined via the right hand side of (4.2) is directed inwards at the remaining part of the boundary of Ω. Since this involves standard arguments we will show it only for one face of the prism Ω, namely $e + i = 1, e, i \geq 0, 0 \leq p \leq m$. The outward normal vector to this face is $(0, 1, 1)$. Therefore it is sufficient to show that $\frac{de}{dt} + \frac{di}{dt} < 0$. We have

$$\begin{aligned}\frac{de}{dt} + \frac{di}{dt} &= \sigma(1 - i)i - [b(p) + (\sigma - \mu)i]e - [b(p) + \mu(1 - i)]i,\\ &= (\sigma - \mu)[1 - (e + i)]i - b(p)(e + i),\\ &= -b(p) < 0.\end{aligned}$$

It follows that the solutions of (4.2) initiated in Ω do not leave this region. Using the fact that Ω is bounded then these solutions exist for $t \in [0, \infty)$. Therefore (4.2) defines a dynamical system on Ω. ■

4.3.2 Threshold quantities

There are two well known ways of a disease control for disease transmission models with varying population size (i.e. a population with increasing or decreasing total size) due to demographic effects [45, 78]. The first way requires that the proportion $i(t)$ of infectives goes to zero, whereas the second requirement is that the absolute number $I(t)$ of infectives approaches to zero. These notions of disease elimination

were given and discussed in some detail in [78]. Thus, the conditions for the linear stability of disease free equilibria and for the existence and stability of endemic proportion equilibria are required. The pertinent threshold parameters are as follows

$$\mathcal{R} = \mathcal{R}(p) = \frac{\delta\sigma}{[\delta + b(p)][\mu + b(p)]}, \tag{4.3}$$

from which, we have

$$\mathcal{R}_0 = \mathcal{R}(1),\ \mathcal{R}_u = \mathcal{R}(u),\ \text{and}\ \mathcal{R}_e = \mathcal{R}(0),$$

according as the population is at its carrying capacity ($p = 1$), minimum survival level ($p = u$) or extinction state ($p = 0$), respectively.

It is important to note that the demographic functions $b(p)$ and $d(p)$ are equal at the carrying capacity state and Allee threshold state. Thus, the threshold parameters $\mathcal{R}_0$ and $\mathcal{R}_u$, are equivalently represented as

$$\mathcal{R}_0 = \frac{\delta\sigma}{[\delta + d(1)][\mu + d(1)]},\quad \mathcal{R}_u = \frac{\delta\sigma}{[\delta + d(u)][\mu + d(u)]}. \tag{4.4}$$

The other threshold parameter at the population extinction state ($p = 0$), is as follows

$$\mathcal{R}_e^* = \frac{\sigma\delta}{[\mu + b(0)][\delta + b(0)] + \{[\sigma - \mu][\mu + \delta + b(0)]/\mu - b(0)\}[b(0) - d(0)]}. \tag{4.5}$$

It is instructive to remark that the threshold parameters $\mathcal{R}$ and $\mathcal{R}_0$ represent the usual replacement and reproduction numbers, respectively, that appear in disease transmission models. The distinction between the two threshold quantities can be found in [64].

4.3.3 Equilibria and their stability

4.3.3.1 Disease-free equilibria

In the absence of the disease, model (4.2) has the following equilibrium points.

(i) $\mathcal{E}_0 = (0, 0, 0)$: trivial extinction state,

(ii) $\mathcal{E}_1 = (u, 0, 0)$: Allee threshold state, and

(iii) $\mathcal{E}_2 = (1, 0, 0)$: carrying capacity state.

Obviously, $\mathcal{R}_0 \leq 1$ if and only if $\delta(\sigma - \mu) - b(1)[\mu + \delta + b(1)] \leq 0 \Rightarrow \sigma - \mu \leq 0$. The condition $\sigma - \mu \leq 0$ leads to the extinction of disease $i(t)$ of system (4.2). Therefore, the disease cannot invade from arbitrarily small introductions into the host population at carrying capacity whenever $\mathcal{R}_0 \leq 1$. Then, we obtain the following results.

Theorem 4.3.2 *Model* (4.2) *has three disease free equilibria:* $\mathcal{E}_0, \mathcal{E}_1$ *and* $\mathcal{E}_2$. *The equilibrium* $\mathcal{E}_0$ *is a stable node if* $\mathcal{R}_e^* < 1$ *and is a saddle point if* $\mathcal{R}_e^* > 1$. *The equilibrium* $\mathcal{E}_2$ *is also a stable node if* $\mathcal{R}_0 < 1$ *and is a saddle point if* $\mathcal{R}_0 > 1$. *The Allee threshold equilibrium* $\mathcal{E}_1$ *is always a saddle point.*

Proof. The Jacobian matrix, denoted by $J^*(p, 0, 0)$ evaluated around a disease-free equilibrium $(p, 0, 0)$ of system (4.2) is given by

$$J_{df}(p, 0, 0) = \begin{pmatrix} g'(p)p + g(p) & 0 & -\mu p \\ 0 & -[\delta + b(p)] & \sigma \\ 0 & \delta & -[\mu + b(p)] \end{pmatrix}.$$

It follows that the matrix $J_{df}(\mathcal{E}_0)$ has eigenvalues $\lambda_1 = b(0) - d(0) < 0$ since $p < u$ and the eigenvalues of the matrix obtained by deleting the first row and column of $J_{df}(\mathcal{E}_0)$, denoted by $J_{df}^*(\mathcal{E}_0)$. Then, the trace and determinant of $J_{df}^*(\mathcal{E}_0)$ are, respectively, given by

$$\text{tr}(J_{df}^*(\mathcal{E}_0)) = -[\mu + \delta + 2b(0)] < 0$$

and

$$\det(J_{df}^*(\mathcal{E}_0)) = [\mu + b(0)][\delta + b(0)] - \delta\sigma \gtrless 0,$$

since $\mathcal{R}_e^* < 1$ if $\delta\sigma \leq [\mu + b(0)][\delta + b(0)]$ and $\mathcal{R}_e^* > 1$ when $\delta\sigma > [\mu + b(0)][\delta + b(0)]$. Furthermore, the corresponding eigenvalues of $J_{df}^*(\mathcal{E}_0)$ are:

$$\lambda_{2,3} = \frac{1}{2}\{-([\mu + b(0)] + [\delta + b(0)]) \pm \sqrt{([\mu + b(0)] - [\delta + b(0)])^2 + 4\delta\sigma}\},$$

which are distinct real and of either negative sign if $\mathcal{R}_e^* < 1$ or opposite sign when $\mathcal{R}_e^* > 1$. Hence, the trivial extinction state $\mathcal{E}_0$ is a stable node whenever $\mathcal{R}_e^* < 1$ and a saddle point otherwise.

For $p = 1$ the first eigenvalue of $J_{df}(\mathcal{E}_2)$ is $\lambda_1 = [b'(1) - d'(1)] < 0$ by (B1). Then, by simply replacing $b(0)$ with $b(1)$ in the above arguments for $J_{df}^*(\mathcal{E}_0)$, one can verify that the carrying capacity state $\mathcal{E}_2$ is also a stable node if $\mathcal{R}_0 < 1$ and a saddle point when $\mathcal{R}_0 > 1$.

Using a similar argument as in the case when $p = 0$ and $p = 1$, the first eigenvalue of $J_{df}(\mathcal{E}_1)$ is $\lambda_1 = [b'(u) - d'(u)]u > 0$ by (B2) and the other two eigenvalues are distinct real and of either negative sign when $\mathcal{R}_0 < 1$ or opposite sign if $\mathcal{R}_0 > 1$. Therefore, the Allee threshold state is always a saddle point. ■

4.3.4 Non-trivial equilibria

The steady states of model (4.2) where at least one of the infected compartment of the model is non-empty are called non-trivial equilibria. These equilibrium points can be obtained by setting the right-hand sides of system (4.2) to zero and solving for the resulting algebraic equations. Thus, setting the right-hand sides of model (4.2) to zero, we obtain

$$p = 0 \text{ or } i = \frac{g(p)}{\mu},\ e = \frac{\sigma(1-i)i}{\delta + b(p) + (\sigma - \mu)i},\ e = \frac{\mu(1-i) + b(p)}{\delta} i, \tag{4.6}$$

thus i satisfies $f(i) = 0$, where

$$\begin{aligned} f(i) =& \mu(\sigma - \mu)i^2 - \{(\sigma - \mu)[\mu + \delta + b(p)] - \mu b(p)\}i \\ &+ [\mu + b(p)][\delta + b(p)](\mathcal{R} - 1). \end{aligned} \tag{4.7}$$

For the non-trivial equilibria to be biologically feasible, we require that $g(p) > 0$ since $g(p) < 0$ for $p \in (0, u) \cup (1, m)$ by (B2) and $\delta + b(p) + (\sigma - \mu)i > 0$ (i.e. $\sigma > \mu$). The second condition also applies to the semi-trivial equilibrium. Conditions for the existence and biological feasibility of the semi-trivial and non-trivial equilibria are presented in the following Lemma.

Lemma 4.3.1 *Model* (4.2) *has*

(i) *a semi-trivial equilibrium* $\mathcal{E}_s = (0, e, i)$ *if* $\mathcal{R}_e > 1$,

(ii) *non-trivial equilibria if* $p \in (u, 1)$ *and* $\mathcal{R}_0 > 1$.

Proof. (i) Let $\mathcal{R}_e > 1 \Rightarrow (\sigma - \mu) > \frac{\mu b(0)}{\delta}$ (i.e. $(\sigma - \mu) > 0$). Then it follows from (4.7) that $f(0) > 0$, and $f(1) = -\{2\mu + [(\sigma - \mu) + \delta + b(0)]b(0)\} < 0$. Therefore, $f(i)$ has a root $i_1 \in (0, 1)$, and a second root $i_2 > 1$. This implies from the last equation of (4.6) that $e \geq 0$. Furthermore, setting the right-hand sides of the second and third equations of (4.2) to zero, adding and simplifying gives

$$b(0)i + [\sigma i + b(0)]e = \{(\sigma - \mu)(1 - i) + \mu e\}i. \tag{4.8}$$

The left-hand side of (4.8) is positive and $\sigma > \mu$. Hence, $i \in (0, 1)$ and this completes the existence proof.
The proof of (ii) follows from the proof of (i) by replacing $\mathcal{R}_e$ with $\mathcal{R}_0$ and $p = 0$ with $p \in (u, 1)$ such that $\mathcal{R}_0 > 1$. ■

Remark 4.3.1

The steady state solutions satisfy the following inequality (noting that $f(0) > 0$ and $f(1) < 0$)

$$i < \frac{[\sigma - \mu][\mu + \delta + b(p)] - \mu b(p)}{2\mu[\sigma - \mu]}.$$

The above results (Lemma 4.3.1) assert that the semi-trivial equilibrium exists if and only if $\mathcal{R}_e > 1$, while the non-trivial equilibrium exists if and only if $\mathcal{R}_0 > 1$. The condition $\mathcal{R}_0 > 1$ implies that $\mathcal{R}_u > 1$ (noting that the denominator of $\mathcal{R}_u$ is less than the denominator of $\mathcal{R}_0$). These existence conditions of endemic stationary state is similar to the finding in [16].

4.3.4.1 Semi-trivial equilibrium

A semi-trivial equilibrium is a steady state of the model (4.2) where the disease exterminates the host population. Let $\mathcal{E}_s = (p_s, e_s, i_s)$ be such equilibrium point of system (4.2). Then from equations (4.6) and (4.7), we have

$$p_s = 0, \; e_s = \frac{\mu(1 - i_s) + b(0)}{\delta} i_s, \tag{4.9}$$

and i_s solves

$$\frac{\sigma\delta(1-i_s)}{[\mu(1-i_s)+b(0)][\delta+(\sigma-\mu)i_s+b(0)]}=1, \tag{4.10}$$

which is obtained by equating the last two expressions for e in (4.6).

Theorem 4.3.3 *The semi-trivial extinction state ($\mathcal{E}_s$) of the model* (4.2) *is locally asymptotically stable if and only if $\mathcal{R}_e^* > 1$ and unstable otherwise.*

Proof. The local stability of the equilibrium solution $\mathcal{E}_s$ can be determined by linearizing the system (4.2) around $\mathcal{E}_s$. This gives the following Jacobian matrix

$$J(\mathcal{E}_s)=\begin{pmatrix} b(0)-d(0)-\mu i_s & 0 & 0 \\ -b'(0)e_s & -\kappa_1 & \kappa_2 \\ -b'(0)i_s & \delta & -[\mu+b(0)-2\mu i_s] \end{pmatrix},$$

where $\kappa_1=\delta+b(0)+(\sigma-\mu)i_s, \kappa_2=-\sigma i_s+\sigma(1-i_s)-(\sigma-\mu)e_s$.
The matrix $J(\mathcal{E}_s)$ has eigenvalues $\lambda_1=b(0)-d(0)-\mu i_s$, and the eigenvalues of the matrix $J_0(\mathcal{E}_s)$ that is obtained by deleting the first row and column of $J(\mathcal{E}_s)$. The trace and determinant of $J_0(\mathcal{E}_s)$, are as follows

$$tr[J_0(\mathcal{E}_s)]=-[\mu+\delta+2b(0)+(\sigma-\mu)i_s]$$

and

$$det[J_0(\mathcal{E}_s)]=[\delta+b(0)+(\sigma-\mu)i_s][\mu+b(0)-2\mu i_s]-\delta[\sigma(1-i_s)-(\sigma-\mu)e_s].$$

Substituting for e_s and $\delta\sigma(1-i_s)$ from (4.9) and (4.10), respectively, we obtain

$$\begin{aligned} det[J_0(\mathcal{E}_s)] &= [\delta+b(0)+(\sigma-\mu)i_s][\mu+b(0)-2\mu i_s]+(\sigma-\mu)[\mu(1-i_s)+b(0)]i_s \\ &\quad +\delta\sigma i_s-[\mu(1-i_s)+b(0)][\delta+b(0)+(\sigma-\mu)i_s], \\ &= \{(\sigma-\mu)[\mu+\delta+b(0)-2\mu i_s]-\mu b(0)\}i_s. \end{aligned}$$

Using that $\sigma-\mu>0$ from Lemma 4.3.1 and the inequality in Remark 1, we have $tr[J_0(\mathcal{E}_s)]<0$ and $det[J_0(\mathcal{E}_s)]>0$. Thus, the eigenvalues of the matrix $J_0(\mathcal{E}_s)$ have negative real parts. Then, it remain to show that $\mu i_s > b(0)-d(0)$. If $b(0)-d(0)>\mu$ then $\mathcal{E}_s$ is unstable, and direct substitution in $\mathcal{R}_e^*$ defined in

equation (4.5) implies that $\mathcal{R}_e^* < 1$. Now, $\mathcal{R}_e^* > 1$ implies from equation (4.7) that $f([b(0) - d(0)]/\mu) > 0$. This requires either $b(0) - d(0) > \mu$ or $\mu i_s > b(0) - d(0)$, but the first possibility has been ruled out. Conversely, $\mathcal{R}_e^* < 1$ implies that $f([b(0) - d(0)]/\mu) < 0$ and $\mu i_s < b(0) - d(0)$. Therefore, $\mu i_s > b(0) - d(0)$ if and only if $\mathcal{R}_e^* > 1$ so that $\lambda_1 < 0$. Hence, the eigenvalues of the matrix $J(\mathcal{E}_s)$ have negative real parts. It follows from Theorem 2.2.2 that $\mathcal{E}_s$ is locally asymptotically stable if and only if $\mathcal{R}_e^* > 1$. ■

It is worth mentioning here that the trivial extinction is solely driven by the Allee effect whereas a semi-trivial extinction occurs as a result of disease infection. However, if the host population goes extinct ($p \to 0$), the fraction of exposed and infected individuals within the disappearing population can either be positive or zero, depending on whether the exposed and infected individuals decay more slowly or more quickly than the host. It should be noted that the semi-trivial equilibrium coincides with the trivial equilibrium whenever expressed in either (N, E, I) or (S, E, I) state variables [16].

4.3.4.2 Endemic equilibria

It follows from Lemma 4.3.1 that if $\mathcal{R}_0 > 1$ and $p \in (u, 1)$, then model (5.2) has non-trivial equilibria. Then, for $p^* \in (u, 1)$ at endemic state, we have from (5.3) that

$$e^* = \frac{\mu(1 - i^*) + b(p^*)}{\delta} i^*, i^* = \frac{g(p^*)}{\mu}, \tag{4.11}$$

and i^* solve

$$\frac{\sigma\delta(1 - i^*)}{[\mu(1 - i^*) + b(p^*)][\delta + (\sigma - \mu)i^* + b(p^*)]} = 1. \tag{4.12}$$

Note that (4.12) is obtained by equating the last two expressions for e in (4.6). Suppose that model (5.2) has two biologically feasible endemic equilibria denoted by $\mathcal{E}_1^* = (p_1^*, e_1^*, i_1^*)$ and $\mathcal{E}_2^* = (p_2^*, e_2^*, i_2^*)$, respectively, where $p_1^* < p_2^*$.

Theorem 4.3.4 *The endemic equilibrium, $\mathcal{E}_2^*$ with a large population size when it exists is locally asymptotically stable in the interior of Ω if $\mathcal{R}_0 > 1$ and is unstable when $\mathcal{R}_0 < 1$. While the endemic equilibrium, $\mathcal{E}_1^*$ with low population size, if it exists is unstable if $\mathcal{R}_0 > 1$.*

Proof. Linearizing system (4.2) around $\mathcal{E}^*$, gives the following Jacobian matrix

$$J(\mathcal{E}^*) = \begin{pmatrix} (b(p^*)' - d(p^*)')p^* & 0 & -\mu p^* \\ -b(p^*)'e^* & -\kappa & \sigma(1-2i^*) - (\sigma-\mu)e^* \\ -b(p^*)'i^* & \delta & -b(p^*) - \mu(1-2i^*) \end{pmatrix}.$$

where $\kappa = [\delta + b(p^*) + (\sigma - \mu)i^*]$. The characteristic equation of the matrix $J(\mathcal{E}^*)$ simplified using equation (4.12) and e^*, i^* in (4.11), is

$$\lambda^3 + a_2\lambda^2 + a_1\lambda + a_0 = 0, \tag{4.13}$$

where

$$\begin{aligned} a_2 &= -(b(p^*)' - d(p^*)')p^* + (\sigma-\mu)i^* + \mu + \delta + 2d(p^*), \\ a_1 &= p^*d(p^*)'[(\sigma-\mu)i^* + \mu + \delta + 2d(p^*)] - p^*b(p^*)'(\sigma i^* + \mu + \delta + 2d(p^*)) \\ &\quad + [(\sigma-\mu)(\mu + \delta + b(p^*) - \mu i^*) - \mu b(p^*)]i^*, \\ a_0 &= p^*i^*\{d(p^*)'[(\sigma-\mu)(\mu + \delta + b(p^*) - \mu i^*) - \mu b(p^*)] - b'\sigma(\mu + \delta + b(p^*))\}. \end{aligned}$$

It follows from the condition $\mathcal{R}_0 > 1$ and Remark 1 that $a_i > 0$ for $i = 0, 1, 2$ if $p^* = p_2^*$. Hence, by Routh-Hurwitz criteria (Theorem 2.2.3), the eigenvalues of the Jacobian matrix $J(\mathcal{E}_2^*)$ have negative real parts if and only if $a_1a_2 > a_0$. To show that $a_1a_2 > a_0$, write $a_i = x_iv + y_iw + z_i$ where $v = -p_2^*b(p_2^*)'$ and $w = p_2^*d(p_2^*)'$ for all $x_i, y_i, z_i, v, w \geq 0$. Then the condition for local stability is

$$\begin{aligned} a_1a_2 - a_0 &= (x_1v + y_1w + z_1)(x_2v + y_2w + z_2) - (x_0v + y_0w + z_0), \\ &= x_1x_2v^2 + y_1y_2w^2 + (x_1y_2 + y_1x_2)vw + (x_1z_2 + z_1x_2 - x_0)v \\ &\quad + (y_1z_2 + z_1y_2 - y_0)w + z_1z_2 - z_0 > 0. \end{aligned}$$

One can easily see that $x_1z_2 > x_0, y_1z_2 > y_0$ and $z_1z_2 - z_0 = z_1z_2 > 0$ so that $a_1a_2 - a_0 > 0$. Then, it follows from Theorem 2.2.2 that $\mathcal{E}_2^*$ is locally asymptotically stable.

For $p^* = p_1^*$ and $\mathcal{R}_0 > 1$ the stability condition $a_1a_2 > a_0$ is not satisfied because $\mathcal{E}_1^*$ establishes an extinction basin above the Allee threshold and, so $\mathcal{E}_1^*$ is unstable. ■

Furthermore, the endemic equilibria of system (4.2) correspond to the roots of the following equation in $(u, 1)$

$$\Psi(p) = [\mu + d(p)]\{\mu[\delta + b(p)] + (\sigma - \mu)g(p)\} + \sigma\delta[g(p) - \mu], \tag{4.14}$$

with

$$e = \frac{\mu(1-i) + b(p)}{\delta} i, \quad i = \frac{g(p)}{\mu}.$$

To investigate the possible number of positive interior equilibria *via* phase plane illustration, equation (4.14) with $g(p) = \mu i$ is rewritten in the form

$$i = \frac{\sigma\delta - [\mu + d(p)][\delta + d(p)]}{\sigma[\mu + \delta + d(p)]}. \tag{4.15}$$

Then, we call (4.15) the infected nullcline or simply i-nullcline. Furthermore, we denote by $\Phi_1(p)$ and $\Phi_2(p)$ the host and infected nullclines, respectively. Therefore, endemic equilibria can be found as the intersections of the i-nullcline in (4.15) above and the p-nullcline $i = \frac{g(p)}{\mu}$. In order to demonstrate this, we use the following demographic functions given in equation (3.9) of Chapter 3.

$$\begin{aligned} b(p) &= k\{-(1-\alpha)p^2 + [1 + (1-\beta)u]p + \gamma\}, \\ d(p) &= k(\alpha p^2 - \beta u p + u + \gamma), \end{aligned} \tag{4.16}$$

where $\beta \leq \min\{1, 2\sqrt{2\alpha}\}, \gamma \geq 0$ and $\alpha \in [0, 1)$ so that both functions are positive in the interval $[0, m]$ for $m = \frac{1+u(1-\beta)}{1-\alpha}$. The non-trivial equilibria of model (4.2) with (4.16) are then depicted in Figure 4.2.

Further, rewriting $\Psi(p)$ as defined in (4.14) in the form

$$\Psi(p) = g(p) - \mu\frac{\sigma\delta - [\mu + d(p)][\delta + d(p)]}{\sigma[\mu + \delta + d(p)]}, \tag{4.17}$$

we obtain

$$\begin{aligned} \Psi(u) &= -\frac{\mu}{\sigma[\mu + d(u)][\delta + d(u)][\mu + \delta + d(u)]}[\mathcal{R}_u - 1], \\ \Psi(1) &= -\frac{\mu}{\sigma[\mu + d(1)][\delta + d(1)][\mu + \delta + d(1)]}[\mathcal{R}_0 - 1]. \end{aligned} \tag{4.18}$$

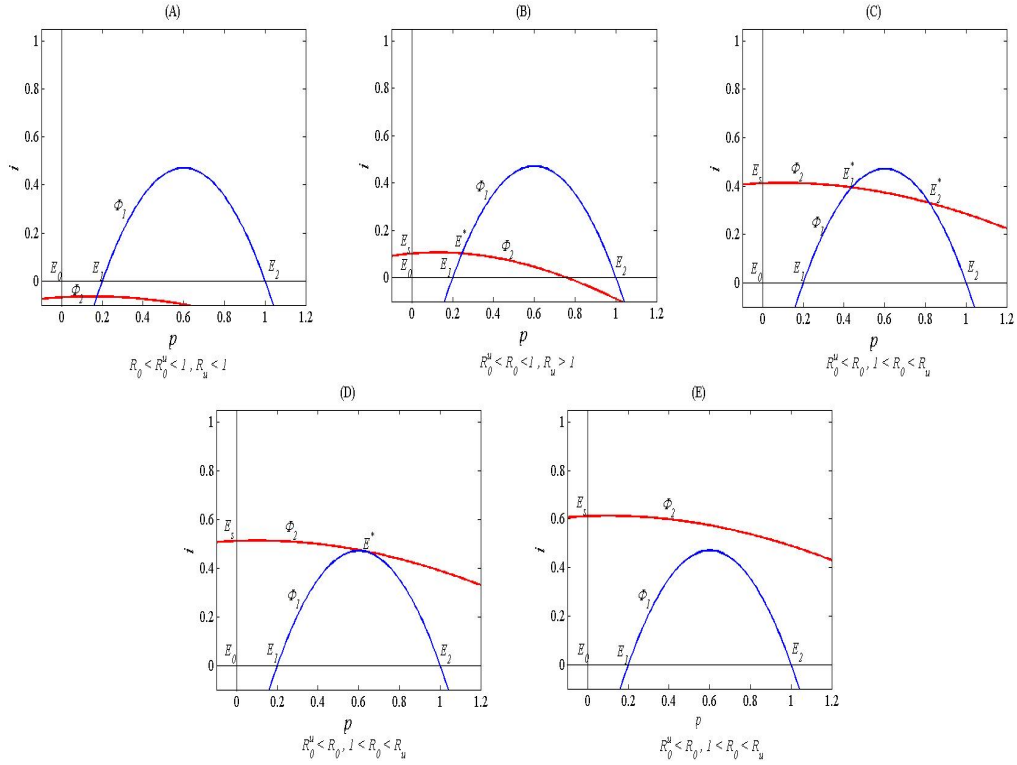

Figure 4.2: Phase plane illustrations with nullclines and endemic states of model (4.2) with (4.16). Parameter values used for all curves are $k = 0.5, u = 0.2, \mu = 0.17$ and other parameters are as would be stated in each part. (A) shows that there is no endemic state in the interval $(u, 1)$, where the curves are drawn with $\alpha = 0.2, \beta = 0.3, \gamma = 0.01, \sigma = 0.7$ and $\delta = 0.06$; (B) shows one endemic state for $\alpha = 0.35, \beta = 0.45, , \gamma = 0.002, \sigma = 0.95$ and $\delta = 0.1$; (C) shows two endemic states with $\alpha = 0.2, \beta = 0.2, \gamma = 0.05, \sigma = 0.995$ and $\delta = 0.55$; (D) shows that the two equilibria in (B) coincide to one when $\gamma = 0.011, \delta = 0.78$; (E) indicates that the two endemic states disappear by saddle-node bifurcation for $\gamma = 0.0001, \sigma = 1.1$ and $\delta = 0.78$.

It follows that $\Psi(u) = 0 \Leftrightarrow \mathcal{R}_u = 1$ and $\Psi(1) = 0 \Leftrightarrow \mathcal{R}_0 = 1$. Using these relations, we define an invasion threshold, denoted by $\mathcal{R}_0^u$ as follows.

$$\mathcal{R}_0^u = \frac{\mathcal{R}_0}{\mathcal{R}_u} = \frac{[\mu + b(u)][\delta + b(u)]}{[\mu + b(1)][\delta + b(1)]}.$$

Thus, we establish the following results.

Theorem 4.3.5 *Model* (4.2) *with* (4.16) *has:*

(i) *no non-trivial equilibrium, if* $\mathcal{R}_0 \leq \mathcal{R}_0^u$ *(i.e.,* $\mathcal{R}_u \leq 1$*),*

(ii) *a unique endemic equilibrium* $\mathcal{E}^* = (p^*, e^*, i^*)$ *if* $\mathcal{R}_0^u < \mathcal{R}_0 \leq 1$ *(i.e.,* $\mathcal{R}_u > 1$*). This equilibrium is always unstable, and, in the presence of disease, is the effective eradication threshold.*

The proof follows from Lemma 4.3.1 and Theorem 4.3.4. Furthermore, the results of Theorem 4.3.5 assert that if $\mathcal{R}_u \leq 1$, then the disease cannot invade a population at the edge of extinction due to the Allee effect. This leads to a bistable system that approaches either one of the extinction states $\mathcal{E}_0/\mathcal{E}_s$ or the carrying capacity state $\mathcal{E}_2$. On the other hand, if $\mathcal{R}_u > 1$, depending on the initial condition the host population either goes extinct or settles at its carrying capacity. Hence host extinction is possible even if the initial size is above the Allee threshold. Therefore, the disease increases the basin of extinction beyond the Allee threshold.

4.4 Bifurcation Analysis

It is evident that, when an epidemiological model admits multiple non-trivial equilibria, the model usually exhibits complex dynamical behavior such as backward bifurcation and forward hysteresis [34, 42, 79].

In order to investigate the existence of such phenomena in model (4.2) with (4.16), we rearrange equation (4.14) with (4.16) and obtain after algebraic manipulations the following quartic polynomial for p.

$$\Psi(p) = Q_4 p^4 + Q_3 p^3 + Q_2 p^2 + Q_1 p + Q_0, \tag{4.19}$$

where

$$
\begin{aligned}
Q_4 &= -k^2\alpha[(\sigma-\mu)+\mu(1-\alpha)],\\
Q_3 &= k^2\{(\sigma-\mu)(\alpha+\beta u)+\alpha[\sigma u+\mu(1-\beta u)]+\beta u\mu(1-\alpha)\},\\
Q_2 &= -k\{(\sigma-\mu)(\mu+\delta+k[2\alpha+\gamma+\beta(1+u)])+\mu(1-\alpha)[\mu+\delta+k(2+u)]\\
&\quad +k\mu[2(1-\alpha)+u(1-\beta u)]\},\\
Q_1 &= k\{(\sigma-\mu)[\mu+\delta+k\gamma(1+u)+ku(1+\beta u)]+k\gamma\mu[u(1-\beta)+(1-\beta u)]\\
&\quad +(\mu+\delta+ku)[\sigma u+\mu(1-\beta u)]\},\\
Q_0 &= k\gamma[\mu^2+\delta+k(u+\gamma)]-(\sigma-\mu)[(\mu+ku)(\delta+ku)+k^2u\gamma].
\end{aligned}
$$

It follows that, if $\mathcal{R}_0 > 1$ (i.e. $(\sigma-\mu) > 0$) the coefficients Q_4, Q_2 of equation (4.19) are negative and Q_3, Q_1 are positive. The constant coefficient Q_0 is either positive or negative. Hence, the sequence of these coefficients has at least three sign changes and so, equation (4.19) will have at least one positive real roots by Descartes' rule of sign (Theorem 2.4.1). Therefore, we obtain the following results.

Theorem 4.4.1 *If $\mathcal{R}_0 > 1$, then model (4.2) with (4.16) has:*

(i) *three non-trivial equilibria or one non-trivial equilibrium if $Q_0 \geq 0$,*

(ii) *four non-trivial equilibria or two non-trivial equilibria if $Q_0 < 0$.*

It can be deduced from Case (ii) of Theorem 4.4.1 and Figure 4.2 (C) that model (4.2) with (4.16) can have two non-trivial steady states when $\mathcal{R}_0 > 1$. Keeping all the parameters fixed other than σ, we take σ as the bifurcation parameter. It should be noted that as bifurcation parameters, σ and $\mathcal{R}_0$ can be considered essentially equivalent. More precisely, $\mathcal{R}_0$ can be regarded as a function of σ so that $\mathcal{R}_0$ is varied by varying transmissibility σ. We denote by σ^c the value of σ at which the two endemic states coincide as in Figure 4.2 (D) with corresponding critical reproduction number $\mathcal{R}_0^c = \mathcal{R}_0(\sigma^c)$. However, in the rest of this section we will discuss the dynamical behavior of model (4.2) with (4.16) in terms of $\mathcal{R}_0$.

Using a numerical bifurcation software 'MatCont', we show in Figure 4.3 how the total population p and prevalence i change with varying the threshold parameter $\mathcal{R}_0$. If $\mathcal{R}_0 < 1$, the disease cannot invade from arbitrarily introductions

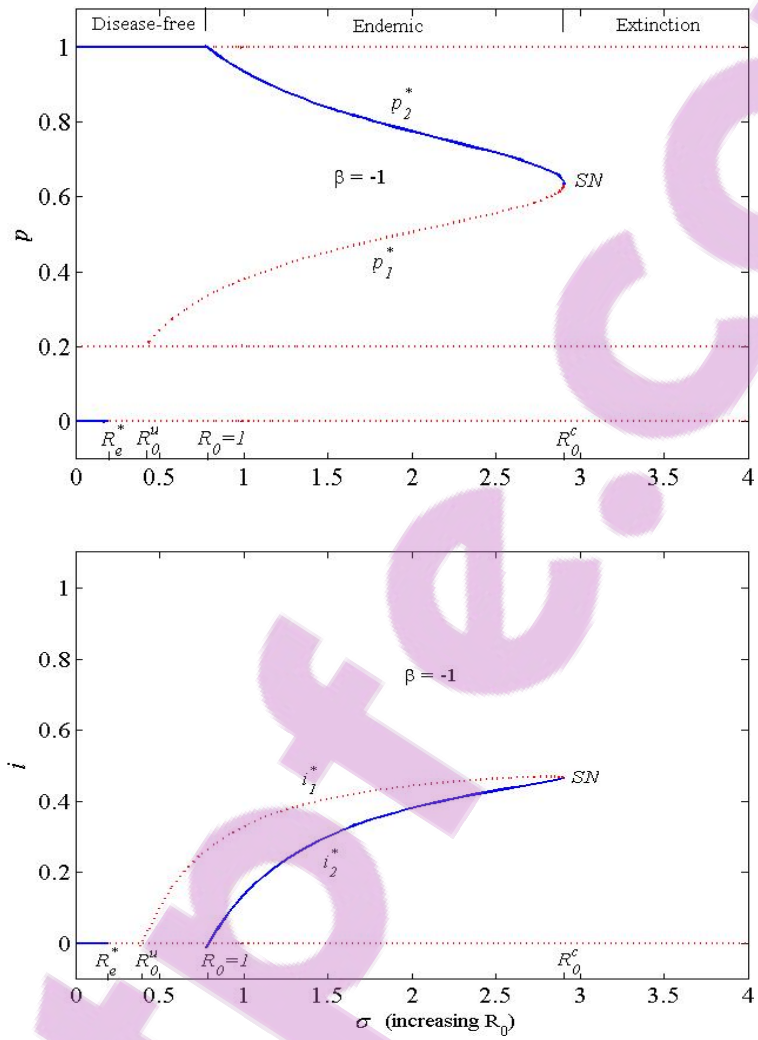

Figure 4.3: Bifurcation diagrams for varying $\mathcal{R}_0$ (by increasing transmissibility σ) with $\beta \leq 1$. Solid (dashed) lines represent stable (unstable) equilibria and the arrow indicates the abrupt population collapse from a level of high population size p_2^* after a saddle-node (SN) bifurcation. Parameter values used are $k = 0.5, u = 0.2, \mu = 0.17, \alpha = 0.2, \gamma = 0.05, \beta = -1$ and $\delta = 0.55$.

into the population at carrying capacity. If $\mathcal{R}_0 > 1$, however, the disease-free equilibrium $\mathcal{E}_2$ loses stability, resulting in the emergence of locally stable endemic equilibrium $\mathcal{E}_2^*$ by transcritical bifurcation. This endemic equilibrium coexists with unstable endemic equilibrium $\mathcal{E}_1^*$ that already arises when $\mathcal{R}_0 > \mathcal{R}_0^u$. The two endemic equilibria coalesce and disappear by a saddle-node (SN) bifurcation at $\mathcal{R}_0 = \mathcal{R}_0^c$. Hence, the population goes extinct.

Furthermore, the sub-threshold $\mathcal{R}_0^c$ is a tipping point for an unanticipated population collapse. Therefore, the dynamics of the system is rendered monostable whenever $\mathcal{R}_0 > \mathcal{R}_0^c$ with a semi-trivial extinction state $\mathcal{E}_s$ being globally stable. If $\mathcal{R}_0 < \mathcal{R}_0^c$, the system is bistable with one of the attractors being an extinction state, either $\mathcal{E}_0$ or $\mathcal{E}_s$ according as $\mathcal{R}_e^* < 1$ or $\mathcal{R}_e^* > 1$, respectively. The other attractor is either the carrying capacity state $\mathcal{E}_2$ if $\mathcal{R}_0 < 1$ or the endemic state $\mathcal{E}_2^*$ when $\mathcal{R}_0 > 1$.

One can observe from Figure 4.6 that the value of the tipping point for the abrupt population collapse $\mathcal{R}_0^c$ increases with decreasing value of β. As it was highlighted in Chapter 3, the mortality rate decreases when $\beta > 0$ and slowly increases for $\beta \leq 0$ at low population. The biological implication of the parameter β as discussed earlier in the introductory section of this chapter is that the mortality rate of species whose individuals benefit from the presence of conspecifics decreases slowly when small. On the other hand, species whose individuals do not benefit from the presence of conspecifics have an increasing mortality rate at low population level. The bifurcation results depicted in Figure 4.6 indicate that the abrupt population collapse from a level of large population size p_2^* is faster when $\beta > 0$ than for $\beta \leq 0$. This reveals that species whose individuals benefit from the presence of conspecifics are more vulnerable to decline and extinction at high population level. The essential mechanism behind this scenario is the simultaneous population size depression and the increase of the extinction threshold owing to disease virulence and the Allee effect.

It is worth mentioning here that all the results of model (4.2) with (4.16) hold true for its special cases. These are the cases when the demographic function $d(p)$ in (4.16) becomes linear and constant for $\alpha = 0$ and $\alpha = \beta = 0$, respectively. For the first case, if $\beta = -1/ku$, then the demographic functions in (4.16) are similar to the dimensional forms of those given in equation (1.4) of Chapter 1.

In such case, we have an extended version of model (1.5) as presented in [16]. Moreover, the bifurcation results here are similar to those in [16], but the novelty of the presented model is the dynamic parameter β that makes the model more general and determines which species are more prone than others to decline and extinction. Determining the range of values of the parameters α and β, however, play a vital role in conservation biology for guiding management actions.

It is to be noted that the threshold $\mathcal{R}_0$ can also be altered by varying the pathogenicity μ. In fact, an increase in $\mathcal{R}_0$ corresponds to a decrease in μ. In such situations, another critical threshold parameter denoted by $\mathcal{R}_0^{c2}$ such that $\mathcal{R}_0^{c2} > \mathcal{R}_0^{c1}$ also exists for which a second saddle-node bifurcation occurs. This scenario gives rise to two non-trivial equilibria again after the extinction regime at $\mathcal{R}_0 = \mathcal{R}_0^{c2}$. The bifurcation diagrams that reveal the second saddle-node bifurcation, which are obtained using the numerical continuation software MatCont [71] are depicted in Figure 4.4.

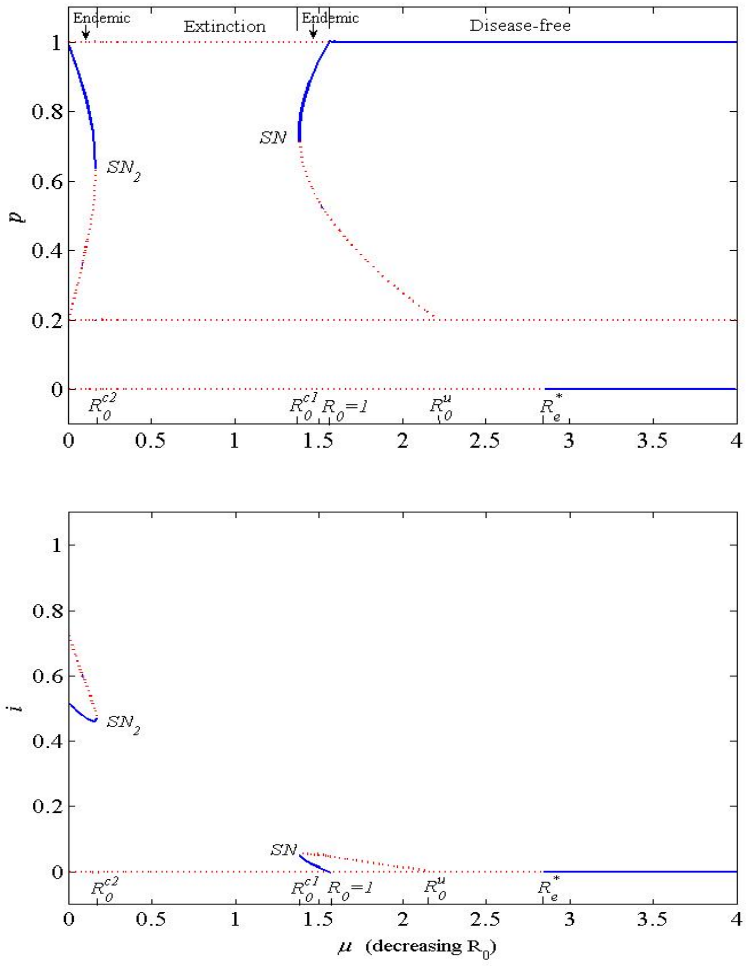

Figure 4.4: Bifurcation diagrams that reveal a second saddle-node bifurcation by changing disease pathogenicity μ (decreasing $\mathcal{R}_0$). The locations of the associated threshold parameters are indicated on μ-axis. The extinction equilibria $\mathcal{E}_0$ and $\mathcal{E}_s$ exchange stability at $\mathcal{R}_e^* = 1$ by transcritical bifurcation. Solid (dashed) lines represent stable (unstable) equilibria and SN indicates a saddle-node bifurcation above which the population collapse. While SN_2 shows a second saddle-node bifurcation for the re-emergence of two endemic equilibria. Parameter values used are $k = 0.5, u = 0.2, \alpha = 0.2, \beta = -1, \sigma = 3, \gamma = 0.05$ and $\delta = 0.55$.

As was reported in [69, 70], the maximum degree of depression of the host population equilibrium (here leading to extinction) is achieved by a disease with intermediate pathogenicity (i.e. moderate to large $\mathcal{R}_0$). When the disease pathogenicity is too small, i.e. too high a $\mathcal{R}_0$, the disease has little detrimental effect on the host. In such a case, the host persists at endemic state with large population size ($\mathcal{R}_0 > \mathcal{R}_0^{c2}$). In contrast, if the level of disease pathogenicity is too high, i.e. too small a $\mathcal{R}_0$, the increased mortality of infected individuals will either prevents effective disease transmission ($1 < \mathcal{R}_0 < \mathcal{R}_0^{c1}$) or even leads to the deletion of infections from the host population ($\mathcal{R}_0 < 1$).

The model behavior in two-parameter space (μ, σ) is depicted in Figure 4.5. Therefore, the dynamical consequence of model (4.2) with (4.16) can be characterized in relations to disease-related parameters σ and μ. The threshold quantities of the model define a linear relationship between σ and μ, while the saddle-node bifurcation conditions define a nonlinear relationship. As highlighted in [16], fixing pathogenicity μ corresponding to saddle-node bifurcation scenario and traversing vertically through Figure 4.5 by altering σ reveals that the saddle-node bifurcation curve can be crossed only once. Similarly, if transmissibility σ is fixed (noting the critical value of σ at the turning point of the saddle-node bifurcation curve) and Figure 4.5 is traversed horizontally by varying μ, the saddle-node bifurcation curve can be crossed twice (revealing a second saddle-node bifurcation). The mathematical implication of these numerical observations is that both nullclines depend on μ, but only one nullcline depends on σ.

4.5 Summary

It is well known that Allee effect is to be more likely to occur when individuals benefit from the presence of conspecifics. However, endangered species whose individuals behave in such manner experience heavy mortality at low population and hence are more susceptible to extinction. This is because they rely on mass numbers and a strategy of predator dilution for survival. The definition of the Allee effect refers to low population levels. Determining impact of the Allee effect at high population level and understanding which species are more vulnerable than others to decline and extinction in a such situation play a relevant role in

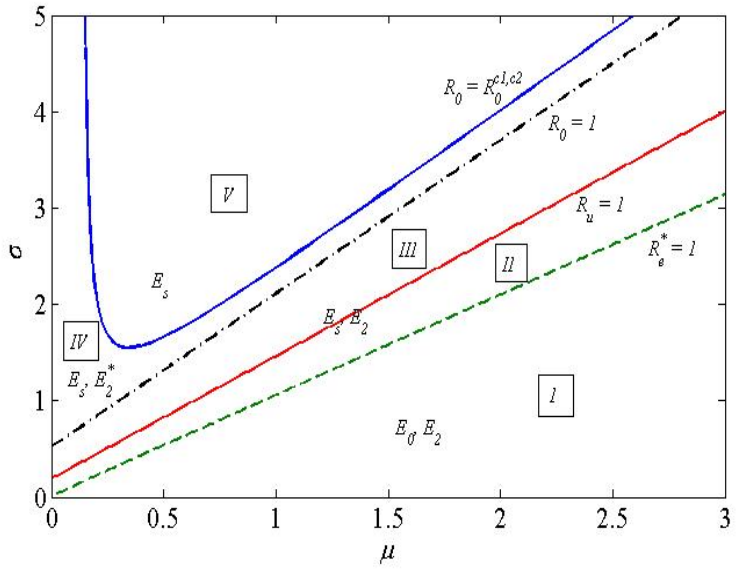

Figure 4.5: Regions of model behavior in the two-parameter space (μ, σ) where σ is the transmission parameter and μ is the disease-induced death rate. In each region, stable equilibria are indicated. The regions marked I through IV are bistable, whereas the region V is monostable with eventual host extinction. Region IV can be endemic, while regions I and II can be disease-free. Host extinction is possible in all regions. The line enclosing region V is a saddle-node bifurcation curve obtained using MatCont, while the dashed and dash-dotted lines are transcritical bifurcation curves. Solid line between the dashed and dash-dotted lines marks the emergence of the unstable non-trivial equilibrium $\mathcal{E}^*$. Parameter values used are $k = 0.5, u = 0.2, \alpha = 0.2, \beta = -1, \gamma = 0.05$ and $\delta = 0.55$.

conservation biology for guiding management actions. This is because such an information would allow biologists to improve the species' chances of survival. The main findings of this chapter are as follows:

(1) If the threshold quantity $\mathcal{R}_0$ is below one, the model has bistable equilibria namely: the trivial extinction state $\mathcal{E}_0$ and the carrying capacity state $\mathcal{E}_2$, which are both stable nodes. This implies that if $\mathcal{R}_0 < 1$ the disease cannot invade from arbitrarily small introductions into the host population at

carrying capacity. Thus, the presence of a strong Allee effect in the host demographics can play a protective and stabilizing role in relations to invasion of a disease.

(2) The disease increases the basin of extinction above the Allee threshold if $\mathcal{R}_0^u < \mathcal{R}_0 \leq 1$ or equivalently $\mathcal{R}_u > 1$.

(3) For $\mathcal{R}_0 > 1$, the model have multiple nontrivial stationary states. The equilibrium point with a large population size is being the only locally asymptotically stable equilibrium.

(4) The model suggests that the joint impact of infectious disease and the Allee effect at high population may lead to a catastrophic crash to extinction. The tipping point marking the unexpected population collapse is mathematically associated with a saddle-node bifurcation.

(5) The bifurcation analysis reveals that species whose individuals benefit from the presence of conspecifics are more prone to decline and extinction.

(6) We shown that the second saddle-node bifurcation can be detected by using a numerical continuation software 'MatCont', despite the comment made by Hilker [16] that it may not be observed by any of such software. Moreover, a transcritical bifurcation at $\mathcal{R}_e^* = 1$, where the trivial extinction state $\mathcal{E}_0$ exchanges stability with a semi-trivial extinction state $\mathcal{E}_s$ is observed on the bifurcation diagrams.

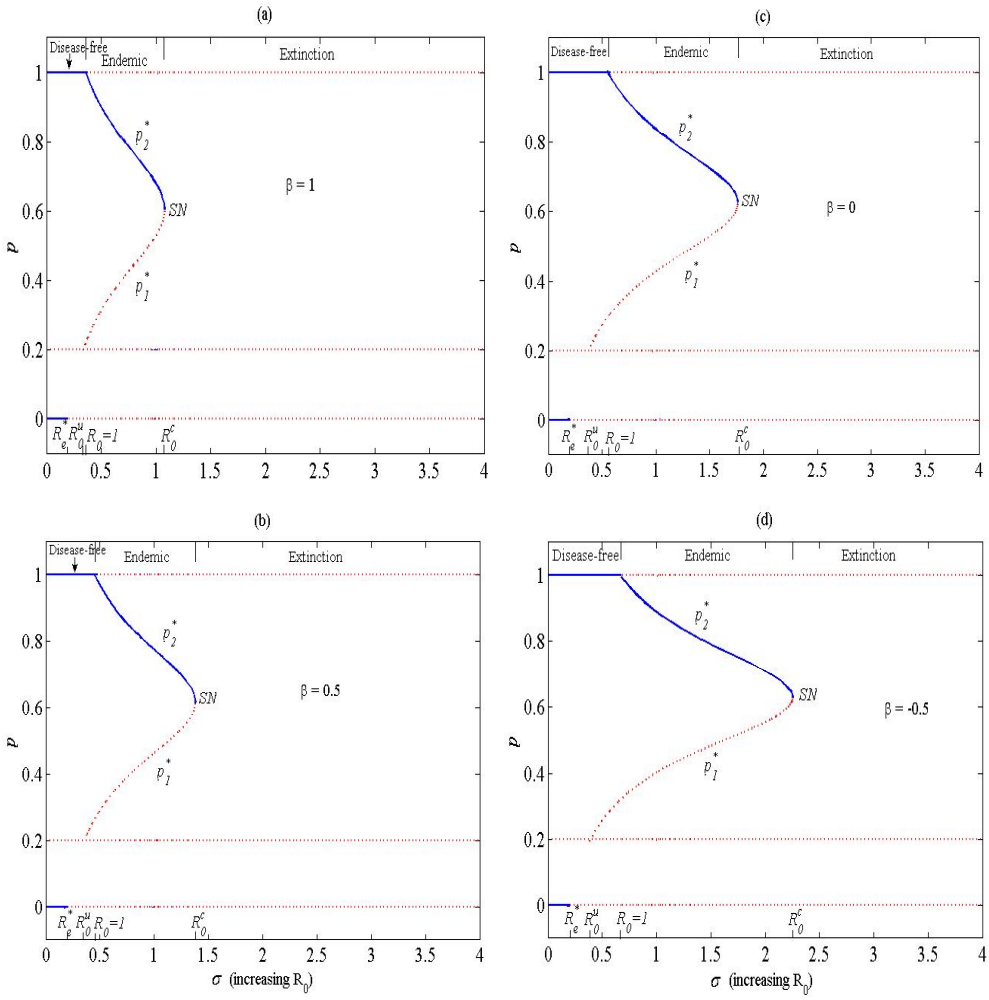

Figure 4.6: Bifurcation diagrams for varying transmissibility σ (increasing $\mathcal{R}_0$) showing the increasing value of $\mathcal{R}_0^c$ with some changing values of β from (a) through (d). The extinction equilibria $\mathcal{E}_0$ and $\mathcal{E}_s$ exchange stability at $\mathcal{R}_e^* = 1$ by transcritical bifurcation. Solid (dashed) lines represent stable (unstable) equilibria and SN indicates a saddle-node bifurcation above which the population collapse. Parameter values used are $k = 0.5, u = 0.2, \mu = 0.17, \alpha = 0.2, \gamma = 0.05$ and $\delta = 0.55$.

CHAPTER 5

Backward bifurcation analysis of an epidemiological model with partial immunity

5.1 Introduction

Bovine tuberculosis (BTB) is a contagious disease caused by a bacterium called *Mycobacterium bovis* (M. bovis), with a wide range of hosts such as domestic livestock, wildlife and humans. Some of such animals include cattle, goats, sheep, Badgers (Meles meles), brushtail possums (Trichosurus vulpecula), deer (Odocoileus virginianus), bison (Bison bison) and African buffalo (Syncerus caffer) which can either be reservoir or spill-over [80]. A reservoir host maintains and spreads infection whereas a spill-over host has a little or no consequence in the maintenance and spread of the infection. However, a spill-over host is referred to a dead-end host when it does not pass on the infection. BTB is a chronic and progressive disease in buffalo that leads to direct or indirect death. In buffalo herds, BTB has a high prevalence of 60% to 92% [81]. It was reported in [82] that the higher the prevalence rate the higher the disease-related mortality and hence

a mortality of up to 10% was detected in buffalo herds having a BTB prevalence of at least 50%. The time from infection to death is not known, but it varies and depends on the animal's immune response, which can wane by factors such as stress, drought or old age.

As in cattle the main source of BTB transmission in buffalo is by direct contact or by aerosol [82]. Vertical (intrauterine) and pseudo-vertical (through infected milk) transmissions are considered to be rare events in buffalo [81]. The mode of transmission and the route of infection within and between species are generally indicated by the locations of the tuberculous lesions in that species [80].

In Africa most animals infected with BTB show clinical signs only when the disease has reached an advanced stage. The clinical signs of BTB in buffalo at such stage include: coughing, debilitation, poor body condition or emaciation and lagging when chased by helicopter [80, 82].

Park management (Kruger National Park (KNP) and Hluhuwe-iMfolozi Park (HiP)) in South Africa have maintained some control measures such as culling, vaccination and some combination of them to control or eradicate BTB owing to its potential effects on buffalo and other host species [81, 83]. However, some modeling work on BTB on buffalo suggest that vaccination may be the best control measure option since BTB may persist in buffalo population even when the population is reduced to low densities [81]. In order to assess the effectiveness of a buffalo vaccination program in South Africa some age structured mathematical models have recently been developed [81, 84].

As discussed in Chapter 1, there is increasing evidence that some animal infections provide partial immunity and spread among seropositive animals, even at a reduce rate. Such disease can be modeled as an $S_1I_1S_2I_2$ (or $SIS_1I_1S_1$) compartmental type [28]. In light of this, we design a two-stage SIS model in animal population with bovine tuberculosis in African buffalo as a guiding example based on the most assumptions of the model introduced in [28] since there is no clinical evidence which suggests that animals recover from BTB infection [81]. And the fact that BTB infection confers partial immunity and spreads among seropositive animals. The model is designed with aim to identify causes of backward bifurcation and to assess vaccine impact in the transmission dynamics of an epidemiological model with partial immunity and variable population.

5.2 Model formulation

Let $N(t)$ be the total population of African buffalo at time t, which is subdivided into four distinct epidemiological classes of those who have never been infected before ($S_1(t)$), those who have experienced at least one previous infection ($S_2(t)$), first time infectious ($I_1(t)$), and at least second time infectious ($I_2(t)$). Hence, the total population at any time t is given by

$$N(t) = S_1(t) + I_1(t) + S_2(t) + I_2(t).$$

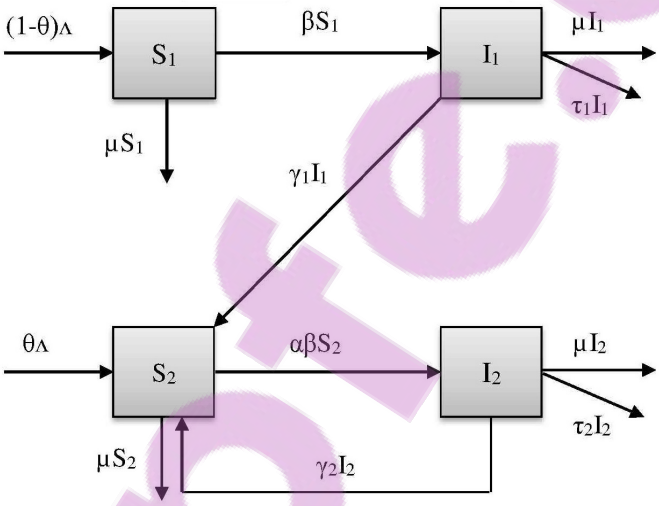

Figure 5.1: Schematic diagram of model (5.1)

The system of ordinary differential equations for the $S_1I_1S_2I_2S_2$ model is presented in equation (5.1), with corresponding flow diagram depicted in Figure 5.1.

All the state variables and parameters of the model are described in Table 5.1.

$$\begin{aligned}
\frac{dS_1}{dt} &= (1-\theta)\Lambda - (\beta+\mu)S_1, \\
\frac{dI_1}{dt} &= \beta S_1 - (\gamma_1+\mu+\tau_1)I_1, \\
\frac{dS_2}{dt} &= \theta\Lambda + \gamma_1 I_1 + \gamma_2 I_2 - (\alpha\beta+\mu)S_2, \\
\frac{dI_2}{dt} &= \alpha\beta S_2 - (\gamma_2+\mu+\tau_2)I_2,
\end{aligned} \tag{5.1}$$

with force of infection

$$\beta = \frac{\sigma_1 I_1 + \sigma_2 I_2}{N}.$$

In (5.1), the parameter Λ is the recruitment rate of susceptible buffalo. A fraction θ of these susceptible buffalo are vaccinated. Furthermore, the population of first time susceptible buffalo acquire infection, following effective contact with infectious buffalo at a rate β. The parameter $\sigma_i \ \ (i = 1, 2)$ is the effective contact rate for the respective infectious class I_i, μ is the natural death rate in all classes. $\gamma_i \ \ (i = 1, 2)$, is the recovery rate of infected buffalo from the I_i class. $\tau_i \ \ (i = 1, 2)$, is the disease induced death rate in each class I_i. It is assumed that second and subsequent times infected buffalo acquire natural immunity after recovery and move to S_2 class. Further, it is assumed that vaccine-induced immunity provides the same protection as the natural immunity. This is a simplifying assumption which helps keep mathematical complexity of the model at a reasonable level, while the model is still relevant. Hence, the S_2 class can be referred to as a vaccinated class as well. The population of vaccinated buffalo in S_2 acquire infection at the rate $\alpha\beta$ where $0 \leq \alpha \leq 1$. Thus, α provides a measure of the efficacy of vaccine in a relative way so that $\alpha = 0$ means the vaccine is completely effective in preventing infection and $\alpha = 1$ means that the vaccine is ineffective. More precisely, in the absence of vaccine the force of infection is β, with vaccine it becomes $\alpha\beta$. The relative reduction $\phi = \frac{\beta-\alpha\beta}{\beta} = 1-\alpha$ of the force of infection is referred to as efficacy of the vaccine.

Table 5.1: Description of state variables and parameters of the model (5.1)

Variable	**Interpretation**	
S_1	First time susceptible buffalo	
I_1	First time infectious buffalo	
S_2	Subsequent times susceptible buffalo	
I_2	Subsequent times infectious buffalo	
Parameter	**Interpretation**	**Unit**
Λ	Recruitment rate	year^{-1}
θ	Fraction of newly-recruited buffalo vaccinated	year^{-1}
μ	Natural death rate	year^{-1}
$\sigma_1,\ \sigma_2$	Effective contact rates	year^{-1}
$\gamma_1,\ \gamma_2$	Recovery rates	year^{-1}
$\tau_1,\ \tau_2$	disease induced death rates	
$\alpha = 1 - \phi$	relative vaccine efficacy	

5.3 Basic properties

The typical epidemiological questions, such as persistence/extinction of the infection, threshold values of the parameter, etc., are mathematically formulated in terms of the asymptotic behavior of the solution of (5.1) considered as a dynamical system as well as the bifurcations of this system.

It is easy to verify that the system of equations (5.1) defines a (positive) dynamical system on the domain

$$\Omega = \left\{ (S_1, I_1, S_2, I_2) \in \mathcal{R}_+^4 : S_1 + I_1 + S_2 + I_2 \leq \frac{\Lambda}{\mu} \right\}.$$

In fact, one can easily see that $\dot{S}_i \geq 0, \dot{I}_i \geq 0$ and $\dot{N} \leq 0$ when $S_i = 0, I_i = 0$ and $N = \lambda/\mu$, respectively. Therefore, at any point on the boundary the vector field is pointing inside Ω. Hence, the system (1) defines a dynamical system on Ω.

5.3.1 Existence and stability of equilibria

5.3.1.1 Disease-free equilibrium (DFE)

In the absence of the disease ($I_1 = I_2 = 0$), the DFE of the model (5.1) obtained at steady state is given by

$$\mathcal{E}_0 = (S_1^*,\ I_1^*,\ S_2^*,\ I_2^*) = \left(\frac{(1-\theta)\Lambda}{\mu},\ 0,\ \frac{\theta\Lambda}{\mu},\ 0\right).$$

To establish conditions for the linear stability of $\mathcal{E}_0$, the next generation operator method is applied to the system (5.1). Using the notation in [58], the matrices F (for the new infection terms) and V (of the transition terms) are given, respectively, by

$$F = \begin{pmatrix} \sigma_1(1-\theta) & \sigma_2(1-\theta) \\ \alpha\sigma_1\theta & \alpha\sigma_2\theta \end{pmatrix},\ V = \begin{pmatrix} \gamma_1+\mu+\tau_1 & 0 \\ 0 & \gamma_2+\mu+\tau_2 \end{pmatrix}.$$

The associated reproduction number denoted by $\mathcal{R}_v$, is the spectral radius of the next generation matrix FV^{-1}, given by

$$\mathcal{R}_v = \frac{\sigma_1 k_2(1-\theta) + \alpha\sigma_2 k_1\theta}{k_1 k_2}, \tag{5.2}$$

where $k_1 = \gamma_1 + \mu + \tau_1$ and $k_2 = \gamma_2 + \mu + \tau_2$.

The threshold quantity, $\mathcal{R}_v$, represents the average number of secondary infections caused by a single infected buffalo in a susceptible buffalo population where a certain fraction of the population is vaccinated [85, 86]. Hence, using [58, Theorem 2], we obtain the following result.

Theorem 5.3.1 *The DFE, $\mathcal{E}_0$ of the model* (5.1) *is locally asymptotically stable* (*LAS*) *if $\mathcal{R}_v < 1$, and unstable if $\mathcal{R}_v > 1$.*

The epidemiological implication of Theorem 5.3.1 is that if $\mathcal{R}_v < 1$, the disease will be eliminated provided the initial sizes of the infected subpopulations of the model are sufficiently small so that the initial state of the system is in basin of attraction of the DFE ($\mathcal{E}_0$).

We note that this result does not exclude the possibility of coexistence of DFE with a stable endemic equilibrium. This coexistence, which results from a backward bifurcation at $\mathcal{R}_v = 1$, is the main issue investigated in the sequel.

5.3.1.2 Endemic equilibria (EE)

The endemic equilibria of model (5.1) are the steady states where the disease may persist in the population, that is when at least one of the infected compartments of the model is non-empty. Let $\mathcal{E}_1 = (S_1^{**}, I_1^{**}, S_2^{**}, I_2^{**})$ be an endemic equilibrium solution of model (5.1). Then, equating the right-hand side of (5.1) to zero, we obtain

$$S_1^{**} = \frac{(1-\theta)\Lambda}{\beta^{**}+\mu}, \; I_1^{**} = \frac{\beta^{**}(1-\theta)\Lambda}{k_1(\beta^{**}+\mu)},$$

$$S_2^{**} = \frac{k_2\Lambda[k_1\theta(\beta^{**}+\mu)+\gamma_1(1-\theta)\beta^{**}]}{k_1(\beta^{**}+\mu)[(\mu+\tau_2)(\alpha\beta^{**}+\mu)+\mu\gamma_2]}, \tag{5.3}$$

$$I_2^{**} = \frac{\alpha\beta^{**}\Lambda[k_1\theta(\beta^{**}+\mu)+\gamma_1(1-\theta)\beta^{**}]}{k_1(\beta^{**}+\mu)[(\mu+\tau_2)(\alpha\beta^{**}+\mu)+\mu\gamma_2]},$$

where

$$\beta^{**} = \frac{\sigma_1 I_1^{**} + \sigma_2 I_2^{**}}{N^{**}} \tag{5.4}$$

and

$$N^{**} = S_1^{**} + I_1^{**} + S_2^{**} + I_2^{**}. \tag{5.5}$$

Equation (5.4) can be written in the form

$$S_1^{**} + \left(1 - \frac{\sigma_1}{\beta^{**}}\right) I_1^{**} + S_2^{**} + \left(1 - \frac{\sigma_2}{\beta^{**}}\right) I_2^{**} = 0. \tag{5.6}$$

Substituting the right-hand sides of (5.3) into equation (5.6), gives the following equation for β^{**}.

$$\begin{aligned} &\frac{(1-\theta)\Lambda}{\beta^{**}+\mu} + \left(1 - \frac{\sigma_2}{\beta^{**}}\right) \frac{\alpha\beta^{**}\Lambda[k_1\theta(\beta^{**}+\mu)+\gamma_1(1-\theta)\beta^{**}]}{k_1(\beta^{**}+\mu)[(\mu+\tau_2)(\alpha\beta^{**}+\mu)+\mu\gamma_2]} \\ &+ \frac{k_2\Lambda[k_1\theta(\beta^{**}+\mu)+\gamma_1(1-\theta)\beta^{**}]}{k_1(\beta^{**}+\mu)[(\mu+\tau_2)(\alpha\beta^{**}+\mu)+\mu\gamma_2]} + \left(1 - \frac{\sigma_1}{\beta^{**}}\right) \frac{\beta^{**}(1-\theta)\Lambda}{k_1(\beta^{**}+\mu)} = 0. \end{aligned} \tag{5.7}$$

Hence, the endemic equilibria of the model (5.1) correspond to positive solutions of the equation (5.7).

5.4 Backward bifurcation analysis

The phenomenon of backward bifurcation occurs in models that have multiple endemic equilibria when $\mathcal{R}_v < 1$ [28, 34, 42]. In this case, the classical epidemiological requirement of having $\mathcal{R}_v < 1$, is necessary but no longer sufficient for effective disease control or elimination.

5.4.1 Existence of endemic equilibria

Re-arranging and simplifying equation (5.7), gives the following quadratic equation in terms of β^{**}

$$a(\beta^{**})^2 + b\beta^{**} + c = 0, \tag{5.8}$$

where,

$$\begin{aligned} a &= \alpha[k_1\theta + (\gamma_1 + \mu + \tau_2)(1-\theta)], \\ b &= k_1\alpha(\mu+\tau_2)(1-\theta) + k_1\alpha\theta(\mu-\sigma_2) + k_2(1-\theta)(\mu+\gamma_1) \\ &\quad + k_1k_2\theta - \sigma_1\alpha(\mu+\tau_2)(1-\theta) - \sigma_2\gamma_1\alpha(1-\theta), \\ c &= k_1k_2\mu(1-\mathcal{R}_v). \end{aligned} \tag{5.9}$$

Thus, the following result is established.

Theorem 5.4.1 *The model* (5.1) *has:*

i. *a unique endemic equilibrium if* $c < 0$,

ii. *a unique endemic equilibrium if* $b < 0$ *and* $c = 0$ *or* $\Delta = b^2 - 4ac = 0$,

iii. *two endemic equilibria if* $b < 0, c > 0$ *and* $\Delta > 0$,

iv. *no endemic equilibrium otherwise.*

If $\alpha > 0$, the proof follows easily from the properties of the roots of a quadratic equation. For $\alpha = 0$, one can verify the statements by inspection.

Note that a is always positive and c is positive or negative according as $\mathcal{R}_v$ is less than or greater than unity. It is clear from Case (i) of Theorem 5.4.1 that the

model (5.1) has a unique endemic equilibrium whenever $\mathcal{R}_v > 1$. Furthermore, the possibility of backward bifurcation (where a stable DFE coexists with a stable EE) in model (5.1) is indicated by Case (iii) of Theorem 5.4.1. To check for the possibility of this phenomenon in (5.1), the discriminant Δ of the equation (5.8), is set to zero and solved for the critical value of $\mathcal{R}_v$, denoted by $\mathcal{R}_v^c$, given by

$$\mathcal{R}_v^c = 1 - \frac{b^2}{4ak_1k_2\mu}.$$

It follows that backward bifurcation occurs for values of $\mathcal{R}_v$ such that $\mathcal{R}_v^c < \mathcal{R}_v < 1$. This is illustrated in Figure 5.2 by simulating the model (5.1) with following set of parameter values : $\mu = 0.097, \sigma_1 = 0.5, \sigma_2 = 0.75, \alpha = 0.8, \tau_1 = 0.36, \tau_2 = 0.162, \gamma_1 = 0.52, \gamma_2 = 0.001$ and $\theta = 0.2$ (so that $\mathcal{R}_v^c = 0.8646438738 < \mathcal{R}_v = 0.8709550431 < 1$). Figure 5.2 clearly shows in this case the coexistence of two stable equilibria of model (5.1).

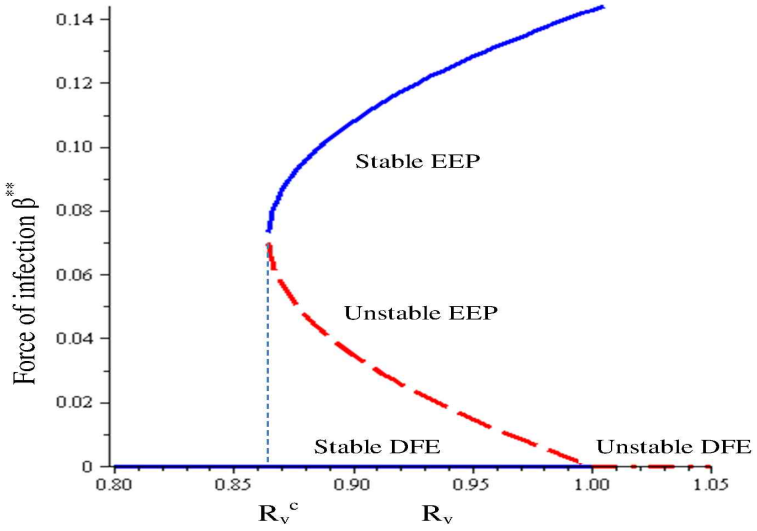

Figure 5.2: Graph of the force of infection β^{**} versus reproduction number $\mathcal{R}_v$ that shows a backward bifurcation diagram for the model (5.1).

Table 5.2: Parameter Values

Parameter	**nominal value**	**references**
Λ	1000	[87]
θ	[0,1]	[81]
μ	0.000648	assumed
σ_1	0.053	[81]
σ_2	0.034	[81]
γ_1	0.1	assumed
γ_2	0.01	assumed
τ_1, τ_2	0.1	assumed
α	0.5	assumed

5.4.2 Coexistence of stable DFE and EE

The parameters θ and α can be considered as controls in the model (5.1) due to their relation to vaccination rate and vaccine efficacy. With all other parameters fixed, the coefficients a, b and c in equation (5.9) are functions of θ and α. Then it follows from Theorem 5.4.1 that a stable DFE coexists with an endemic equilibrium for values of θ and α in the region

$$M = \{(\theta, \alpha) \in [0,1] \times [0,1] : b < 0, c \geq 0, b^2 - 4ac \geq 0\}.$$

The graph of the coexistence region M on the $(\theta,\ \alpha)$ plane is presented on Figure 5.3. One can observe that although the region covers wide range of values of θ and α, for any fixed value of one parameter the range of the other is rather small. Further, the curves $\Delta = 0,\ b = 0$ and $\mathcal{R}_v = 1$ intersect at one point, say P $= (\hat{\theta},\ \hat{\alpha})$. Indeed, it is easy to see that if two of the equations hold then so does the third one, e.g. $\Delta = 0,\ b = 0 \Rightarrow c = 0 \Leftrightarrow \mathcal{R}_v = 1$.

Note that for values of θ larger than $\hat{\theta}$ or values of α smaller than $\hat{\alpha}$ there is no coexistence of DFE with any endemic equilibrium. Depending on the values

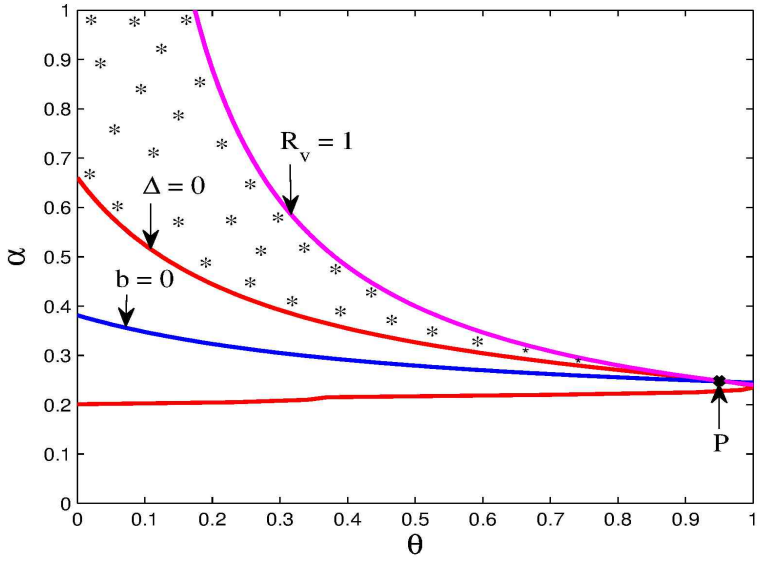

Figure 5.3: Region with stars in the $(\theta,\ \alpha)$ space is defined by $\mathcal{R}_v < 1, b < 0$ and $\Delta > 0$ where stable DFE and EE of model (5.1) coexist. Parameter values used are: $\mu = 0.01, \sigma_1 = 0.07, \sigma_2 = 0.5$, and the values of $\gamma_1, \gamma_2, \tau_1, \tau_2$ are as in 5.2.

of the other parameters the region M may vary in shape and size. However, we will show later that there are always threshold values $\hat{\theta}$ and $\hat{\alpha}$ with the above stated properties. The proof is based on the two special cases given in the next subsection.

5.5 Two special cases

5.5.1 All new recruits are vaccinated $(\theta = 1)$

In this case we have

$$\mathcal{R}_v = \frac{\alpha\sigma_2}{k_2} \tag{5.10}$$

and the coefficients of equation (5.8) in (5.9) are now

$$a = \alpha, \quad b = \alpha\mu + k_2(1 - \mathcal{R}_v), \quad c = k_2\mu(1 - \mathcal{R}_v). \tag{5.11}$$

Then it follows from Theorem 5.4.1 that there is no endemic equilibrium when $\mathcal{R}_v \leq 1$. The following theorem shows that if $\mathcal{R}_v \leq 1$, the DFE is globally asymptotically stable on Ω.

Theorem 5.5.1 *The DFE ($\mathcal{E}_0$) of the model* (5.1) *is GAS on* Ω *whenever* $\mathcal{R}_v \leq 1$ *and* $\theta = 1$.

proof. Since for $\theta = 1$ there are no recruits in the compartment S_1 both S_1 and I_1 approach zero as $t \to \infty$. This essentially means that the model is reduced to a two dimensional system

$$\begin{aligned} \frac{dS_2}{dt} &= \Lambda + \gamma_2 I_2 - \frac{\alpha\sigma_2 I_2}{N} S_2 - \mu S_2, \\ \frac{dI_2}{dt} &= \frac{\alpha\sigma_2 I_2}{N} S_2 - (\gamma_2 + \mu + \tau_2) I_2. \end{aligned} \tag{5.12}$$

This argument can be made precise by using LaSalle's Invariance Principle (Theorem 2.3.2) with Lyapunov function

$$G(S_1, I_1, S_2, I_2) = S_1 + I_1.$$

Indeed, we have

$$\dot{G} = \frac{dS_1}{dt} + \frac{dI_1}{dt} = -\mu S_1 - (\gamma_1 + \mu + \tau_1) I_1 \leq 0$$

and

$$\dot{G} = 0 \Leftrightarrow S_1 = I_1 = 0.$$

Therefore, the subdomain of Ω given by

$$\begin{aligned} \hat{\Omega} &= \{(S_1, I_1, S_2, I_2) \in \Omega : S_1 = I_1 = 0\} \\ &= \left\{(0, 0, S_2, I_2) \in \Omega : S_2 \geq 0, I_2 \geq 0, S_2 + I_2 \leq \frac{\Lambda}{\mu}\right\} \end{aligned}$$

is a stable and attractive invariant set of (5.1). Hence, $\mathcal{E}_0$ is GAS equilibrium of (5.1) on Ω if $\mathcal{E}_0$ is GAS equilibrium of (5.1) on $\hat{\Omega}$ or equivalently that $\tilde{\mathcal{E}}_0 = (S_2^*, I_2^*) = \left(\frac{\Lambda}{\mu}, 0\right)$ is a GAS equilibrium of (5.12) on

$$\tilde{\Omega} = \left\{(S_2, I_2) \in \mathbb{R}_+^2 : S_2 + I_2 \leq \frac{\Lambda}{\mu}\right\}.$$

In order to prove this, we apply again the LaSalle's Invariance Principle with quadratic Lyapunov function as in [88]

$$\mathcal{F}(S_2, I_2) = \frac{1}{2} I_2^2.$$

We have

$$\begin{aligned}
\dot{\mathcal{F}} = I_2 \frac{dI_2}{dt} &= I_2(\alpha\beta S_2 - k_2 I_2), \\
&= I_2 \left(\frac{\alpha\sigma_2 I_2 S_2}{S_2 + I_2} - k_2 I_2\right), \\
&= -k_2 \frac{I_2^2}{S_2 + I_2} \left(S_2 + I_2 - \frac{\alpha\sigma_2 S_2}{k_2}\right), \\
&= -k_2 \frac{I_2^2}{S_2 + I_2} [S_2(1 - \mathcal{R}_v) + I_2].
\end{aligned}$$

Thus, if $\mathcal{R}_v \leq 1$ we have $\dot{\mathcal{F}} \leq 0$ with $\dot{\mathcal{F}} = 0$ if and only if $I_2 = 0$. Substituting $I_2 = 0$ in the first equation of (5.12) we obtain that S_2 approaches $\frac{\Lambda}{\mu}$ as $t \to \infty$. Therefore, $\tilde{\mathcal{E}}_0$ is GAS equilibrium of (5.12) on $\tilde{\Omega}$ by Theorem 2.3.2 and consequently $\mathcal{E}_0$ is GAS equilibrium of (5.1) on Ω. ■

5.5.2 Recovery from infection confers permanent immunity ($\alpha = 0$)

In this case we have $\mathcal{R}_v = \frac{\sigma_1(1-\theta)}{k_1}$ and the coefficients of (5.8) in equation (5.9) become

$$a = 0, \quad b = k_1\theta + (\mu + \gamma_1)(1 - \theta), \quad c = k_1\mu(1 - \mathcal{R}_v). \tag{5.13}$$

It then follows from Theorem 5.4.1 that there is no endemic equilibrium when $\mathcal{R}_v \leq 1$. Furthermore, the following theorem shows that if $\mathcal{R}_v \leq 1$, the DFE is globally asymptotically stable on Ω.

Theorem 5.5.2 *The DFE ($\mathcal{E}_0$) of the model* (5.1) *is GAS on* Ω *whenever* $\mathcal{R}_v \leq 1$ *and* $\alpha = 0$.

proof. Since for $\alpha = 0$ recovery from infection confers permanent immunity then the infected compartment I_2 approaches zero as $t \to \infty$. In fact, this reduces (5.1) to the following three dimensional system

$$\begin{aligned} \frac{dS_1}{dt} &= (1-\theta)\Lambda - \frac{\sigma_1 I_1}{N} S_1 - \mu S_1, \\ \frac{dI_1}{dt} &= \frac{\sigma_1 I_1}{N} S_1 - (\gamma_1 + \mu + \tau_1) I_1, \\ \frac{dS_2}{dt} &= \theta\Lambda + \gamma_1 I_1 - \mu S_2. \end{aligned} \tag{5.14}$$

We make this statement precise by using LaSalle's Invariance Principle in a similar way as in the proof of Theorem 5.5.1. We consider the Lyapunov function

$$U(S_1, I_1, S_2, I_2) = \begin{cases} I_2 + \frac{1}{2}(\theta S_1 - (1-\theta)S_2)^2 & \text{if } S_1 > \frac{1-\theta}{\theta} S_2, \\ I_2 & \text{if } S_1 \leq \frac{1-\theta}{\theta} S_2. \end{cases}$$

Then

$$\dot{U} = \begin{cases} \dot{I}_2 + (\theta S_1 - (1-\theta)S_2)(\theta \dot{S}_1 - (1-\theta)\dot{S}_2) & \text{if } S_1 > \frac{1-\theta}{\theta} S_2, \\ \dot{I}_2 & \text{if } S_1 \leq \frac{1-\theta}{\theta} S_2. \end{cases}$$

We have

$$\begin{aligned} \theta \dot{S}_1 - (1-\theta)\dot{S}_2 &= -\mu(\theta S_1 - (1-\theta)S_2) - \theta\beta S_1 - (1-\theta)(\gamma_1 I_1 + \gamma_2 I_2) \\ &\leq -\mu(\theta S_1 - (1-\theta)S_2. \end{aligned}$$

Therefore

$$\dot{U} \leq \begin{cases} -k_2 I_2 - \mu(\theta S_1 - (1-\theta)S_2)^2 & \text{if } S_1 > \frac{1-\theta}{\theta} S_2, \\ -k_2 I_2 & \text{if } S_1 \leq \frac{1-\theta}{\theta} S_2. \end{cases}$$

Hence, $\dot{U} \leq 0$ with $\dot{U} = 0$ if and only if $I_2 = 0$ and $\theta S_1 - (1-\theta)S_2 = 0$. Then it follows that

$$\check{\Omega} = \{(S_1, I_1, S_2, I_2) \in \Omega : \theta S_1 \leq (1-\theta)S_2, I_2 = 0\}$$

is a stable and attractive invariant subdomain of Ω by Theorem 2.3.2. Therefore, $\mathcal{E}_0$ is GAS equilibrium of (5.1) on Ω if it is GAS equilibrium of (5.1) on $\check{\Omega}$ or equivalently that $\bar{\mathcal{E}}_0 = (S_1^*, I_1^*, S_2^*) = \left(\frac{\Lambda(1-\theta)}{\mu}, 0, \frac{\Lambda\theta}{\mu}\right)$ is a GAS equilibrium of (5.14) on

$$\bar{\Omega} = \left\{(S_1, I_1, S_2) \in \mathbb{R}^3_+ : S_1 + I_1 + S_2 \leq \frac{\Lambda}{\mu},\ \theta S_1 \leq (1-\theta)S_2\right\}.$$

For the dynamical system defined by (5.14) on $\bar{\Omega}$, we consider the Lyapunov function $F(S_1, I_1, S_2) = \frac{1}{2}I_1^2$ as in [88]. Then

$$\dot{F} = I_1\frac{dI_1}{dt} = I_1\left(\frac{\sigma_1 I_1}{N}S_1 - k_1 I_1\right) = I_1^2\left(\frac{\sigma_1 S_1}{N} - k_1\right).$$

But on $\check{\Omega}$, we have

$$S_1 = (1-\theta)S_1 + \theta S_1 \leq (1-\theta)S_1 + (1-\theta)S_2 \leq (1-\theta)(S_1+S_2) \leq (1-\theta)N.$$

Therefore

$$\dot{F} \leq I_1^2\left(\frac{\sigma_1(1-\theta)N}{N} - k_1\right) = I_1^2 k_1(\mathcal{R}_v - 1) \leq 0.$$

It is easy to see that $\dot{F} = 0$ if and only if $I_1 = 0$. Substituting $I_1 = 0$ in the first and third equations of (5.14) implies that S_1 approaches $\frac{\Lambda(1-\theta)}{\mu}$ and S_2 approaches $\frac{\Lambda\theta}{\mu}$ as $t \to \infty$. Hence, $\bar{\mathcal{E}}_0$ is GAS equilibrium of (5.14) on $\bar{\Omega}$ by Theorem 2.3.2 and subsequently $\mathcal{E}_0$ is GAS equilibrium of (5.1) on Ω. ■

5.5.3 Existence of thresholds for θ and α

The functions a, b and c in (5.9) used in the equations defining the coexistence region M are all continuous functions of θ and α. Therefore, the topological closure of M is

$$\bar{M} = \{(\theta, \alpha) : b \leq 0, c \geq 0, b^2 - 4ac \geq 0\}.$$

Let

$$\hat{\theta} = \max\{\theta \in [0,1] : \exists\ \alpha \in [0,1] : (\theta, \alpha) \in \bar{M}\}$$

and

$$\hat{\alpha} = \min\{\alpha \in [0,1] : \exists\ \theta \in [0,1] : (\theta, \alpha) \in \bar{M}\}.$$

Assume $\hat{\theta} = 1$, then there exists $\check{\alpha}$ such that $(1, \check{\alpha}) \in \bar{M}$. However, from the discussion in Subsection 3.3.1 we have $(1, \check{\alpha}) \notin M$. Therefore $b = 0$ at the point $(1, \check{\alpha})$ in Figure 5.3. Then it follows from (5.11) that $\alpha = 0$ and $\mathcal{R}_v = 1$ which contradicts (5.10). Thus $\hat{\theta} < 1$. Similarly, using Subsection 3.3.2 we show that $\hat{\alpha} > 0$.

These results show that the backward bifurcation can be removed if either (i) significantly large proportion of the population are vaccinated or (ii) the vaccine efficacy $\phi = 1 - \alpha$ is high enough. Indeed, in the parameter regime of the coexistence region (Figure 5.3) $\hat{\alpha} = 0.25$ and $\hat{\theta} = 0.95$, so that at least 75% vaccine efficacy or 95% vaccination coverage is required to remove backward bifurcation.

5.6 Impact of vaccine

Since preliminary data from a previous study of African buffalo suggests that the Bacille Calmette-Guerin (BCG) vaccine was not effective [89] despite its potential impact in some alternative BTB hosts, it is useful to investigate whether or not the widespread application of such imperfect vaccine in free-ranging African buffalo will be beneficial or not. The impact of such vaccine is usually qualitatively assessed *via* threshold analysis of the associated vaccinated reproduction number $\mathcal{R}_v$ defined in (5.2) [85, 86]. More precisely, $\mathcal{R}_v$ is considered as a function of the fraction θ of vaccinated individuals at DFE ($\theta = S_2^*/N^*$). Then the vaccine is said to have positive or negative impact according as $\frac{\partial \mathcal{R}_v}{d\theta} < 0$ or $\frac{\partial \mathcal{R}_v}{d\theta} > 0$, respectively [86]. It is common for this analysis to be carried out in terms of the vaccine efficacy (ϕ) [86]. Then from (5.2), we obtain

$$\frac{\partial \mathcal{R}_v}{d\theta} = \frac{-\sigma_1 k_2 + \sigma_2 k_1(1-\phi)}{k_1 k_2}. \tag{5.15}$$

The sign of $\frac{\partial \mathcal{R}_v}{d\theta}$ is characterized *via* the critical value of ϕ,

$$\phi^c = 1 - \frac{k_2\sigma_1}{k_1\sigma_2}.$$

More precisely, $\frac{d\mathcal{R}_v}{d\theta} < 0$ if and only if $\phi > \phi^c$. In practical terms this means that when ϕ is larger than the threshold ϕ^c, any increase in the vaccinated fraction θ reduces $\mathcal{R}_v$ and, in this sense, the vaccine is having a positive impact [85, 86].

An alternative approach is by using the concept of vaccine impact [90, 91, 92, 93, 94].

$$\Pi = \frac{S_2^*}{N^*}\left(1 - \frac{\alpha k_1\sigma_2}{k_2\sigma_1}\right) = \frac{S_2^*}{N^*}\left(1 - \frac{\mathcal{R}_1}{\mathcal{R}_0}\right), \tag{5.16}$$

where $\mathcal{R}_0 = \frac{\sigma_1}{k_1}$ is the reproduction number of model (5.1) with no vaccination and $\mathcal{R}_1 = \frac{\alpha\sigma_2}{k_2}$ is the reproduction number with population fully-vaccinated.

Note that

$$\mathcal{R}_v = \mathcal{R}_0(1 - \Pi). \tag{5.17}$$

Therefore, the positive impact ($\frac{\partial \mathcal{R}_v}{d\theta} < 0$) is equivalent to $\Pi > 0$. The discussion results are summarized in the following theorem.

Theorem 5.6.1 *For an imperfect BTB vaccine*

(i) *if $\phi > \phi^c$ then the vaccine has positive impact* ($\Pi > 0$),

(ii) *if $\phi = \phi^c$ then the vaccine has no impact* ($\Pi = 0$),

(iii) *if $\phi < \phi^c$ then the vaccine has negative impact* ($\Pi < 0$).

proof. (i) Suppose $\phi > \phi^c$, then $(1-\alpha) > (1 - \frac{k_2\sigma_1}{k_1\sigma_2})$. Therefore, $\alpha < \frac{k_2\sigma_1}{k_1\sigma_2}$ which implies that $\mathcal{R}_1 < \mathcal{R}_0$ so that $\Pi > 0$. Then it follows from (5.17) that $\mathcal{R}_v < \mathcal{R}_0$ indicating that the vaccine has positive impact. Similarly, $\phi = \phi^c$ and $\phi < \phi^c$ implies that $\mathcal{R}_1 = \mathcal{R}_0$ and $\mathcal{R}_1 > \mathcal{R}_0$, respectively. Using these relations in (5.16) give $\Pi = 0$ and $\Pi < 0$ which from (5.17) lead to $\mathcal{R}_v = \mathcal{R}_0$ and $\mathcal{R}_v > \mathcal{R}_0$, respectively. Therefore, the results of (ii) and (iii) follows. ■

The result in Theorem 5.6.1, is numerically validated, by depicting $\mathcal{R}_v$ as a function of the vaccinated susceptible buffalo θ, in Figure 5.4 , for the cases where $\phi > \phi^c$ and $\phi < \phi^c$. The figure indicates that, the reproduction threshold, $\mathcal{R}_v$, decreases with increasing values of θ when $\phi > \phi^c$. On the other hand, $\mathcal{R}_v$ increases as θ increases when $\phi < \phi^c$.

To get a clear insight of vaccine impact in reducing the spread of infection at endemic state, a plot of the BTB prevalence as a function of time is depicted in Figure 5.5. It is evident from Figure 5.5 that prevalence decreases with decreasing value of the vaccinated reproduction number ($\mathcal{R}_v$). It should be noted that the reproduction number before the vaccination ($\mathcal{R}_0$), is always greater than the reproduction number in the presence of vaccination ($\mathcal{R}_v$) at the endemic state. Thus, vaccination reduces the prevalence of the disease.

A contour plot of the reproduction threshold $\mathcal{R}_v$, as a function of vaccine efficacy (ϕ) and fraction of vaccinated buffalo (θ), is depicted in Figure 5.6. The contours indicate that for effective disease elimination, a vaccine efficacy (ϕ) and fraction of vaccinated susceptible buffalo (θ) are to be high enough. For instance, if 90% of susceptible African buffalo are vaccinated, an efficacy level of at least 85% would be required to eradicate the disease.

5.7 Summary

A two-stage deterministic epidemiological model in animal population with bovine tuberculosis in African buffalo as a guiding example, is designed and rigorously analyzed, in this chapter. Some of the main findings of the study are:

(1) The presented model exhibits the phenomenon of backward bifurcation for certain values of the parameters.

(2) The presence of backward bifurcation does not arise under each of the following scenarios:

   (i) sufficiently large fraction (at least 95%) but not necessarily all of recruited buffalo are vaccinated,

(ii) if the efficacy of the vaccine is high enough (at least 75%), although it need not be perfect.

(3) The disease-free equilibrium is proved to be globally-asymptotically stable whenever all new recruits are vaccinated ($\theta = 1$) or the vaccine is 100% effective ($\alpha = 0$).

(4) Numerical simulations of the model demonstrate that, the use of an imperfect vaccine can lead to effective control of the disease if the vaccination coverage and the efficacy of vaccine are high enough, at least 90% each.

(5) Vaccination with BCG is a means of reducing levels of bovine TB, thereby, diminishing the spread and severity of the disease in African buffalo population. This follows from the model result in the parameter regime of the coexistence region (Figure 3), that for effective disease eradication a high vaccination coverage or vaccine efficacy is required. But in the field high coverage is very challenging and efficacy of the BCG vaccine may wane with prior exposure to mycobacteria [95]. This conclusion is in line with the finding in [81] that eradication of BTB *via* vaccination alone may not be an effective control strategy .

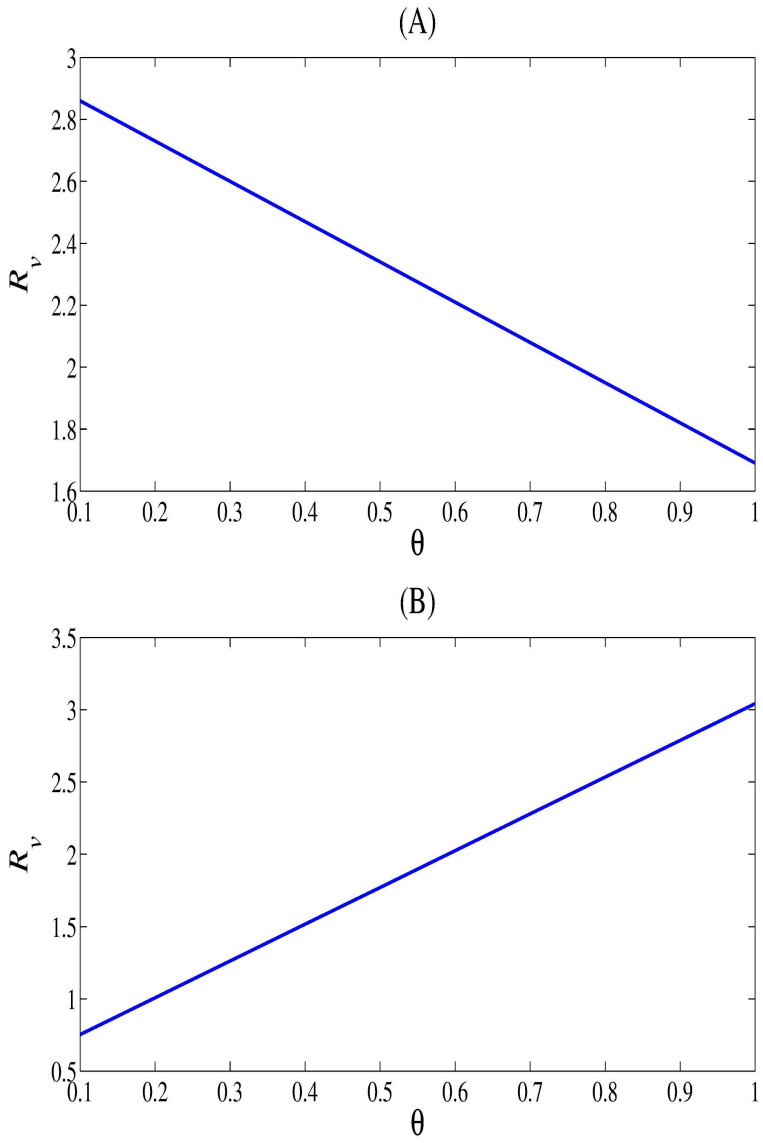

Figure 5.4: Simulation of model (5.1), showing $\mathcal{R}_v$ as a function of the fraction of vaccinated susceptible buffalo at DFE ($\theta = S_2^*/N^*$). Parameter values used are as in Table 5.2 (A): $\phi = 0.5$, $\mathcal{R}_0 = 0.2641$, $\mathcal{R}_1 = 0.1536$ (so that $0.5 = \phi > \phi^c = 0.1404$ and $\mathcal{R}_0 > \mathcal{R}_1 \Rightarrow \Pi > 0$); (B): $\phi = 0.01$, $\mathcal{R}_0 = 0.2641$, $\mathcal{R}_1 = 0.3042$ (so that $0.01 = \phi < \phi^c = 0.1404$ and $\mathcal{R}_0 < \mathcal{R}_1 \Rightarrow \Pi < 0$).

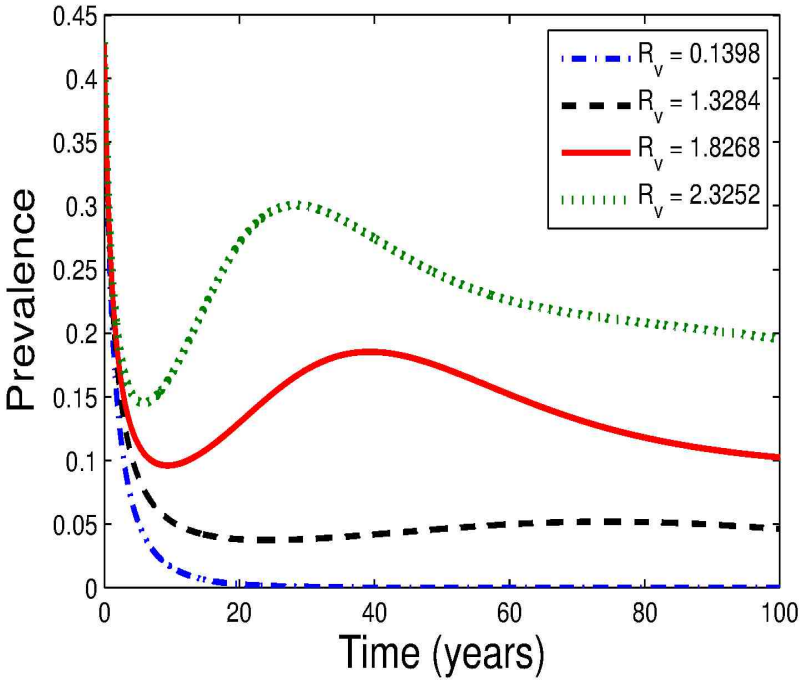

Figure 5.5: Prevalence as a function of time for model (5.1) showing positive impact of vaccine: when $\sigma_1 = 0.93$ then $\mathcal{R}_v = 2.3252 < \mathcal{R}_0 = 4.6350$; when $\sigma_1 = 0.73$ then $\mathcal{R}_v = 1.8268 < \mathcal{R}_0 = 3.6382$; when $\sigma_1 = 0.53$ then $\mathcal{R}_v = 1.3284 < \mathcal{R}_0 = 2.6414$; when $\sigma_1 = 0.053$ then $\mathcal{R}_v = 0.1398 < \mathcal{R}_0 = 0.2641$. Other parameter values used are as given in Table 2 with $\sigma_2 = 0.0034$.

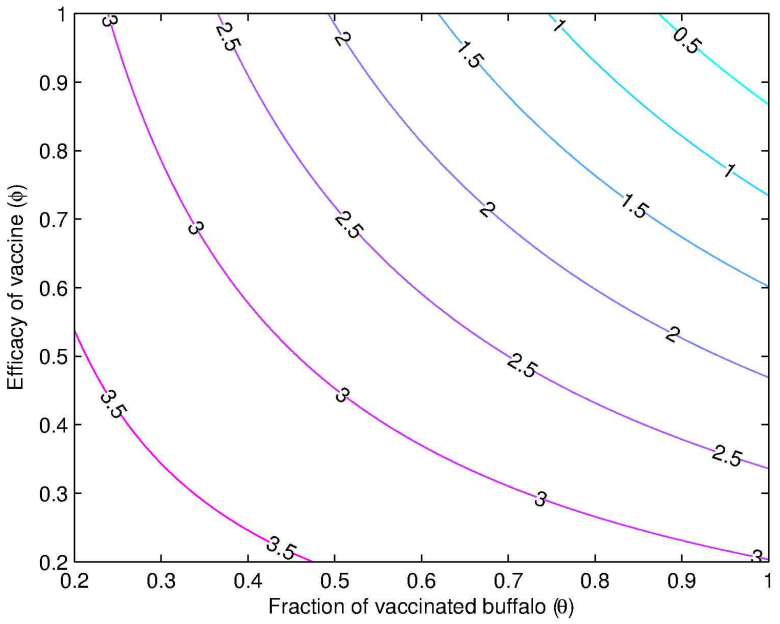

Figure 5.6: Contour plot of $\mathcal{R}_v$ of the model (5.1) as a function of vaccine efficacy (ϕ) and fraction of vaccinated susceptible buffalo (θ). Parameter values used are $\mu = 0.000648, \sigma_1 = 0.83, \sigma_2 = 0.3, \gamma_1 = 0.09, \gamma_2 = 0.01, \tau_1 = 0.12, \tau_2 = 0.069$. The reproduction number without vaccination is $\mathcal{R}_0 = 3.94$ which indicates that vaccination always has positive impact.

CHAPTER 6

Conclusion and Future Work

In this thesis, we have presented an in-depth mathematical study of some epidemiological models that exhibit complex and non-trivial outcomes on the dynamics of a population. We have presented in the first part (Chapter 3 and Chapter 4) of our study the combined impact of infectious disease and Allee effect. These are some of the extinction drivers that recently received considerable attention in the extinction research. Indeed, their joint interplay have long been recognized to drive host population to extinction. In the last part (Chapter 5) of this study, we have considered the role of structured acquired-immunity on the dynamics of a population due to repeated exposure to mycobacteria. We developed the three presented models from the models introduced in [23], [16] and [28], respectively.

In Chapter 3, an SI model with demographic Allee effect in which the vital dynamics (birth and death) are both modeled as quadratic polynomials is designed and rigorously analyzed. This approach provides ample opportunity for taking into account the major contributors to the Allee effect given in Table 1.1 and makes the presented model more general and biologically relevant. It also provides a more realistic representation of the population dynamics particularly at low density or small population size, in the sense that the specific choice of the quadratic mortality rate function arises from the Allee mechanisms that affect survival or

both survival and reproduction at all densities and intraspecific competition. This allow us to explore a range of values of the parameter α and that of β, which determine the intensity of the Allee effects on both fertility and mortality rate functions. More specifically, the mortality rate decreases when $\beta > 0$ and it increases if $\beta \leq 0$ while the values of all the other parameters are fixed, testifying that some species are more susceptible to the Allee effects than others. This follows from the fact that species whose individuals benefit from the presence of conspecifics are more susceptible to the Allee effects than others [26, 68]. This study generalizes some of the previous studies in the literature as if $\alpha = \beta = 0$, we have a nonlinear fertility function and a constant mortality rate as in [20]. For $\alpha = 0, \beta = -\frac{1}{ku}$, the demographic functions of the proposed model are quadratic and linear similar to those in [23]. In this case the presented model can be considered as an extension of the model of [23]. Stability analysis of both disease-free and endemic equilibria are carried out, which reveal that if $\mathcal{R}_0 < 1$ the model has two bistable attractors: the trivial extinction state and the carrying capacity state. In such a case the disease cannot invade from arbitrarily small introductions into the host population at carrying capacity. From biological point of view, in the absence of disease the presence of an Allee effect in the host demographic plays a protective and a stabilizing role in relations to the disease invasion. On the other hand, in the presence of infection an additional disease-related mortality increases the likelihood of population extinction. More precisely, the disease establishes an effective host eradication threshold above the Allee threshold u. On the other hand, if $\mathcal{R}_0 > 1$ a locally asymptotically stable endemic equilibrium may exist. Moreover, the model suggests that additional disease related mortality increases the likelihood of population extinction.

It is well known that the maximum degree of depression of a host population equilibrium is achieved by intermediate disease pathogenicity, i.e. low to moderate pathogenicity [69, 70]. In view of that, we obtain two important threshold quantities λ_0 and λ_1 of the transmissibility λ. If the disease pathogenicity is low ($\mu < \mu^*$) such that $\lambda > \lambda_0$, the disease could establish itself in the host population (Figure 3.4). On the other hand, if the disease pathogenicity is high, i.e. $\mu > \mu^*$ such that $\lambda \in (\lambda_0, \lambda_1)$, the disease can either invade the population or drive the host population to extinction depending on the initial sizes of the host

and infected sub-populations due to the strong Allee effect. For some high value of μ, the dynamics of the model could undergo some substantial changes as λ decreases from λ_1 to λ_0. First, the stable endemic equilibrium becomes unstable and so, both the total population and the infected sub-population start oscillating in form of stable limit cycles (illustrated in Figure 3.5C). This mathematically corresponds to a Hope bifurcation scenario. Then, the oscillations disappear as a results of a coalition between the increasing limit cycles and the Allee threshold state $\mathcal{E}_1$, which is known as a Homoclinic bifurcation. Despite the disappearance of the limit cycles, the unstable endemic equilibrium still persist and so, there is no endemic attractor any more. This leads to the extinction of the whole population. Moreover, the unstable endemic equilibrium also disappears when the total population falls below the Allee threshold due to disease related mortality. As expected, the model presented in [23] exhibits all these dynamical behaviors being a special case of the model presented in this chapter. In addition, if the disease pathogenicity is high ($\mu > \mu^*$) and $\lambda > \lambda_1$ the disease drive the host population to extinction. Thus, the system is rendered monostable with the trivial extinction state $\mathcal{E}_0$ being the only global attractor, see for example Figure 3.5A. In particular, when $\lambda > \lambda_1$ there is a disease-induced extinction for any initial state.

For the special cases of the model, verifiable conditions that guarantee host persistence (with or without infected individuals) and extinction are derived. The extinction scenario shows that a small perturbation to the disease-free equilibrium can lead to a catastrophic extinction of the host population in the presence of a strong Allee effect. Indeed, when a fatal disease invades the host population whose demographics are manifested with a strong Allee effect an effective extinction threshold above the Allee threshold is established, see similar results in [15, 22, 24]). Numerical simulations under the special cases of the model show that the persistence and extinction regions of the host population vary in size with altering value of β.

In Chapter 4, we extended the SI model introduced in Chapter 3 by adding the compartment of exposed individuals and replacing the density-dependent transmission with frequency-dependent transmission. While Chapter 3 basically provides a more realistic representation of a population dynamics at low population

density, Chapter 4 focusses on the combined impact of infectious disease and Allee effect at high population level despite the fact that the definition of an Allee effect does not imply any impact at high population. However, investigating such impact and understanding which species are more vulnerable than others to decline and extinction at high population play a relevant role in conservation biology for guiding management actions. This is because such an information would allow biologists to predict the vulnerability of species to extinction even before they decline, thereby improving the species' chances of survival [74]. There is an increasing evidence that the Allee effect is to be more likely to occur when individuals benefit from the presence of conspecifics [1, 26]. Therefore, endangered species whose individuals behave in a such manner experience heavy mortality at low population and hence are more susceptible to extinction because they rely on mass numbers and a strategy of predator satiation for survival [77]. In light of this, the model suggests that the joint impact of infectious disease and the Allee effect at high population may lead to a catastrophic crash to extinction. The tipping point marking the unexpected population collapse is mathematically associated with a saddle-node bifurcation. When the two endemic equilibria $\mathcal{E}_1^*$ and $\mathcal{E}_2^*$ coalesce and disappear, there is no endemic attractor left and extinction is an eventual outcome. The endemic state $\mathcal{E}_2^*$ emerges from the carrying capacity state if $\mathcal{R}_0 > 1$, which has a larger population size than $\mathcal{E}_1^*$. $\mathcal{E}_1^*$ bifurcates from the Allee threshold state on the disease-free boundary into the interior of the domain if $\mathcal{R}_u > 1$ or equivalently $\mathcal{R}_0 > \mathcal{R}_0^u$. The emergence of the unstable equilibrium $\mathcal{E}_1^*$ establishes the extinction basin above the Allee threshold and it is essential for the saddle-node bifurcation to occur.

From biological point of view, the underlying mechanisms of the spontaneous population collapse are: the regulatory potential of disease, which leads to a depression of the host population size p_2^* at endemic equilibrium and additional disease induced mortality that increases the likelihood of extinction (i.e. the effective extinction threshold becomes larger). Therefore, the infection attacks the host from two ends of the population size spectrum, thereby reducing the range of possible endemic persistence. Hence extinction takes place when the range of viable population sizes could not exist. The bifurcation analysis of the model reveals that species whose individuals benefit from the presence of conspecifics

are more prone to decline and extinction at high population level. This is because the value of the tipping point $\mathcal{R}_0^c$ marking the unanticipated population collapse is smaller when $\beta > 0$ than for $\beta \leq 0$. Indeed, determining the range of values of the parameters α and β makes the model more general and biologically relevant than the model of Hilker in [16].

Mathematically, we provide a new approach to investigate species' differential susceptibility to the Allee effects. An approach which makes the presented models more general than some of those in the previous studies [16, 20, 23]. Indeed, determining the range of values of the parameters α and β which determine the intensity of the Allee effects on both the fertility and the mortality rate functions $B(P)$ and $D(P)$ would be of crucial importance in ecology and conservation for identifying potential extinction risks and guiding management actions.

In Chapter 5, we have presented a two-stage deterministic epidemiological model in animal population with bovine tuberculosis in African buffalo as a guiding example. The model is rigorously analyzed to get insight for the role of acquired-immunity due to repeated exposure to mycobacteria. This chapter extends the model of Greenhalgh *et al.* introduced in [28] by incorporating vital dynamics in a population with varying size which makes the model more realistic and practically relevant. We show that the model exhibits the phenomenon of backward bifurcation for certain values of the parameters. The existence of this phenomenon makes disease control more difficult owing to endemic persistence when $\mathcal{R}_0 < 1$. Indeed, for effective disease elimination when a backward bifurcation occurs $\mathcal{R}_0$ must be reduced below the sub-threshold $\mathcal{R}_0^c < 1$.

Furthermore, we identified some scenarios under which a backward bifurcation does not arise. These are the cases when either sufficiently large fraction (at least 95%) but not necessarily all of recruited buffalo are vaccinated or if the efficacy of the vaccine is high enough (at least 75%), although it need not be perfect. In each of these scenarios the classical requirement of having $\mathcal{R}_0 < 1$ is sufficient for disease eradication. Furthermore, the disease-free equilibrium is proved to be globally asymptotically stable whenever all new recruits are vaccinated ($\theta = 1$) or the vaccine is 100% effective ($\alpha = 0$). Numerical simulations of the model demonstrate that, the use of an imperfect vaccine can lead to effective control of the disease if the vaccination coverage and the efficacy of vaccine are high enough,

at least 90% each. The numerical observation reveals that vaccination with BCG is a means of reducing levels of bovine TB, thereby, diminishing the spread and severity of the disease in African buffalo population. This is for the fact that in the field high coverage is very challenging and efficacy of the BCG vaccine may wane with prior exposure to mycobacteria [95]. This conclusion is in line with the finding in [81] that eradication of BTB *via* vaccination alone may not be an effective control strategy.

In future work the models presented in this thesis will be extended by considering more complex dynamics. For example, the models described in Chapter 3 and Chapter 4 will be extended by incorporating either migration between at least two patches or including a control strategy such as vaccination and culling. The two-stage model presented in Chapter 5 will be reformulated by separating the vaccinated compartment from the compartment of the subsequent times susceptible individuals and incorporating the waning rate of vaccine-induced immunity. It can also be extended by either using n-stages or including combined control strategies such as vaccination and culling.

BIBLIOGRAPHY

[1] P. Stephens, W. Sutherland, and R. Freckleton, "What is the Allee effect?," *Oikos*, pp. 185–190, 1999.

[2] W. Allee, "Animal Aggregations, a Study in General Sociology. 1931."

[3] W. Allee, *The Social Life of Animals*. New York, 1938.

[4] F. Courchamp, L. Berec, and J. Gascoigne, *Allee Effect in Ecology and Conservation*. Oxford University Press, New York, 2008.

[5] D. L. Clifford, J. A. Mazet, E. J. Dubovi, D. K. Garcelon, T. J. Coonan, P. A. Conrad, and L. Munson, "Pathogen exposure in endangered island fox (urocyon littoralis) populations: implications for conservation management," *Biological Conservation*, vol. 131, no. 2, pp. 230–243, 2006.

[6] E. Angulo, G. W. Roemer, L. BEREC, J. Gascoigne, and F. Courchamp, "Double allee effects and extinction in the island fox," *Conservation Biology*, vol. 21, no. 4, pp. 1082–1091, 2007.

[7] R. Burrows, H. Hofer, and M. L. East, "Population dynamics, intervention and survival in african wild dogs (lycaon pictus)," *Proceedings of the Royal Society of London. Series B: Biological Sciences*, vol. 262, no. 1364, pp. 235–245, 1995.

[8] F. Courchamp, T. Clutton-Brock, and B. Grenfell, "Multipack dynamics and the allee effect in the african wild dog, lycaon pictus," *Animal Conservation*, vol. 3, no. 4, pp. 277–285, 2000.

[9] C. Walters and J. F. Kitchell, "Cultivation/depensation effects on juvenile survival and recruitment: implications for the theory of fishing," *Canadian Journal of Fisheries and Aquatic Sciences*, vol. 58, no. 1, pp. 39–50, 2001.

[10] Y. Willi, J. Van Buskirk, and M. Fischer, "A threefold genetic Allee effect population size affects cross-compatibility, inbreeding depression and drift load in the self-incompatible ranunculus reptans," *Genetics*, vol. 169, no. 4, pp. 2255–2265, 2005.

[11] F. Courchamp, E. Angulo, P. Rivalan, R. J. Hall, L. Signoret, L. Bull, and Y. Meinard, "Rarity value and species extinction: the anthropogenic Allee effect," *PLoS biology*, vol. 4, no. 12, pp. 2405–2406, 2006.

[12] L. Berec, E. Angulo, and F. Courchamp, "Multiple Allee effects and population management," *Trends in Ecology & Evolution*, vol. 22, no. 4, pp. 185–191, 2007.

[13] D. S. Boukal, M. W. Sabelis, and L. Berec, "How predator functional responses and Allee effects in prey affect the paradox of enrichment and population collapses," *Theoretical Population Biology*, vol. 72, no. 1, pp. 136–147, 2007.

[14] A. Friedman and A.-A. Yakubu, "Host Demographic Allee Effect, Fatal Disease, and Migration: Persistence or Extinction," *SIAM Journal on Applied Mathematics*, vol. 72, no. 5, pp. 1644–1666, 2012.

[15] F. M. Hilker, M. Langlais, S. V. Petrovskii, and H. Malchow, "A diffusive SI model with Allee effect and application to FIV," *Mathematical Biosciences*, vol. 206, no. 1, pp. 61–80, 2007.

[16] F. M. Hilker, "Population collapse to extinction: the catastrophic combination of parasitism and Allee effect," *Journal of Biological Dynamics*, vol. 4, no. 1, pp. 86–101, 2010.

[17] L.-l. Chen and C. Hui, "Habitat destruction and the extinction debt revisited: The Allee effect," *Mathematical Biosciences*, vol. 221, no. 1, pp. 26–32, 2009.

[18] Y. Kang and C. Castillo-Chavez, "A simple epidemiological model for populations in the wild with Allee effects and disease-modified fitness.," *Discrete & Continuous Dynamical Systems-Series B*, vol. 19, no. 1, pp. 89–130, 2014.

[19] S. R.-J. Jang, "Discrete-time host–parasitoid models with Allee effects: density dependence versus parasitism," *Journal of Difference Equations and Applications*, vol. 17, no. 04, pp. 525–539, 2011.

[20] H. R. Thieme, T. Dhirasakdanon, Z. Han, and R. Trevino, "Species decline and extinction: synergy of infectious disease and Allee effect?," *Journal of Biological dynamics*, vol. 3, no. 2-3, pp. 305–323, 2009.

[21] D. S. Boukal and L. Berec, "Single-species models of the Allee effect: extinction boundaries, sex ratios and mate encounters," *Journal of Theoretical Biology*, vol. 218, no. 3, pp. 375–394, 2002.

[22] A. Deredec and F. Courchamp, "Combined impacts of Allee effects and parasitism," *Oikos*, vol. 112, no. 3, pp. 667–679, 2006.

[23] F. M. Hilker, M. Langlais, and H. Malchow, "The Allee effect and infectious diseases: extinction, multistability, and the (dis-) appearance of oscillations," *The American Naturalist*, vol. 173, no. 1, pp. 72–88, 2009.

[24] A. Friedman and A.-A. Yakubu, "Fatal disease and demographic Allee effect: population persistence and extinction," *Journal of Biological Dynamics*, vol. 6, no. 2, pp. 495–508, 2012.

[25] L. Cai, G. Chen, and D. Xiao, "Multiparametric bifurcations of an epidemiological model with strong Allee effect," *Journal of Mathematical Biology*, vol. 67, no. 2, pp. 185–215, 2013.

[26] F. Courchamp and D. W. Macdonald, "Crucial importance of pack size in the african wild dog lycaon pictus," *Animal Conservation*, vol. 4, no. 02, pp. 169–174, 2001.

[27] M. Kermack and A. McKendrick, "Contributions to the mathematical theory of epidemics. part i," in *Proc. R. Soc. A*, vol. 115, pp. 700–721, 1927.

[28] D. Greenhalgh, O. Diekmann, and M. de Jong, "Subcritical endemic steady states in mathematical models for animal infections with incomplete immunity," *Mathematical Biosciences*, vol. 165, no. 1, pp. 1–25, 2000.

[29] M. Safan, H. Heesterbeek, and K. Dietz, "The minimum effort required to eradicate infections in models with backward bifurcation," *Journal of Mathematical Biology*, vol. 53, no. 4, pp. 703–718, 2006.

[30] Z. Ma, J. Liu, and J. Li, "Stability analysis for differential infectivity epidemic models," *Nonlinear Analysis: Real World Applications*, vol. 4, no. 5, pp. 841–856, 2003.

[31] J. M. Hyman and J. Li, "Differential susceptibility epidemic models," *Journal of Mathematical Biology*, vol. 50, no. 6, pp. 626–644, 2005.

[32] S. M. Moghadas and A. B. Gumel, "Global stability of a two-stage epidemic model with generalized non-linear incidence," *Mathematics and Computers in simulation*, vol. 60, no. 1, pp. 107–118, 2002.

[33] J. M. Hyman and J. Li, "Differential susceptibility and infectivity epidemic models," *Mathematical Biosciences and Engineering*, vol. 3, no. 1, pp. 89–100, 2006.

[34] D. Greenhalgh and M. Griffiths, "Backward bifurcation, equilibrium and stability phenomena in a three-stage extended BRSV epidemic model," *Journal of Mathematical Biology*, vol. 59, no. 1, pp. 1–36, 2009.

[35] A. Schweitzer and R. Anderson, "Dynamic interaction between $CD4^+$ T cells and parasitic helminths: mathematical models of heterogeneity in outcome," *Parasitology*, vol. 105, no. 03, pp. 513–522, 1992.

[36] C. Castillo-Chavez, K. Cooke, W. Huang, and S. Levin, "Results on the dynamics for models for the sexual transmission of the human immunodeficiency virus," *Applied Mathematics Letters*, vol. 2, no. 4, pp. 327–331, 1989.

[37] C. Castillo-Chavez, K. L. Cooke, W. Huang, and S. A. Levin, "On the role of long incubation periods in the dynamics of acquired immunodeficiency syndrome (AIDS). part 2: Multiple group models," in *Mathematical and statistical approaches to AIDS epidemiology*, pp. 200–217, Springer, 1989.

[38] W. Huang, K. L. Cooke, and C. Castillo-Chavez, "Stability and bifurcation for a multiple-group model for the dynamics of HIV/AIDS transmission," *SIAM Journal on Applied Mathematics*, vol. 52, no. 3, pp. 835–854, 1992.

[39] B. Buonomo and D. Lacitignola, "On the backward bifurcation of a vaccination model with nonlinear incidence," *Nonlinear Analysis: Modelling and Control*, vol. 16, no. 1, pp. 30–46, 2011.

[40] S. M. Garba, M. A. Safi, and A. Gumel, "Cross-immunity-induced backward bifurcation for a model of transmission dynamics of two strains of influenza," *Nonlinear Analysis: Real World Applications*, vol. 14, no. 3, pp. 1384–1403, 2013.

[41] A. Gumel, "Causes of backward bifurcations in some epidemiological models," *Journal of Mathematical Analysis and Applications*, vol. 395, no. 1, pp. 355–365, 2012.

[42] K. Hadeler and P. Van den Driessche, "Backward bifurcation in epidemic control," *Mathematical Biosciences*, vol. 146, no. 1, pp. 15–35, 1997.

[43] J. Arino, C. C. McCluskey, and P. van den Driessche, "Global results for an epidemic model with vaccination that exhibits backward bifurcation," *SIAM Journal on Applied Mathematics*, vol. 64, no. 1, pp. 260–276, 2003.

[44] M. Safan and K. Dietz, "On the eradicability of infections with partially protective vaccination in models with backward bifurcation.," *Mathematical Biosciences and Engineering: MBE*, vol. 6, no. 2, pp. 395–407, 2009.

[45] S. Busenberg and P. Van den Driessche, "Analysis of a disease transmission model in a population with varying size," *Journal of Mathematical Biology*, vol. 28, no. 3, pp. 257–270, 1990.

[46] H. W. Hethcote and P. Van den Driessche, "An SIS epidemic model with variable population size and a delay," *Journal of Mathematical Biology*, vol. 34, no. 2, pp. 177–194, 1995.

[47] J. Zhou and H. W. Hethcote, "Population size dependent incidence in models for diseases without immunity," *Journal of Mathematical Biology*, vol. 32, no. 8, pp. 809–834, 1994.

[48] R. Anguelov, S. M. Garba, and S. Usaini, "Backward bifurcation analysis of epidemiological model with partial immunity," *Computers & Mathematics with Applications*, vol. 68, no. 9, pp. 931–940, 2014.

[49] A. Stuart and A. R. Humphries, *Dynamical Systems and Numerical Analysis*, vol. 2. Cambridge University Press, 1998.

[50] S. Wiggins and M. Golubitsky, *Introduction to Applied Nonlinear Dynamical Systems and Chaos*, vol. 2. Springer, 1990.

[51] J. D. Meiss, *Differential Dynamical Systems*, vol. 14. SIAM, 2007.

[52] J. Hale, *Ordinary Differential Equations*. Interscience, New York, 1969.

[53] H. K. Khalil and J. Grizzle, *Nonlinear Systems*, vol. 3. Prentice hall Upper Saddle River, 2002.

[54] J. M. Pena, "Characterizations and stable tests for the routh–hurwitz conditions and for total positivity," *Linear algebra and its applications*, vol. 393, pp. 319–332, 2004.

[55] D. A. Sánchez, *Ordinary Differential Equations and Stability Theory: an Introduction*. Courier Dover Publications, 1979.

[56] F. Z. Castillo-Chavez C and H. W, "On the computation of R_0 and its role in global stability," in *Mathematical approaches for emerging and reemerging infectious diseases: an introduction (Mineapolis, MN, 1999), IMA Vol. Math Appl.*, vol. 125, pp. 229–250, 2002.

[57] O. Diekmann, J. Heesterbeek, and J. A. Metz, "On the definition and the computation of the basic reproduction ratio R_0 in models for infectious diseases in heterogeneous populations," *Journal of Mathematical Biology*, vol. 28, no. 4, pp. 365–382, 1990.

[58] P. van den Driessche and J. Watmough, "Reproduction numbers and subthreshold endemic equilibria for compartmental models of disease transmission," *Mathematical Biosciences*, vol. 180, no. 1, pp. 29–48, 2002.

[59] N. P. Bhatia and G. P. Szegö, *Dynamical Systems: Stability Theory and Applications*. Springer Berlin-Heidelberg-New York, 1967.

[60] P. N. Tu, *Dynamical Systems: An Introduction with Applications in Economics and Biology*. Springer-Verlag Berlin, 1994.

[61] M. W. Hirsch, S. Smale, and R. L. Devaney, *Differential Equations, Dynamical Systems, and an Introduction to Chaos*, vol. 60. Academic press, 2004.

[62] A. D. Polyanin and A. V. Manzhirov, *Handbook of Mathematics for Engineers and Scientists*. CRC Press, 2006.

[63] F. Dercole and S. Rinaldi, "Dynamical systems and their bifurcations," *Advanced Methods of Biomedical Signal Processing, IEEE-Wiley Press, New York, USA*, pp. 291–325, 2011.

[64] H. W. Hethcote, "The mathematics of infectious diseases," *SIAM review*, vol. 42, no. 4, pp. 599–653, 2000.

[65] H. R. Thieme, *Mathematics in Population Biology*. Princeton University Press, 2003.

[66] H. W. Hethcote, "Qualitative analyses of communicable disease models," *Mathematical Biosciences*, vol. 28, no. 3, pp. 335–356, 1976.

[67] A. Berman and R. J. Plemmons, "Nonnegative matrices," *The Mathematical Sciences, Classics in Applied Mathematics*, vol. 9, 1979.

[68] P. Stephens and W. Sutherland, "Consequences of the Allee effect for behaviour, ecology and conservation," *Trends Ecol. Evol.*, vol. 14, no. 10, pp. 401–405, 1999.

[69] R. M. Anderson, "Parasite pathogenicity and the depression of host population equilibria," *Nature*, vol. 279, pp. 150–152, 1979.

[70] R. M. Anderson and R. M. May, "Population biology of infectious diseases: Part I," *Nature*, vol. 280, pp. 361–367, 1979.

[71] A. Dhooge, W. Govaerts, and Y. A. Kuznetsov, "Matcont: a MATLAB package for numerical bifurcation analysis of ODEs," *ACM Transactions on Mathematical Software (TOMS)*, vol. 29, no. 2, pp. 141–164, 2003.

[72] E. J. Doedel, "Auto: A program for the automatic bifurcation analysis of autonomous systems," *Congr. Numer*, vol. 30, pp. 265–284, 1981.

[73] B. Ermentrout, *Simulating, analyzing, and animating dynamical systems: a guide to XPPAUT for researchers and students*, vol. 14. SIAM, 2002.

[74] G. Caughley, "Directions in conservation biology," *Journal of animal ecology*, pp. 215–244, 1994.

[75] S. L. Pimm, H. L. Jones, and J. Diamond, "On the risk of extinction," *American Naturalist*, pp. 757–785, 1988.

[76] C. Bessa-Gomes, S. Legendre, and J. Clobert, "Allee effects, mating systems and the extinction risk in populations with two sexes," *Ecology Letters*, vol. 7, no. 9, pp. 802–812, 2004.

[77] Y. Tanaka, J. Yoshimura, C. Simon, J. R. Cooley, and K.-i. Tainaka, "Allee effect in the selection for prime-numbered cycles in periodical cicadas," *Proceedings of the National Academy of Sciences*, vol. 106, no. 22, pp. 8975–8979, 2009.

[78] K. L. C. S. Busenberg and H. Thieme, "Demographic change and persistence of HIV/AIDS in a heterogeneous population," *Journal of Applied Mathematics*, vol. 51, no. 04, pp. 1030–1052, 1991.

[79] H. Gulbudak and M. Martcheva, "Forward hysteresis and backward bifurcation caused by culling in an avian influenza model," *Mathematical biosciences*, vol. 246, no. 1, pp. 202–212, 2013.

[80] G. W. de Lisle, C. Mackintosh, and R. Bengis, "Mycobacterium bovis in free-living and captive wildlife, including farmed deer.," *Revue scientifique et technique (International Office of Epizootics)*, vol. 20, no. 1, pp. 86–111, 2001.

[81] P. C. Cross and W. M. Getz, "Assessing vaccination as a control strategy in an ongoing epidemic: Bovine tuberculosis in African buffalo," *Ecological Modelling*, vol. 196, no. 3, pp. 494–504, 2006.

[82] V. De Vos, R. G. Bengis, N. Kriek, A. L. Michel, D. Keet, J. Raath, and H. Huchzermeyer, "The epidemiology of tuberculosis in free-ranging African buffalo (syncerus caffer) in the Kruger National Park, South Africa," *Onderstepoort Journal of Veterinary Research*, vol. 68, pp. 119–130, 2001.

[83] A. E. Jolles, D. V. Cooper, and S. A. Levin, "Hidden effects of chronic tuberculosis in African buffalo," *Ecology*, vol. 86, no. 9, pp. 2358–2364, 2005.

[84] R. Anguelov and H. Kojouharov, "Continuous Age-structured model for bovine tuberculosis in African buffalo," in 1^{st} *international conference on applications of mathematics in technical and natural sciences*, vol. 1186, pp. 443–450, AIP Publishing, 2009.

[85] S. M. Garba, A. B. Gumel, and M. R. Abu Bakar, "Backward bifurcations in dengue transmission dynamics," *Mathematical Biosciences*, vol. 215, no. 1, pp. 11–25, 2008.

[86] M. A. Safi and A. B. Gumel, "Mathematical analysis of a disease transmission model with quarantine, isolation and an imperfect vaccine," *Computers & Mathematics with Applications*, vol. 61, no. 10, pp. 3044–3070, 2011.

[87] B. M. Buddle, D. N. Wedlock, M. Denis, H. M. Vordermeier, and R. G. Hewinson, "Update on vaccination of cattle and wildlife populations against tuberculosis," *Veterinary Microbiology*, vol. 151, no. 1, pp. 14–22, 2011.

[88] C. Vargas-De-León, "On the global stability of SIS, SIR and SIRS epidemic models with standard incidence," *Chaos, Solitons & Fractals*, vol. 44, no. 12, pp. 1106–1110, 2011.

[89] L.-M. de Klerk-Lorist, *The evaluation of BCG vaccine against bovine tuberculosis in African buffaloes (Syncerus caffer)*. PhD thesis, University of Pretoria, 2005.

[90] S. Blower and A. McLean, "Prophylactic vaccines, risk behavior change, and the probability of eradicating HIV in san francisco," *Science*, vol. 265, no. 5177, pp. 1451–1454, 1994.

[91] C. Chiyaka, J. M. Tchuenche, W. Garira, and S. Dube, "A mathematical analysis of the effects of control strategies on the transmission dynamics of malaria," *Applied Mathematics and Computation*, vol. 195, no. 2, pp. 641–662, 2008.

[92] E. H. Elbasha and A. B. Gumel, "Theoretical assessment of public health impact of imperfect prophylactic HIV-1 vaccines with therapeutic benefits," *Bulletin of Mathematical Biology*, vol. 68, no. 3, pp. 577–614, 2006.

[93] A. R. Mclean and S. M. Blower, "Imperfect vaccines and herd immunity to HIV," *Proceedings of the Royal Society of London. Series B: Biological Sciences*, vol. 253, no. 1336, pp. 9–13, 1993.

[94] A. R. McLean and S. M. Blower, "Modelling HIV vaccination," *Trends in Microbiology*, vol. 3, no. 12, pp. 458–463, 1995.

[95] B. Buddle, G. De Lisle, A. Pfeffer, and F. Aldwell, "Immunological responses and protection against Mycobacterium bovis in calves vaccinated with a low dose of BCG," *Vaccine*, vol. 13, no. 12, pp. 1123–1130, 1995.